Improving the testing of padding safety in short track speed skating

Graduation Project

Jurian de Klerk

Delft University of Technology

TU Delft

Improving the testing of padding safety in short track speed skating

by

Jurian de Klerk

5298742

Mentor:	G. Hoekstra
Chair:	A. Jansen
KNSB:	E. Reijmer
Innovatielab Thialf:	I. Stoter
Faculty:	Faculty of Industrial Design, TU Delft

TU Delft

Preface

This report is conducted as part of the Integrated Product Design Masters program in Industrial Design Engineering at the Delft University of Technology. The project was carried out in collaboration with the Koninklijke Nederlandse Schaatsenrijdersbond (KNSB) and Innovatielab Thialf with the aim of contributing to the further development of the ICE-G1 testing system and improving the biomechanical representativeness of padding impact simulations in short track speed skating.

Improving athlete safety in high speed sports requires a careful balance between theoretical insight, engineering feasibility, and practical constraints. This project challenged me to integrate crash dynamics, material behavior, and design methodology into a coherent testing approach.

I would like to express my sincere gratitude to Gonny Hoekstra and Arjen Jansen for their supervision and feedback throughout the project. My appreciation extends to Ellen Reijmer, Inge Stoter, Wilf OReilly and the coaches and experts who contributed through interviews and technical input. Their practical insights were essential in grounding the project in real-world relevance. Finally, I would like to thank my family and friends for their continuous support during this graduation period.

Generative AI tools have been used during this project solely to improve the readability and clarity of written text and to support structured brainstorming in the early exploration of the solution space. In chapter 5, AI has been used to improve the quality of one drawing. All technical content, theoretical interpretations, experimental results, and factual claims presented in this report are based on independent research, analysis, and design work conducted by the author. Generative AI has not been used to generate factual research content, data, or conclusions.

I hope this report contributes to the continued development of safer testing methods within short track speed skating and provides a foundation for future improvements in padding safety evaluation.

Jurian de Klerk
Delft, May 2026

Abstract

Short track speed skating is characterized by high velocities and close athlete interactions, resulting in frequent crashes and a substantial risk of injury. To mitigate injury severity, protective padding systems are installed around the ice rink; however, current evaluation methods insufficiently represent the complex interaction between athlete and padding. Existing standardized tests rely on simplified geometries and perpendicular impacts, leading to unrealistic pressure distributions and limited biomechanical relevance. This study aims to improve the realism of padding safety evaluation by developing a projectile that more accurately simulates the interaction between a short track speed skater and padding, while remaining compatible with the ICE-G1 on-site testing system.

A comprehensive theoretical framework was established, integrating foam mechanics, crash dynamics, injury mechanisms, and scaling principles. Foam behavior was analyzed using a mass-spring-damper model, highlighting the importance of impact velocity, contact area, and geometry in determining deformation and energy absorption. To define representative crash conditions, a video analysis of 62 real-world short track incidents was conducted. Results show that the majority of crashes occur at velocities above 40 km/h, with impact angles predominantly between 35 and 55°, and back-first impacts identified as the most frequent and representative scenario. Furthermore, impacts were found to occur primarily in the lower region of the padding, often involving a single padding element.

A key limitation of existing test methods was identified in the mismatch between mass and contact area, resulting in stress levels that are not representative of real athlete impacts. To address this, a scaling strategy was developed based on preserving the mass-to-contact-area ratio, ensuring comparable stress distributions within the padding. This led to the design of a scaled projectile that more closely mimics the geometry and loading characteristics of a skater during impact, which is shown below (left).

Experimental validation demonstrated that the redesigned projectile produces higher and likely more representative peak accelerations compared to current testing approaches, indicating improved simulation fidelity. The findings emphasize that accurate representation of contact geometry and mass distribution is essential for realistic padding evaluation. Additionally, there is a difference between moveable and traditional padding. As the current standardized test method (ISU drop test) is unable to test moveable padding, this highlights yet another flaw in the current standard. The proposed method provides a significant step toward more representative and reliable testing of safety of padding systems in short track speed skating, and offers a foundation for future improvements in both testing methodology and athlete safety. However, as sensor limitations were encountered during experimental validation, the exact differences between the redesigned projectile and the current standardized test method is unknown, and more testing is required.

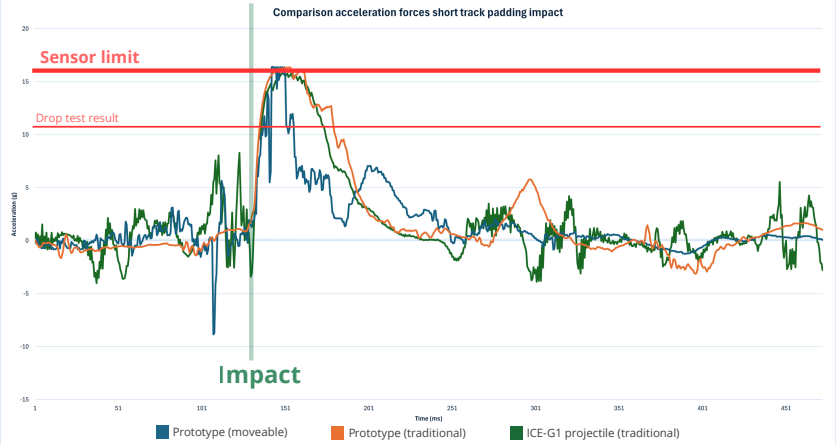

Contents

1

Introduction

Short track speed skating is not a sport without risks. Falls could lead to significant injuries, but the padding surrounding the ice rink should prevent serious injuries. Different test methods can be used to check the safety of padding, but these methods lack realism. This is where a new design can make a difference. In this chapter, the context will be explained first. Then, the main project objective will be shared and explained.

1.1. Context and background

Short track speed skating is a relatively young discipline within ice skating (Fig. 1.1). Although early forms of the sport date back to the beginning of the twentieth century, it was officially recognized by the International Skating Union (ISU) only in 1967 (Hurdis, 1998). Since its formal introduction, the sport has undergone continuous development, with recent changes focusing on athlete safety and injury prevention.

Figure 1.1: Short track speed skaters racing in the Milano Ice Skating Arena at the Olympic Winter Games 2026 (OWIA, 2025).

In short track speed skating, multiple athletes compete by skating laps around a small oval track, 111 meters in length in a racing format (Fig. 1.2). The winner is determined by finishing position rather than time. This results in close proximity racing and frequent overtake manoeuvrers, which combined with speeds up to 60 km/h create a high-risk environment where collisions and falls are common. During a single competitive season, a large number of falls may occur, and previous studies indicate that a significant proportion of short track speed skaters sustain injuries during competition (Hillis, 2018; Hendricks et al., 2024).

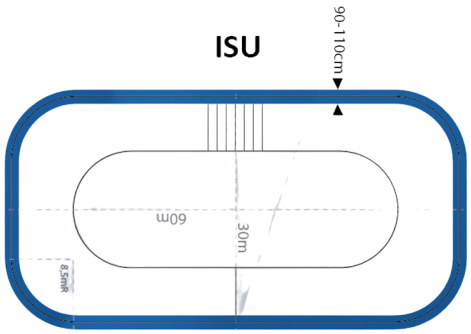

Figure 1.2: Schematic drawing of short track ice rink using moveable padding (Engo GmbH, n.d.)

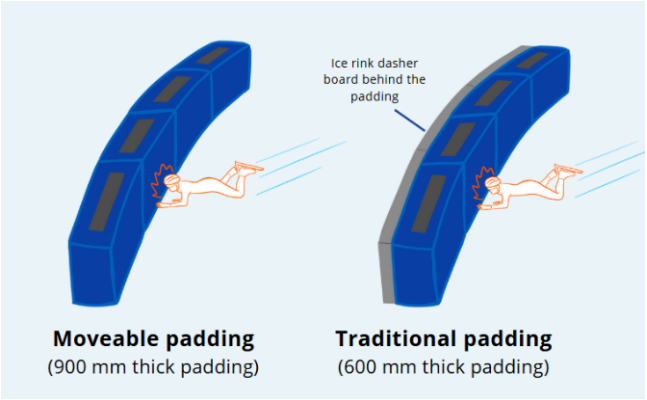

Figure 1.3: Schematic drawing of the two padding varieties used in short track speed skating.

To reduce the risk of serious injury during crashes, safety padding is installed along the perimeter of the ice rink, shown as the blue perimeter in Fig. 1.2. The primary function of padding is to decelerate the short track speed skater in a controlled manner after a fall (Fig. 1.4), limiting peak forces acting on the skaters body. In short track speed skating, two padding varieties are used: traditional padding and moveable padding. Traditional padding is 600 mm thick and placed against hard boarding in ice hockey rinks while moveable padding is usually 900 mm thick and placed on ice rinks without any hard boarding (Fig. 1.3). In official elite short track events, only moveable padding is allowed to be used. Traditional padding can only be used for junior competition or training sessions (KNSB, 2025).

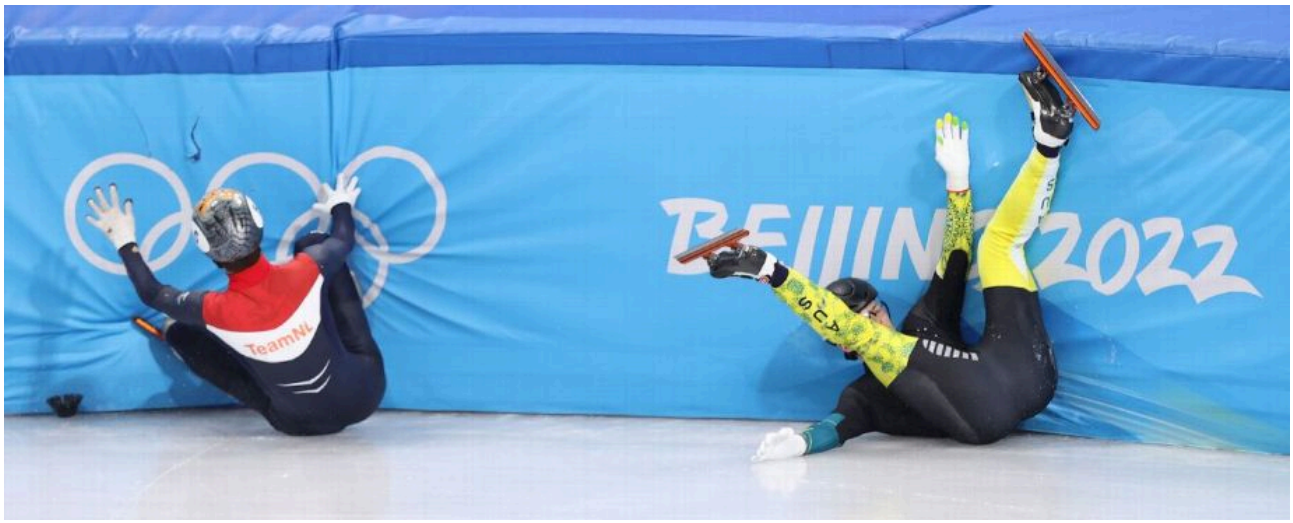

Figure 1.4: Short track speed skaters crashing in padding (AAP, 2022)

As new padding systems are developed, their performance must be evaluated before being implemented in competition. The ISU currently prescribes a standardized test, commonly referred to as the ISU drop test, to assess padding safety (Fig. 1.5). In this test, a cylindrical mass of 32 kg with a diameter of 20 cm is dropped vertically at the center of a single piece of padding which is placed on the ground. An accelerometer attached to the cylindrical mass is used to measure peak forces during the impact. If the measurement is below a specified threshold, the padding is deemed safe and is allowed to be used at ice rinks during official competitions and training sessions (KNSB, 2025). While the ISU drop test provides repeatable and controllable results, an evaluation commissioned by the Koninklijke Nederlandse Schaatsenrijdersbond (KNSB) identified several limitations. These include the inability to assess moveable padding behavior, the absence of interactions between connected padding elements, the use of a rigid cylindrical mass to represent a human body, and the assumption of perpendicular, centrally located impacts (Beets et al., 2024).

In response to these limitations, a new on-site testing system, the Impact & Crash Evaluator 1st Generation (ICE-G1), was developed by Industrial Design Engineering Master students at the Delft University of Technology (Fig. 1.7) (Beets et al., 2024). The ICE-G1 allows padding to be tested directly on the ice rink using a rail-based launching mechanism that propels a projectile into the padding. This approach improves realism by enabling the assessment of both traditional and moveable padding under more representative conditions. A detailed explanation of the ICE-G1 test method can be found in Appendix C.

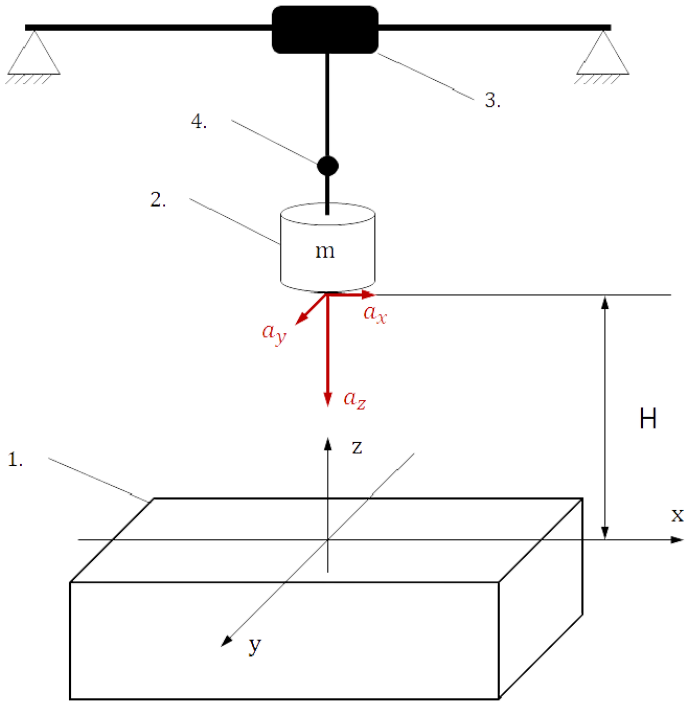

Figure 1.5: The standardized ISU drop test. 1) the piece of padding to test, 2) a cylindrical mass (m) of 32 kg, 3) a winch, and 4) the drop triggering device. The cylindrical mass is hoisted to a height of 4 meters with a winch. This mass is then dropped on the padding by the drop triggering device. An accelerometer attached to the mass measures peak acceleration.

However, while the ICE-G1 is designed to simulate a back-first impact of an average male short track speed skater at 60 km/h, it still relies on a flat circular ram with a diameter of 20 cm as the contact area during impact (Fig. 1.6), which likely results in a different pressure distribution, stopping distance and foam behavior. This raises the question how well it simulates the interaction between a short track speed skater and padding, which forms the main focus of this project.

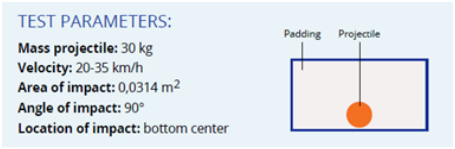

Figure 1.6: Test parameters of the ICE-G1 test method.

Figure 1.7: The Impact & Crash Evaluator 1st Generation (ICE-G1), a circular ram designed to be launched at padding on ice rinks (Beets et al., 2024)

1.2. Project objective

The aim of this project is to improve the simulation of the interaction between a short track speed skater and padding when performing physical tests (Appendix A). This project aims to develop a new projectile that better represents the short track speed skater - padding interaction which can still be used with the existing ICE-G1 modular launching mechanism. This leads to the following main research and design question:

How should a projectile look like to simulate the impact interaction between short track speed skaters and padding more realistically than the ICE-G1 projectile, while remaining compatible with the ICE-G1 launching mechanism?

To answer this question, the project has been structured using the double diamond method (Fig. 1.8). This means that the project is split into two distinct phases. The first phase is used to gather the theoretical knowledge necessary to create a meaningful design, and concludes with a clear scope and detailed design objective. The second phase revolves around the correct application of this knowledge within the scope to design a solution that fits the project objective best.

In the research phase, the aim is to clarify the research question and to define the scope and boundaries of the project. Therefore, four sub-questions have been phrased to help with the scope and detailed project objective definition:

SQ1: How does padding behave when a short track speed skater collides with it?

SQ2: What are the most common types of crashes involving padding in short track speed skating?

SQ3: What type of crash can cause the most serious injury during a collision with padding?

SQ4: How can the dimensions of a short track speed skater be scaled to keep the short track speed skating padding interaction equal in a scaled design?

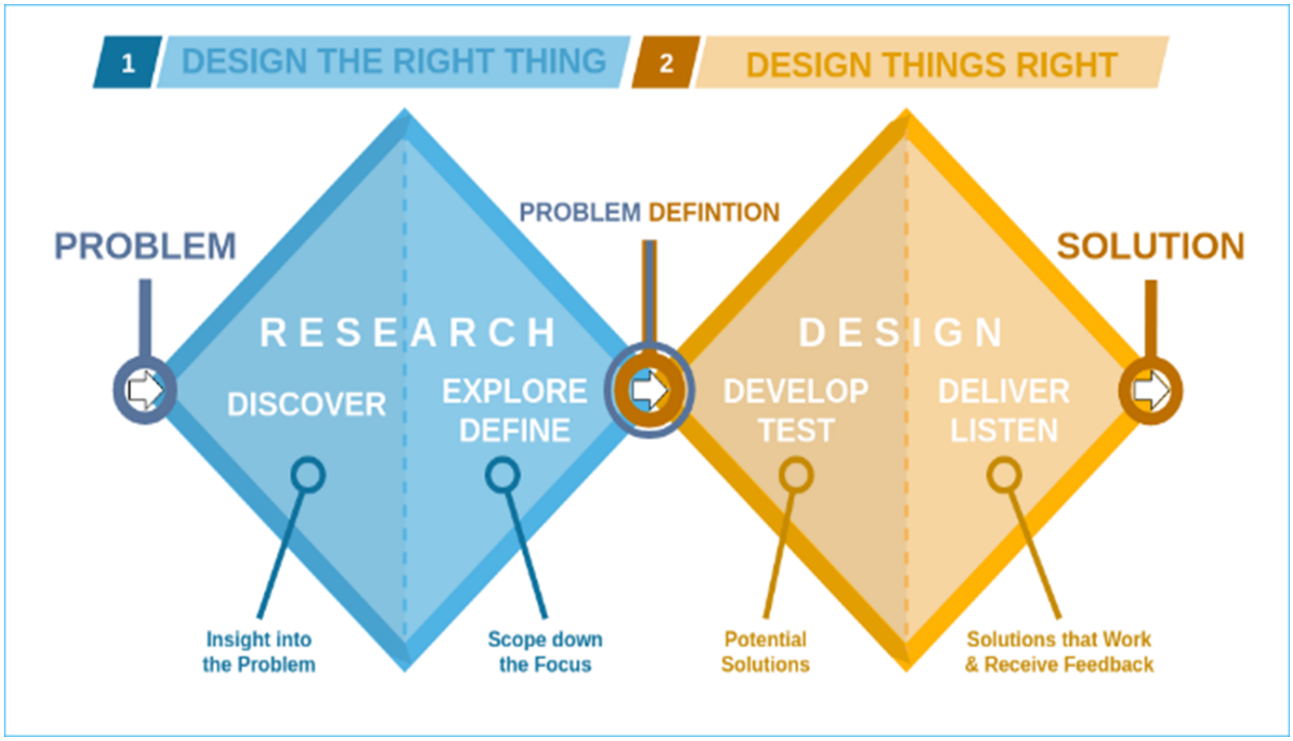

Figure 1.8: Visualisation of the double diamond method (Godesky, 2023).

Answers to these questions will help define design criteria, the clear definition of the project scope and what a realistic crash scenario is exactly, which should be simulated by the design. In the next phase, this knowledge is applied to design a projectile that is best suited for the project objective. This phase is guided by the following sub-questions:

SQ5: How can the form of the projectile be designed to physically simulate the short track speed skater - padding interaction of the most impactful crash scenario?

SQ6: Which parameters are essential to measure when evaluating padding performance using the redesigned projectile?

Using these questions as guidance, a new projectile will be designed. To test if the theory is translated correctly into the design, a prototype will be constructed to test how well the design succeeds to fulfill the project objective. The project concludes with a physical prototype of the design used to answer the main research question, and recommendations for improvements or future iterations.

The report is also structured using the double diamond method. The analysis is presented first, including research methods and important insights from the analyses. Next, these insights are used to create a more detailed project objective and to clarify the scope. After creating the design frame, the design process and final design, including the prototype, are shared, followed by the experimental validation, including test plans and results. Finally, the report addresses the project's limitations and concludes with recommendations.

2

Theoretical Framework

Before a meaningful solution can be designed, it is important to understand the problem itself. In this chapter, the athlete-padding interaction will be explained in four directions. First, the general behavior of foam padding and how this behavior is influenced will be explained. Then, an extensive crash analysis will be presented, and general crash dynamics and impact types will be clarified. Next, injury mechanics and dangerous crash types will be briefly explained. Finally, how to scale down short track speed skater dimensions to ensure compatibility with the ICE-G1 infrastructure will be described.

2.1. Padding systems and energy absorption

When short track speed skaters fall, foam padding is placed in the perimeter of the ice rink to catch these athletes. The use of padding can lead to many questions, such as why foam is the chosen material to create padding, what type of foam is used in short track padding and how padding in short track speed skating is designed. These questions all link back to SQ1: analyzing how padding behaves during a crash. This chapter will first explain how foam functions, followed by an explanation why foam is used. The chapter concludes with an explanation of what types of foam are used in padding and how padding for short track speed skating is designed.

2.1.1. Dynamic behavior of foam padding

Trying to understand padding starts with taking a closer look to the short track speed skater padding interaction. The behavior of foam can be explained by using an example of a short track speed skater crashing in padding (Fig. 2.1). During impact, a short track speed skater collides with padding with a certain velocity, and the padding deforms around the skaters body (Fig. 2.2). This simplified scenario highlights that two factors play a role during impact: the short track speed skater, and the piece of padding. The ice floors friction resistance is deemed negligible, as the friction force is estimated to have almost no influence in the force distribution during impact.

Figure 2.1: A short track speed skater crashes in padding.

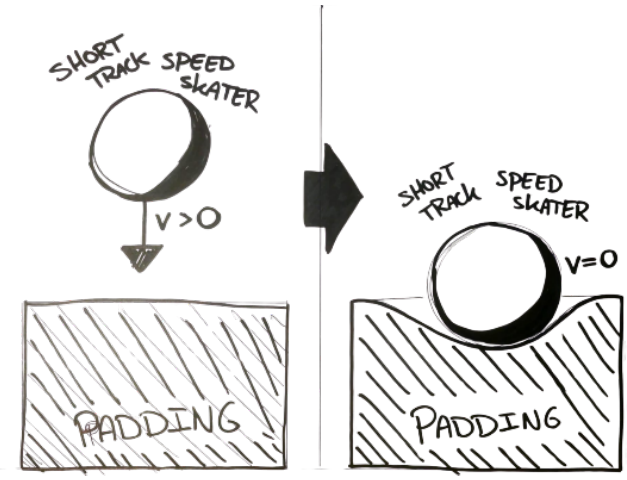

Figure 2.2: A simplified drawing of what happens during impact. v is the velocity of the short track speed skater.

During impact, the padding responds through a combination of elastic deformation and energy dissipation. This interaction can be effectively described using a massspringdamper model (Equation 2.1) (Idema, 2023). While this model does not

aim to predict exact impact forces, it is used here to illustrate the relationships between key parameters that explain padding behavior. Besides that, it is important to emphasize that this model is a simplified linear model that explains what happens during impact.

$$m\ddot{x}(t) + c\dot{x}(t) + kx(t) = F(t) \tag{2.1}$$

Equation 2.1: The mass spring damper model, where m is mass (kg), $\ddot{x}(t)$ is acceleration (m/s^2), c is the damping coefficient (N·s/m), $\dot{x}(t)$ is velocity (m/s), k is the spring constant (N/m), $x(t)$ is displacement (m), and $F(t)$ is the impact force (N).

Although the mass spring damper model provides useful insight, it remains a simplification. Real padding impacts are influenced by additional factors such as impact area and velocity. Foam does not deform purely in one dimension, and its response depends on the size of the contact area. This effect can be incorporated by extending the model to include a non-linear deformation term related to contact area (Equation 2.2) (Nayfeh & Mook, 1995).

$$m\ddot{x}(t) + c\dot{x}(t) + kx(t) + \alpha x(t)^3 = F(t) \tag{2.2}$$

Equation 2.2: Mass spring damper model with added non-linear deformation component, where α is the cubic stiffness (N/m^3) and $x(t)$ is displacement (m).

More importantly, foam is a viscoelastic material, meaning that its mechanical response depends on the rate at which it is deformed. As a result, impact velocity directly affects the apparent stiffness and damping of the foam. This strain-rate dependency can be described by velocity dependent damping behavior (Christensen, 1971). At higher impact velocities, foam behaves stiffer, resulting in higher reaction forces and reduced deformation, which can be added to a mass spring damper model with the addition (Equation 2.3).

$$m\ddot{x}(t) + (c_0 + c_1|\dot{x}(t)|)\dot{x}(t) + kx(t) + \alpha x(t)^3 = F(t) \tag{2.3}$$

Equation 2.3: Mass spring damper model with added non-linear deformation component and included velocity dependent damping component. 'c_0' is linear damping coefficient in N*(m/s), 'c_1' is the velocity-dependent damping coefficient in N*(s^2/m^2), '$\dot{x}(t)$' is velocity in m/s.

The modified mass spring damper model has been used to identify important criteria to consider for the designing phase. First, foam exhibits strain-rate dependency, which means that the impact velocity must be equal for both the real and simulated crash scenarios. In addition, the contact area and geometry at impact also changes foams deformation in all directions, meaning that defining the contact area and geometry is important in the design phase and will be carefully considered for the design.

2.1.2. Energy absorption characteristics of foam

To understand why foam is used for short track padding, it is important to understand what happens with the short track speed skaters kinetic energy during impact. Energy is not dissipated equally throughout a crash, but exhibits a pronounced peak deceleration (Fig. 2.3) (De Bruijn et al., 2023). In addition, Tremblay (2012) found that a larger stopping distance results in a decrease of acceleration forces (Fig. 2.4).

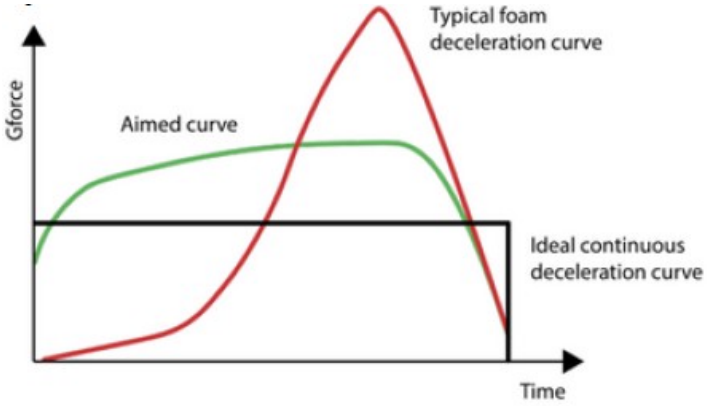

Figure 2.3: A typical foam curve with a pronounced peak force vs. the ideal flat curve without a clear peak.

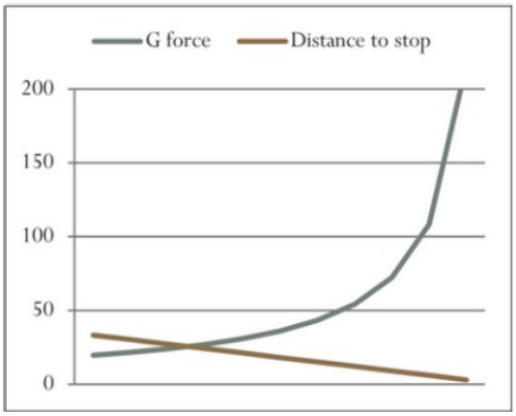

Figure 2.4: Graph showing G-force versus stopping distance. y-axis unit for g-forces in g, y-axis unit for stopping distance in cm

In short track speed skating, the primary foam type used is open cell polyurethane (PU) with varying densities (Maw & Johnston, 2010). This foam is used, as its deformation capabilities increase the stopping distance in a crash, decreasing the experienced g-forces and flattening the peak towards the aimed curve. In addition to its deformation capabilities, this foam is also an excellent energy absorber, demonstrated by its stress-strain curve compared to a dense solid material (Fig. 2.5) (Grilec et al., 1970). For conventional dense solid materials, stress increases linear with strain, resulting in limited energy absorption. Initially, foam behaves similarly. This is then followed by a plateau, during which stress remains relatively constant while the material continues to deform. This plateau enables foam to absorb large amounts of energy while maintaining relatively low reaction forces. When too much stress is applied however, the foam reaches its densification point where it stiffens rapidly, leading to a sudden reduction in energy absorption capacity (Grilec et al., 1970).

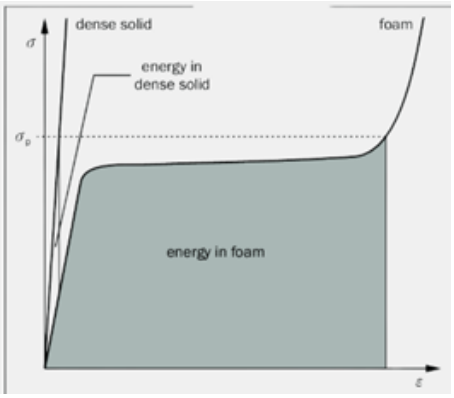

Figure 2.5: The difference in energy absorption between foam and a dense solid material, where the area under the graph visualizes the amount of absorbed energy.

To simulate the athlete - padding interaction as realistically as possible, the stress applied to the padding with the projectile should be as equal as possible for both the real and simulated crash scenario. For a similar stress, the contact geometry should also remain similar to ensure a similar applied pressure. Therefore, in addition to contact area previously mentioned, keeping the contact geometry of the projectile similar to its simulated crash scenario is another criterium that needs careful consideration for the design.

2.1.3. Padding used in short track speed skating

In short track speed skating, two types of padding are used: moveable and traditional padding (Fig. 1.3). Moveable padding is the standard issued padding for elite competition. This padding is able to move back with the speed skater during impact, increasing stopping distance and lowering impact forces. Traditional padding is used in ice hockey rinks where its placed against the dasher boards, which prevent the padding from moving back. This padding type is also thinner, which results in shorter stopping distances and higher impact forces, deeming it less safe than moveable padding. Therefore, traditional padding is only used for junior competitions and training sessions. The standardized ISU drop test is currently unable to test the effects op moveable padding, so the new design should be able to test both padding types to compare measurements between both padding types.

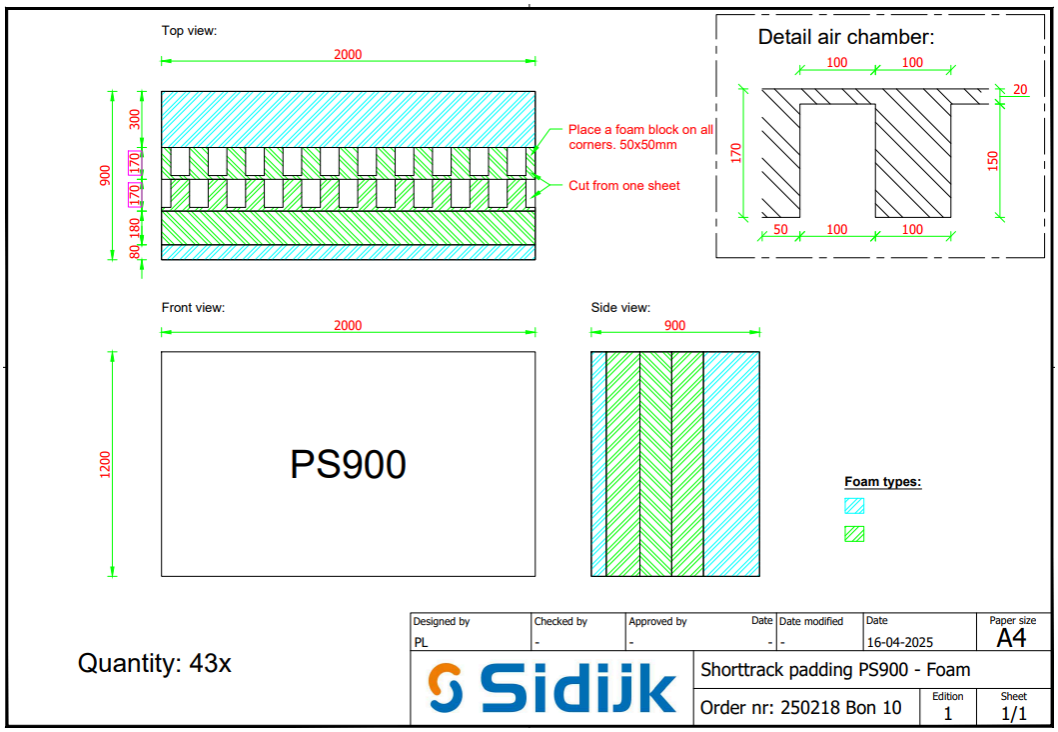

Figure 2.6: Schematic drawing of a piece of moveable short track padding.

As padding in short track speed skating should protect athletes with very different sizes and masses, its design needs to

be carefully considered to protect all athletes equally. To accommodate this variability, manufacturers such as Sidijk use layered foam constructions (Fig. 2.6). Typically, a thin layer of denser foam is used at the front to distribute forces, followed by less dense foam layers to absorb moderate impacts, and a final dense layer to manage extreme crashes. Therefore, to simulate a crash realistically, all foam layers that deform during a real crash should deform with the projectile of the test.

This underlines the importance of equal stress levels applied to padding by a new design. Therefore, the contact geometry and area of the new design should be similar to the contact geometry and area of the simulated crash scenario.

2.2. Crash dynamics in short track speed skating

For a good simulation of a typical crash, it is important to understand what a typical crash is. Therefore, it is essential to understand how short track speed skaters collide with padding. This chapter refers back to SQ2 about the commonality of short track crash scenarios. In this chapter, the crash dynamics in short track speed skating crashes are explained by first defining a short track crash, followed by a detailed video analysis of crashes where all variables are explained individually. Finally, relationships between variables are examined to identify recurring patterns and underlying crash mechanics.

2.2.1. Definition of a crash event

In short track speed skating, crashes occur regularly, but what exactly is a crash event? The term crash can be interpreted in various ways depending on context. In this project, a crash is defined as follows:

"A crash in short track speed skating includes everything that happens from the moment that the short track speed skater is about to fall until the moment that the short track speed skater comes to a complete stop."

For a better understanding of this definition, a crash has been divided into 5 distinct phases from the initial cause of the crash to post-impact observations (Fig. 2.7). These phases do not imply strict temporal separation. In reality, they may partially overlap. However, the phased structure provides a clear analytical framework for studying complex crash behavior.

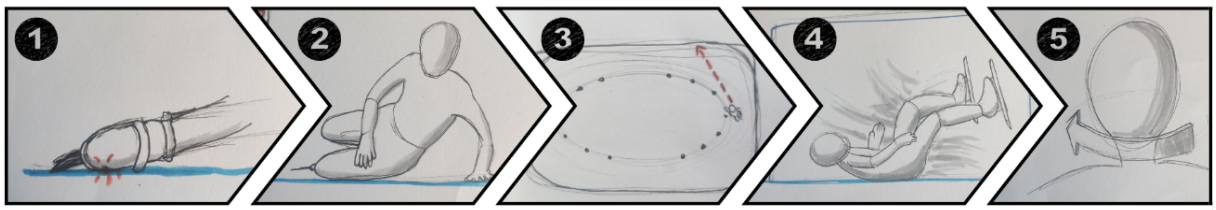

Figure 2.7: Overview of the 5 phases of a crash. 1: the cause of falling, 2: body configuration at ice contact, 3: sliding dynamics, 4: impact interaction with padding, 5: post-impact

For this analysis, 62 crash videos have been analyzed of short track talent teams in the Netherlands for both competition events and training sessions. Due to varying camera views, not all parameters were visible in all videos, which resulted in varying sample sizes per parameter. For each crash phase, the crash phase is first explained, followed by an overview of the variables and their occurrences. Each crash phase chapter ends with clear interpretation of findings.

2.2.2. Crash phase 1: Cause of falling

The first crash phase explains the moment where the crash originates and what happened to make a short track speed skater crash. In 60 crashes, seven different causes for falling have been observed (Fig. 2.8). While the cause of falling provides useful contextual information, it does not directly influence the interaction between the skater and the padding. Therefore, it is not considered a primary design variable for the projectile but rather a background factor that helps explain subsequent crash behavior.

The distribution across the causes of falling differed significantly ($\chi^2(7) = 16.533, p < 0.02$) (Table 2.1). Ice breaking away is the primary cause of falling in the observed instances with 26.7% occurrences. In 30% of crashes, multiple athletes are involved.

Table 2.1: Cause of falling observations. $N = 60, \chi^2(7) = 16.533; p = 0.02.^{*}(Z > 1.96 \rightarrow p < 0.05)^{**}(Z > 2.58 \rightarrow p < 0.01)^{***}(Z > 3.29 \rightarrow p < 0.001)$, significance Z-scores is based on standardized residuals

Cause of falling					
Variable	**n**	**% Obs.**	**Exp. %**	**Z**	**Sig.**
Front skate in ice	7	11,7%	14,3%	-0,58	
Shoe on ice	11	18,3%	14,3%	0,90	
Ice breaking away	16	26,7%	14,3%	2,74	**
Push by other athlete	6	10,0%	14,3%	-0,95	
Loss of balance	7	11,7%	14,3%	-0,58	
Collision other athlete	12	20,0%	14,3%	1,26	
Skating over block	1	1,7%	14,3%	-2,79	**

Figure 2.8: Visual overview of all observed fall initiation causes.

2.2.3. Crash phase 2: Body configuration

The second crash phase explains how short track speed skaters fall on the ice after the cause of falling. The initial fall consists of both a falling direction in comparison to the ice rink perimeter and a body orientation of the short track speed skater. The falling direction explains in what direction the body is oriented compared to the ice rink perimeter (Fig. 2.9) and the body orientation explains what body parts of the short track speed skater hit the ice first (Fig. 2.13). Similar to the first crash phase, this crash phase does not directly influence the interaction between the athlete and the padding. Insights from this phase are therefore not translated into design criteria, but could influence test protocols when relationships between variables are explored.

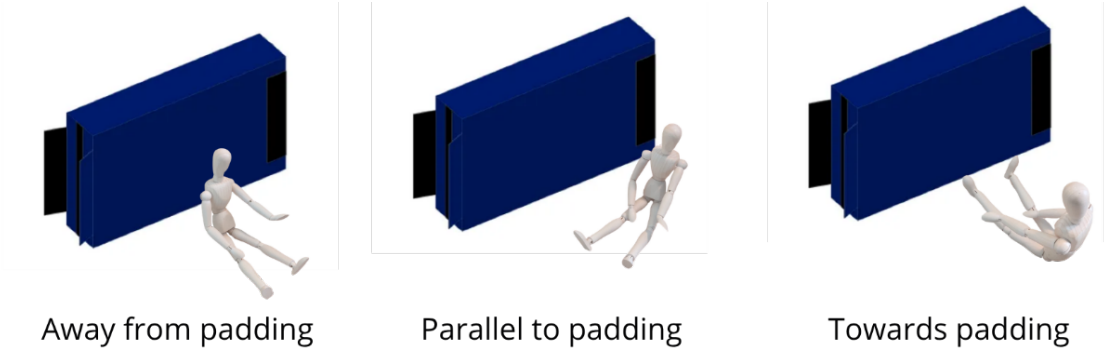

Figure 2.9: Visualization of all observed falling directions in crash phase 2.

The distribution across the falling directions differed significantly (χ^2(n=3) = 21.100, $p = 0.0002$) (Table 2.2). In 58.3% of crashes, short track speed skaters fall parallel to the ice rink perimeter. In only 10% of crashes, athletes fall facing away from padding, which shows significantly less occurrences then the other falling directions.

Table 2.2: Falling directions observations. $N = 60$, χ^2(n = 3) = 21.100; $p = 0.0002.^*(Z > 1.96 \rightarrow p < 0.05)^{**}(Z > 2.58 \rightarrow p < 0.01)^{***}(Z > 3.29 \rightarrow p < 0.001)$, significance Z-scores is based on standardized residuals

Direction of falling					
Variable	**n**	**% Obs.**	**Exp. %**	**Z**	**Sig.**
Towards padding	19	31,7%	33,3%	-0,27	
Parallel to padding	35	58,3%	33,3%	4,11	***
Away from padding	6	10,0%	33,3%	-3,83	***

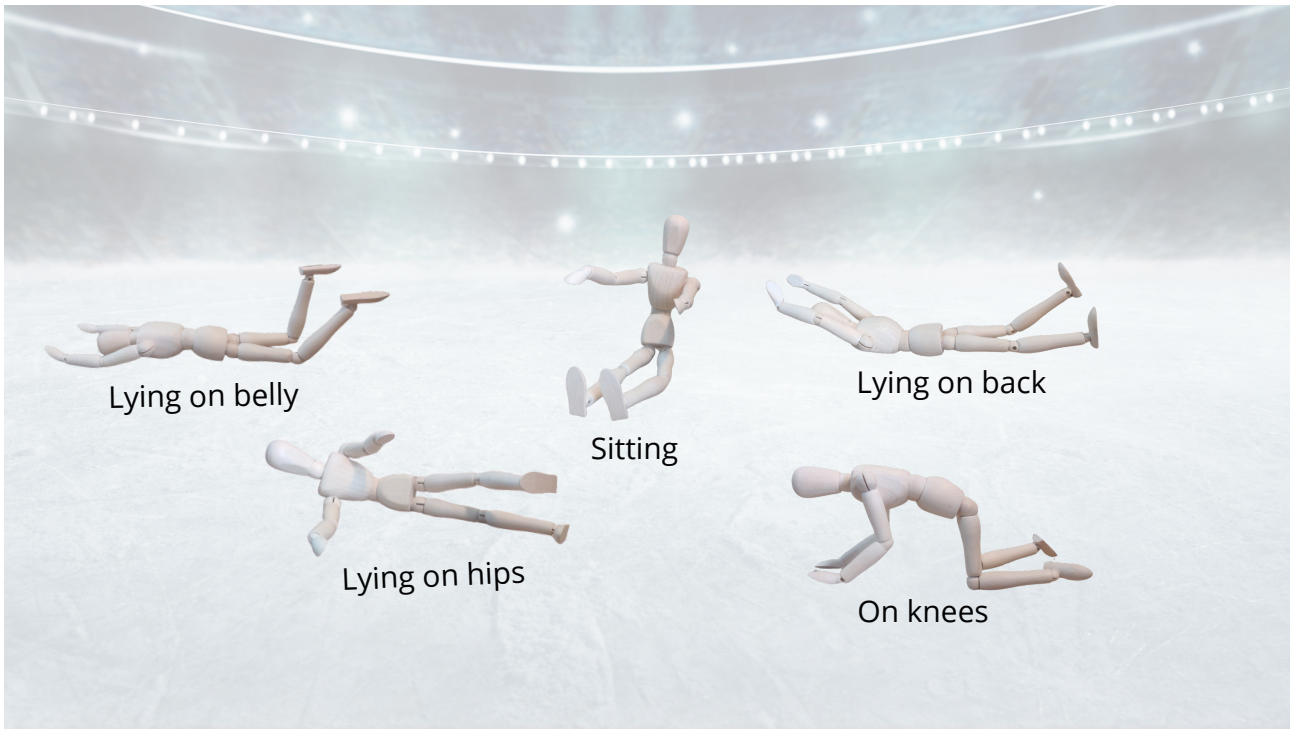

Figure 2.10: Visualization of all observed body orientations in crash phase 2.

The distribution across the body orientations at initial ice contact differed significantly (χ^2(n=5) = 73.333, $p = 3.57 * 10 - 15$) (Table 2.3). In 91,7% of observed falls, short track speed skaters either hit the ice lying on their hips (56,7%) or sitting (35,0%). All other observed body orientations at initial ice contact occur significantly less frequently.

Table 2.3: Falling orientations observations. $N = 60$, χ^2(n=5) = 73.833; $p = 3.57 \cdot 10^{-15}$.*$(Z > 1.96 \rightarrow p < 0.05)$**$(Z > 2.58 \rightarrow p < 0.01)$***$(Z > 3.29 \rightarrow p < 0.001)$, significance Z-scores is based on standardized residuals

Orientation when falling					
Variable	**n**	**% Observed**	**Expected %**	**Z-score**	**Sig.**
Lying on hips	34	56,7%	20,0%	7,10	***
Sitting	21	35,0%	20,0%	2,90	**
Lying on belly	1	1,7%	20,0%	-3,55	***
Lying on back	2	3,3%	20,0%	-3,23	**
On knees	2	3,3%	20,0%	-3,23	**

2.2.4. Crash phase 3: Sliding dynamics

The third crash phase explains the slide towards padding after initial ice contact until the short track speed skater is about to make contact with padding, which encompasses sliding angle and sliding velocity. Sliding angle is the angle of attack compared to the piece of padding which the short track speed skater will impact and is determined by using tracker software to get an estimated angle (Fig. 2.11). The sliding velocity determines the speed of sliding, which is determined by taking the average velocity of the skater in the lap before the crash, as this is the most reliable method to estimate crash velocities for the used videos (Fig. 2.12). This crash phase does not yield any direct design criteria for the design of a projectile, as it does not explain the interaction between the athlete and padding explicitly. However, as this crash phase explains how a short track speed skater arrives at padding, This crash phase will be used to determine test protocols, such as velocity, and test setups, such as angle of impact.

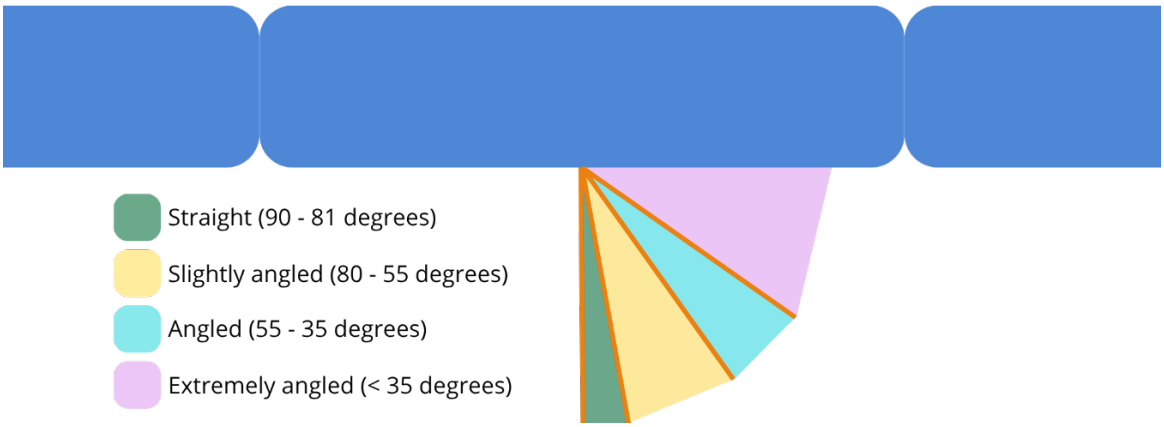

Figure 2.11: Visualization of all observed crash angle ranges, seen in top view.

The distribution across the observed crash angles differed significantly ($\chi^2(n = 4) = 14.242, p = 0.005$) (Table 2.4). 42.4% of impacts happen at an angle of approximately 45 degrees, and occur significantly more frequently than any other range. Straight impacts, which is the only impact angle range currently tested by the standardized testing method, occur 20.3% of crashes. Simulating a typical crash scenario would therefore include tests in the 55-35 degree range. Crashes angled lower than 35 degrees only occurred 8.5% in the observed videos, and occur significantly infrequent.

Table 2.4: Crash angle observations. $N = 59, \chi^2(4) = 14.242; p = 0.005.^*(Z > 1.96 \rightarrow p < 0.05)^{**}(Z > 2.58 \rightarrow p < 0.01)^{***}(Z > 3.29 \rightarrow p < 0.001)$, significance Z-scores is based on standardized residuals

Crash angle					
Variable	**n**	**% Obs.**	**Exp. %**	**Z**	**Sig.**
90 - 80 degrees	12	20,3%	25,0%	-0,83	
79 - 56 degrees	17	28,8%	25,0%	0,68	
55 - 35 degrees	25	42,4%	25,0%	3,08	**
34 - 1 degrees	5	8,5%	25,0%	-2,93	**

Figure 2.12: Visualization of all observed velocities during crashes.

Table 2.5: Sliding velocities observations. $N = 61, \chi^2(5) = 99.902; p = 2.2 \cdot 10^{-16}.^*(Z > 1.96 \rightarrow p < 0.05)^{**}(Z > 2.58 \rightarrow p < 0.01)^{***}(Z > 3.29 \rightarrow p < 0.001)$, significance Z-scores is based on standardized residuals

Sliding velocity					
Variable	**n**	**% Obs.**	**Exp. %**	**Z**	**Sig.**
10-20 km/h	2	3,3%	20,0%	-3,26	**
20-30 km/h	5	8,2%	20,0%	-2,30	*
30-40 km/h	9	14,8%	20,0%	-1,02	
40-50 km/h	43	70,5%	20,0%	9,86	***
50-60 km/h	2	3,3%	20,0%	-3,26	**

The distribution across the observed sliding velocities differed significantly ($\chi^2(5) = 99.902, p = 2.2 \cdot 10^{-16}$) (Table 2.5). In 73.8% of observed crashes, short track speed skaters had a sliding velocity greater than 40 km/h. Crashes with slide velocities below 30 km/h occurred only in 11.5% of all observed crashes.

However, an important sidenote, is that the observed videos centered around talent teams, which involved junior and early senior short track speed skaters. While sliding velocities may be higher at elite skating levels, this still highlights that the majority of crashes occur at high speeds, and that a typical crash scenario would have a velocity of at least 40 km/h.

2.2.5. Crash phase 4: Impact interaction

The fourth crash phase explains the interaction between the short track speed skater and padding, and is thus the most important phase to consider for design criteria. This crash phase highlights how a short track speed skater impacts padding by looking at the body impact type, padding usage, height of the impact and the crash zone. The body impact type explains the athletes body orientation at the moment of impact (Fig. 2.13). The padding usage explains how many padding pieces are directly engaged at the moment of impact (Fig. 2.15). Padding height explain the height of the impact (Fig. 2.14). The crash zone explains where on the ice rink the impact happens (Fig. 2.16). As this crash phase directly focuses on skater padding interaction, insights gathered from this crash phase can directly be translated in design criteria.

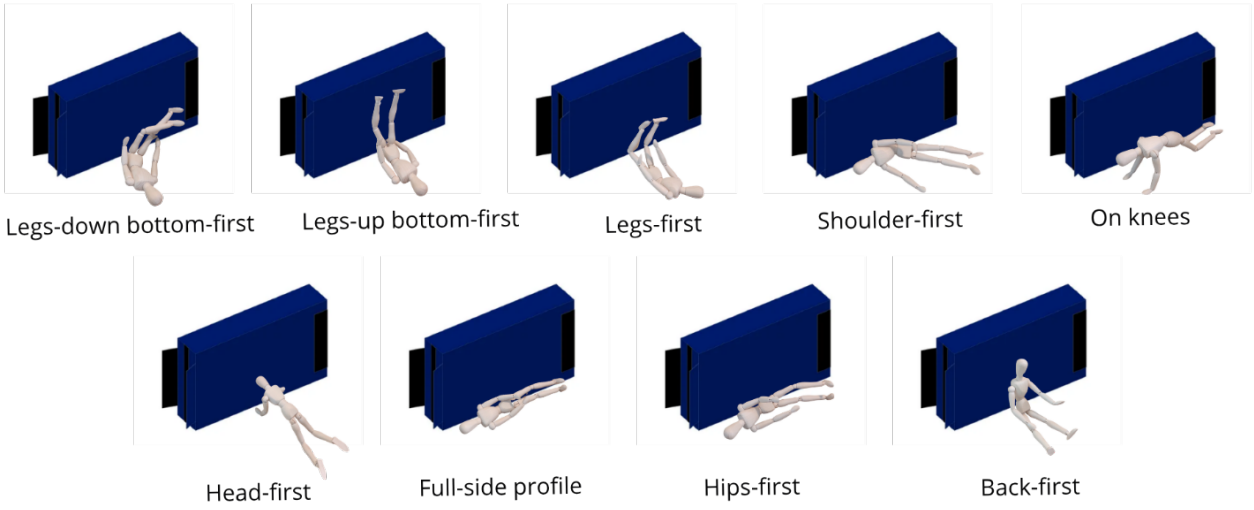

Figure 2.13: Visualization of all observed body impact types

Table 2.6: Body impact type observations.
$N = 59, \chi^2(9) = 38.492; p = 1.7 \cdot 10^{-5}$.*$(Z > 1.96 \rightarrow p < 0.05)$**$(Z > 2.58 \rightarrow p < 0.01)$***$(Z > 3.29 \rightarrow p < 0.001)$, significance Z-scores is based on standardized residuals

Body impact type					
Variable	**n**	**% Obs.**	**Exp. %**	**Z**	**Sig.**
Back first	18	30,5%	11,1%	4,18	***
Shoulder first	4	6,8%	11,1%	-1,33	
Legs up, bottom first	12	20,3%	11,1%	1,82	
Head first	0	0,0%	11,1%	-	
Full side profile laying	5	8,5%	11,1%	-0,93	
Full side profile knees	1	1,7%	11,1%	-2,51	*
Hips first	14	23,7%	11,1%	2,61	**
Legs down, bottom first	3	5,1%	11,1%	-1,72	
Legs first	2	3,4%	11,1%	-2,12	*

The distribution across the observed body impact types differed significantly ($\chi^2(9) = 38.492, p = 1.7 \cdot 10^{-5}$) (Table 2.6). In 30.5% of observed crashes, the athlete hit the padding back-first, which occurs significantly more frequently than any other impact type.

In 74.5% of crashes, skaters impact padding either back-first, hips-first or legs-up bottom-first. This suggests that skaters try to adjust their bodies during crash phase three to collide in one of these three types. However, as back-first impacts occur significantly most frequent, this should be the focus impact type of the design.

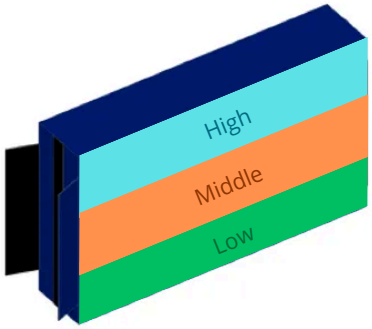

Figure 2.14: Visualization of observed padding heights.

Table 2.7: Padding impact height observations.
$N = 42, \chi^2(3) = 34.381; p = 3.6 \cdot 10^{-8}$.

Variable	**n**	**% Obs.**	**Sig.**
High	0	0,0%	
Medium	2	4,8%	***
Low	40	95,2%	***

The distribution across the observed padding impact height differed significantly ($\chi^2(3) = 34.381, p = 3.6 \cdot 10^{-8}$) (Table 2.7). More than 95% of crashes occur in the lower region of short track padding. No impacts in the high region of padding has been observed in the videos. A typical crash therefore includes an impact in the lower region of padding.

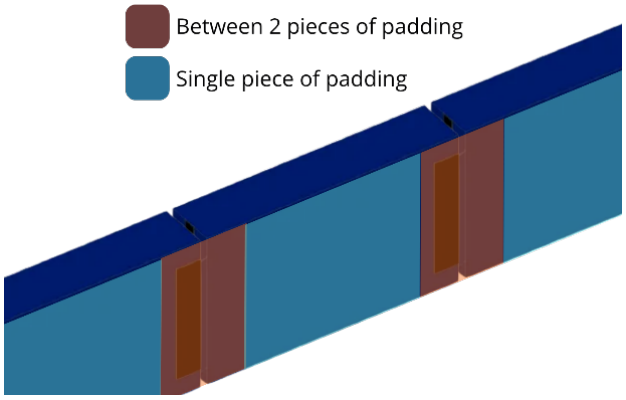

Figure 2.15: Visualization of observed padding usage.

Table 2.8: Padding usage observations. $N = 42, \chi^2(2) = 3.429, p = 0.06$.

Variable	n	% Obs.	Sig.
Single piece	27	64,3%	
Between two pieces	15	35,7%	

The distribution across the observed padding usage did not differ significantly ($\chi^2(2) = 3.429, p = 0.06$) (Table 2.8). Although impacts in a single piece occurred more frequently, the difference is not significant. This means a typical crash could occur in both scenarios, but single piece impacts will be the main focus for test protocols.

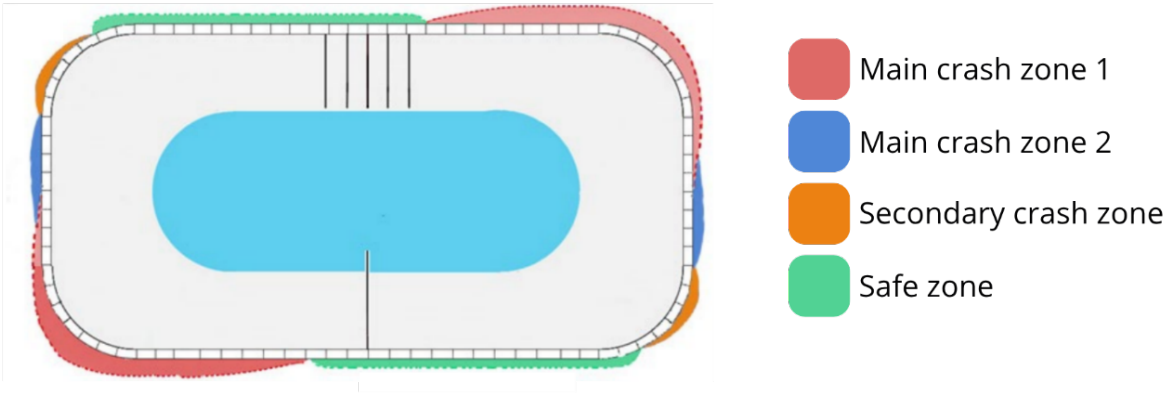

Figure 2.16: Visualization of the crash zones. Red is one of the main crash zones in the corners of the rink. Blue is the other main crash zone, just after a corner. The safe zone is the straight just after the main crash zone (red) and just before the secondary crash zone (orange).

The distribution across the observed crash zones differed significantly ($\chi^2(4) = 105.62, p = 2.2 \cdot 10^{-16}$) (Table 2.9). More than 82% of all observed crashes occur in main crash zone 1 (red).

Interesting to note is that crashes in main crash zone 2 (blue) and the safe zone (green) occur equally frequently, although main crash zone 2 is smaller in size than the safe zone. While the crash zone analysis does not yield any design criteria, it does firmly confirm that the test protocol should focus around pieces of padding located in main crash zone 1.

Table 2.9: Crash zone observations. $N = 61, \chi^2(4) = 105.62; p = 2.2 \cdot 10^{-16}$. $^*(Z > 1.96 \rightarrow p < 0.05)^{**}(Z > 2.58 \rightarrow p < 0.01)^{***}(Z > 3.29 \rightarrow p < 0.001)$, significance Z-scores is based on standardized residuals

	Crash zone				
Variable	**n**	**% Obs.**	**Exp. %**	**Z**	**Sig.**
Main crash zone 1 (red)	50	82,0%	25,0%	10,28	***
Main crash zone 2 (blue)	4	6,6%	25,0%	-3,33	***
(orange)	3	4,9%	25,0%	-3,62	***
Safe zone (green)	4	6,6%	25,0%	-3,33	***

2.2.6. Crash phase 5: Post-impact effects

The final crash phase revolves around post-impact effects. In this analysis, the only post-impact effect considered is post-impact movement of body parts after the initial crash. If the main body of the athlete is stopped by padding, its possible that limbs which do not impact padding immediately keep their momentum, creating a sort of whiplash-like movement. In this crash phase, this movement has been observed (Fig. 2.17). This crash phase is not directly linked to design criteria, as it reveals more about the biomechanics of a short track speed skater during a crash, but it provides context and a deeper understanding of crash dynamics as a whole and may provide useful insights for future iterations.

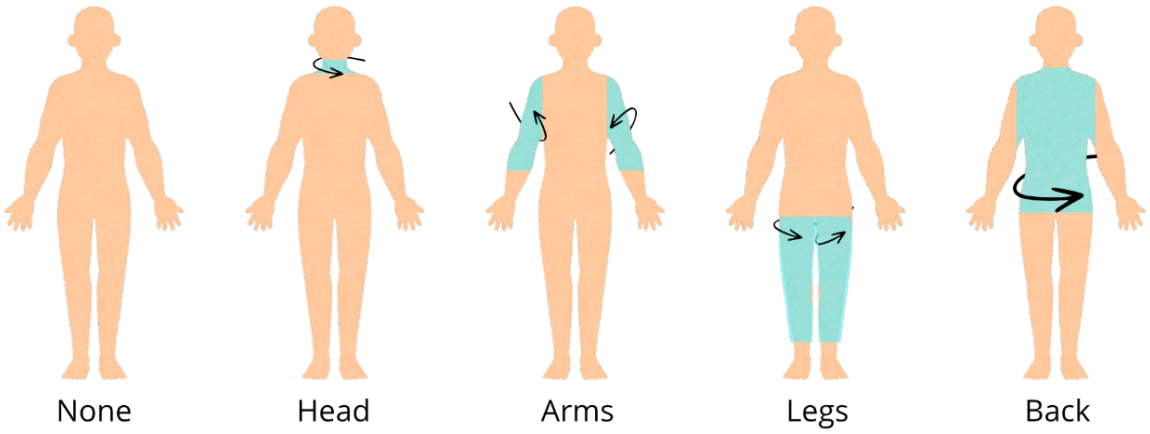

Figure 2.17: Visualization of observed post-impact movement of limbs.

Table 2.10: Post-impact movement observations. $N = 34, \chi^2(5) = 19.529; p = 0.002.^{*}(Z > 1.96 \rightarrow p < 0.05)^{**}(Z > 2.58 \rightarrow p < 0.01)^{***}(Z > 3.29 \rightarrow p < 0.001)$, significance Z-scores is based on standardized residuals

Post-impact movement					
Variable	**n**	**% Obs.**	**Exp. %**	**Z**	**Sig.**
None	12	35,3%	20,0%	2,23	*
Head	13	38,2%	20,0%	2,66	**
Arms	1	2,9%	20,0%	-2,49	*
Legs	7	20,6%	20,0%	0,09	
Back	1	2,9%	20,0%	-2,49	*

The distribution across the observed post-impact body movement differed significantly ($\chi^2(5) = 19.529, p = 0.002$) (Table 2.10). In 35.3% of observed crashes, no post-impact movement can be detected, which means that in 64.7% of crashes, post-impact movement of body parts takes place.
The majority of post-impact movements can be observed around the head and neck, with an occurrence of 38.2%. For biomechanical-focused iterations, post-impact head movement is worth testing, although it is not a core requirement for this design scope.

2.2.7. Patterns and correlations in crash behavior

To understand short track crash dynamics in a structured manner, a representative and frequently occurring crash scenario must be taken as a starting point. Based on the analysis of crash phase 4, a back-first impact is the most common impact type and therefore serves as the primary reference scenario for understanding relationships between variables. A Multiple Correspondence Analysis (MCA) was performed to uncover relationships between variables (Appendix D).

A back-first impact typically originates from a sitting orientation at the moment of initial ice contact, where the torso remains relatively upright and often experiences limited rotation before impact. This results in a direct transition from sliding to impact where the back makes first contact. Due to the simultaneous deceleration of a large portion of the torso, these impacts generally lead to more stable post-impact behavior. This is in contrast to legs-up bottom-first impacts where post-impact movement can be observed more frequently. This suggests and highlights that the contact area and pressure distribution is an important factor when trying to simulate real crashes.

This observation also highlights a key principle in crash dynamics: early-phase body orientation constrains the subsequent crash pathway. The initial contact with the ice determines how the body rotates, slides and impacts the padding for a given impact type. A sitting orientation leads more often to back-first impacts, while a lying on hips orientation more often leads to a hips-first of legs-up bottom-first impact type. Both crash pathways show signs of rotation being present before impact, as the body direction at initial ice contact and padding impact often differ. When looking at biomechanics at impact, these crash phases cannot be considered in isolation. While these are very relevant mechanics to explain crash dynamics, this project excludes biomechanics and has a focus on athlete - padding interaction. Therefore, these rotational dynamics do not play a role for the designing phase.

Additionally, a clear relationship exists between fall direction, sliding angle, and impact orientation. Crashes in which the fall direction is parallel to the padding most frequently result in impact angles between 35 and 55 degrees. In these cases, fall direction, sliding direction, and impact orientation are largely aligned, reducing the need for late-stage body rotation and resulting in more stable and predictable impacts. In contrast, straight impacts often require reorientation shortly before contact, introducing additional rotational dynamics and increasing the likelihood of residual motion after impact. While rotational dynamics are excluded from the scope of this project, this indicates that straight impacts are not necessarily the most representative condition, and that angled impacts within this range should be included in experimental setups.

Some crash conditions are observed to occur within a relatively narrow range across all crash pathways. Sliding velocities are predominantly above 40 km/h, impacts occur almost exclusively in the lower region of the padding, and crashes mainly occur in main crash zone 1. This indicates that realistic simulations should focus on a limited set of representative conditions rather than extreme cases. Additionally, while more impacts happen in single padding pieces, impacts between two padding pieces also occur regularly. However, for experimentation in this project, the main focus remains on single padding usage as it does have a higher occurrence.

From these relationships, several design criteria emerge. The dominance of back-first impacts establishes this as the primary and typical crash in short track speed skating and should be represented by the projectile. Furthermore, the importance of a representative contact area and pressure distribution for a realistic athlete - padding interaction implies that geometry and mass distribution of the design must be similar to a back-first impact type to allow for a realistic athlete padding simulation. Finally, the consistent location of impacts defines boundary conditions for the test setup as impacts in the lower region of a single piece of padding with a velocity preferably above 40 km/h. Test protocols should also include tests with straight impacts to compare data to current standardized tests as well as impacts with angles between 35 and 55 degrees.

2.3. Injury mechanics related to padding impacts

The main functionality of short track padding is to prevent injuries, or at least limit the seriousness of injuries as much as possible. While injury mechanics are prominently biomechanical in nature, and thus not in scope of this project, analyzing injuries in short track speed skating may highlight dangerous crash types which should be prioritized. This chapter aims to answer SQ3 to find the most dangerous and serious type of crash. First, general injury mechanics relevant for collisions with short track padding will be explained. Then, based on these injury mechanics, dangerous crash types can be identified. Finally, the most dangerous crash type will be shared and explained.

2.3.1. General injury mechanics

Short track speed skating is a high speed and physically demanding sport, which inherently carries a risk of injury. Although each sport places different demands on the human body, the fundamental mechanical principles underlying injury occurrence are similar across sports. In general, injuries can be divided into two categories: acute injuries and repetitive strain injuries (Sports Injuries, 2025). In the context of padding impacts, acute injuries are the primary concern. Palmer-Green et al. (2014) found that 25% of short track injuries are caused by contact with a static object, and that this injury cause, in combination with overuse injuries, can result in the most severe injuries.

For an acute injury to occur, the load experienced by a body part must exceed its mechanical tolerance. During a collision with padding, the skaters kinetic energy must be dissipated over a short distance and time. Ideally, the padding absorbs most of this energy. However, the skaters body inevitably absorbs part of the load as well. If the padding absorbs insufficient energy or does so too abruptly, the remaining energy is transferred to the skaters body, resulting in high internal loads. When these loads exceed tissue limits, injury occurs (Chen et al., 2009). The severity of the injury is determined by both the magnitude and the rate of load application: small excess loads may result in bruising, while large excess loads can cause fractures or severe trauma.

Two primary mechanical loading modes play a role in injury during padding impacts: linear acceleration and rotational acceleration. Linear acceleration occurs when forces act directly on a body part, causing rapid deceleration of the body. Rotational acceleration involves angular motion, such as twisting or bending of body segments. While safety features in short track are often less effective in mitigating injuries caused by rotational acceleration (Karton et al., 2013) (Meaney et al., 2011), this mainly concerns biomechanics and are out of scope for this project. The main injury mechanic investigated in this project will therefore be excessive linear deceleration during padding impact.

2.3.2. Collision related injuries

Based on discussions and interviews with short track coaches and athletes, excessive linear deceleration can cause a variety of injuries. Minor injuries such as muscle stiffness or contusions are a more regular occurrence, whereas more extreme crashes may result in fractures or severe brain trauma. Beyond this expert input, a lack of scientific studies specifically quantifying injuries caused by padding collisions makes it difficult to identify recurring injury patterns. While several studies address injuries in the sport more generally, expert input indicates that many of these findings are no longer fully representative of the current situation. Short track is a relatively young sport, and safety regulations have evolved rapidly. When recurring injury patterns are identified, governing bodies such as the ISU often respond with rule changes or equipment requirements, which alters injury distributions over time. As a result, older injury statistics may not reflect present day risks.

Despite this limitation, meaningful qualitative insights can still be derived. Interviews with coaches indicate that minor injuries occur very frequently following high speed crashes. This includes muscle stiffness and contusions. In extreme crashes, fractures can occur, with spinal fractures often named as one of the more serious injuries. In short track speed skating, concussions have also been relatively common injuries with a possible major impact on athletes (Hillis, 2018).

However, the underlying injury mechanic is not linear acceleration, but motion relative to the skull due to rotational acceleration (Romeu-Mejia et al., 2019), which falls outside the scope of the project. Therefore, supported by expert input, spinal fractures are considered one of the most dangerous injuries short track speed skaters can sustain after a high-speed collision with padding.

Talking to coaches and padding manufacturers, it is indicated that head-first crashes have the highest likelihood of spinal fractures or other serious injuries, and thus are considered the most dangerous crash type. Luckily, this crash type is rare, supported by the previous chapter where 0 head-first crashes have been observed. This does however not mean that head-first crashes never happen, shown by the crash of Daan Breeuwsma in 2017 (Van der Linden, 2017). For the design, a head-first injury will not be the main crash type that needs to be simulated. While it is potentially very dangerous, and possibly the most dangerous crash type, its rarity does mean that it tests for a very unlikely scenario. This crash type should absolutely be included in future iterations if multiple crash types can be simulated with a single design.

2.4. Scaling strategy

An important criteria for the design is keep the design compatible with the current ICE-G1 launching mechanism. This does limit the scale of the design, as it is impossible to use a full-scale design with the ICE-G1 infrastructure. This chapter aims to answer SQ4, as the design needs to represent the athlete padding interaction accurately while scaled. First, dimensions of the average male short track speed skater will be shared. Then, a scaling strategy will be described. Finally, a scaling factor which can be used to scale linear measurements will be shared.

2.4.1. Dimensions and mass of average short track speed skater

Before investigating how to scale a short track speed skater to ensure a similar athlete–padding interaction, it is important to know the dimensions of a short track speed skater. In this project, dimensions of an average male short track speed skater are used. This skater is chosen as the ICE-G1 also is designed to simulate an average male short track speed skater, and more clear data is available.

To define a representative skater profile, anthropometric data must first be established. Although limited literature exists specifically on short track speed skaters, Matyk & Raschka (2012) studied elite short-distance roller speed skaters, a discipline comparable to short track speed skating. They report an average height of 177.3 cm and an average body mass of 73.2 kg for male athletes. These values are adopted in this project as representative for an average male short track speed skater.

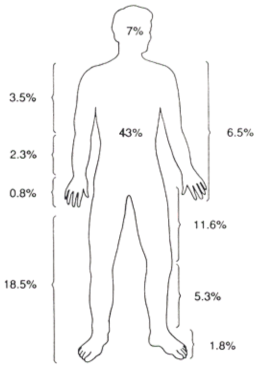

Figure 2.18: Average mass distribution percentages across body segments of average humans(Maastricht UMC, n.d.)

Figure 2.19: : 3D model of an average short track speed skater

Body composition of short track speed skaters differs from that of the general population. Athletes in this discipline typically exhibit lower body fat percentages and greater muscle mass, particularly around the legs. This results in a relatively lean torso and more pronounced muscles in the legs (Sovak & Hawes, 1987). Traditional anthropometric datasets, such as those summarized by Maastricht UMC (n.d.) and refined by De Leva (1996), provide average mass distribution percentages across body segments (Fig. 2.18). While more recent refinements exist, these distributions remain broadly comparable. To approximate the morphology of a short track speed skater, the relative mass distribution is adjusted by increasing the proportional mass of the legs and decreasing the proportional mass of the torso compared to general population averages (Fig. 2.19. This modification reflects the sport-specific muscular development pattern. It should be noted that this adjustment is an approximation intended to better represent segmental loading during impact.

Using the CEASAR (NL) database within DINED, a height of 177.3 cm is entered to determine corresponding normal distribution percentile to find anthropometric dimensions for other body segments (Dined, n.d.) (Figure 27). Based on this dataset, and incorporating the adjusted mass distribution, a three-dimensional model of an average male short track speed skater is constructed (Fig. 2.20). This model forms the geometric basis for further scaling.

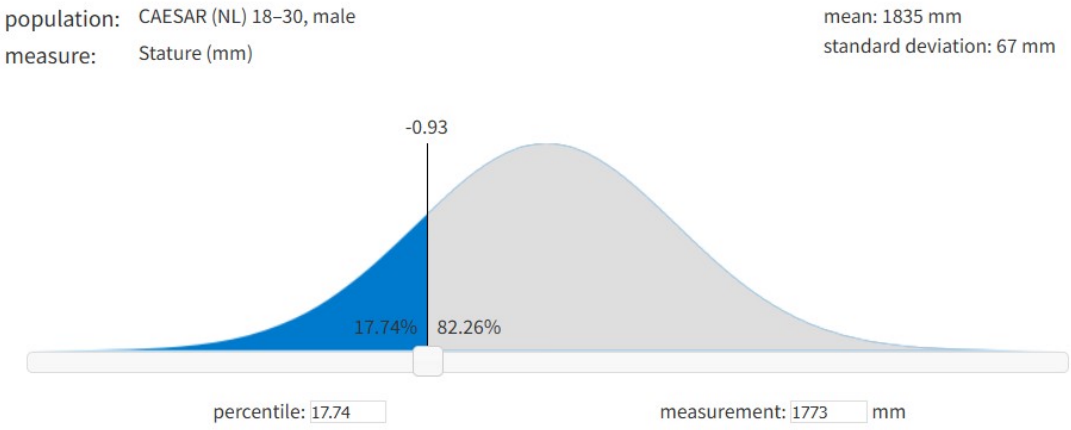

Figure 2.20: Normal distribution showing the percentile of average male short track speed skaters based on their average height.

2.4.2. Scaling down short track speed skater dimensions

After defining the full-scale anthropometric model, the next step is to determine how to scale the dimensions and mass distribution to ensure compatibility with the ICE-G1 launching system while preserving relevant crash dynamics. As established earlier in chapter 3.1, foam padding exhibits strain-rate dependency. Changing impact velocity would therefore alter foam behavior and compromise comparability. For this reason, velocity is treated as a fixed parameter.

The objective of scaling is to approximate similar acceleration behavior during impact between the scaled design and a real short track speed skater. Newtons second law states that acceleration is given by:

$$a = \frac{F}{m} \tag{2.4}$$

where a is acceleration (m/s^2), F is force (N), and m is mass (kg). During impact with padding, the kinetic energy of the skater is dissipated through deformation of the foam. The work performed by the padding can be expressed as:

$$W = F \cdot d \tag{2.5}$$

where d is the stopping distance within the padding (m). Assuming that the padding absorbs the initial kinetic energy of the skater, conservation of energy gives:

$$\frac{1}{2}mv^2 = F \cdot d \tag{2.6}$$

where v is impact velocity (m/s). Substituting this into Newtons second law yields:

$$a = \frac{\frac{1}{2}mv^2/d}{m} \Rightarrow a = \frac{1}{2}\left(\frac{v^2}{d}\right) \tag{2.7}$$

This expression shows that acceleration during impact depends on velocity and stopping distance, but not directly on mass. Since velocity is kept constant, achieving similar acceleration requires maintaining a similar stopping distance in the padding.

Stopping distance in viscoelastic foam is governed by stressstrain behavior. The stress applied to the foam is related to the kinetic energy distributed over the contact area. A useful first-order approximation is to consider the kinetic energy per unit area:

$$E_{area} = \frac{\frac{1}{2}mv^2}{A} \tag{2.8}$$

where A is the effective contact area (m^2). For identical padding material, identical velocity, and comparable pressure distribution, similar energy per unit area will result in comparable stress levels in the foam. This corresponds to similar deformation depth and thus similar stopping distance, provided densification is not prematurely reached.

Under these controlled assumptions, maintaining a constant ratio between mass and contact area (m/A) between the real skater and the scaled design approximates similar stress levels and therefore similar stopping distances, as velocity (v) must be equal for both. It must be emphasized that this is a first-order approximation valid under the following conditions:

- Identical padding material and construction.
- Identical impact velocity.
- Comparable pressure distribution.
- Densification of foam is not prematurely reached.

Given these assumptions, geometric scaling can be derived. For the representative skater, the mass is 73.2 kg and the back contact area, calculated from the DINED-based model, is 0.189 m^2. The primary constraint for the scaled design is that the total mass should approximate 30 kg, as this is the mass the launching system is designed to accelerate. For the scaled design with a target mass of 30 kg, maintaining the same m/A ratio yields a required contact area of 0.0775 m^2.

Because contact area scales with the square of linear dimensions, the scaling factor (λ) for all linear measurements must equal the square root of the area ratio:

$$\lambda = \sqrt{\frac{A_{scaled}}{A_{real}}} \approx 0.64 \tag{2.9}$$

By multiplying all relevant linear dimensions of the anthropometric model by 0.64, a geometrically similar scaled representation is obtained. This approach preserves the ratio between mass and contact area.

Comparing the m/A ratio of an average skater to the ISU drop test and the ICE-G1 test reveals significant flaws, as their ratios are almost three times as high. This means these tests apply much more pressure to the padding than a real skater would, resulting in a greater stopping distance and lower measured g-forces. It is therefore expected that a design scaled with the correct m/A ratio yields higher g-forces than the current tests available, suggesting that standardized ISU drop test results may not effectively represent the forces experienced by athletes.

3

Refined design assignment

Using insights gained from the theoretical framework, the initial design assignment can be detailed, providing a clear scope for the design phase. In this chapter, this refined design assignment in shared. First, a short summary of the most important insights of the theoretical framework will be shared. Then, a clear scope will be created, where will be explained what insights will be used as criteria, and what parts of crash dynamics will be outside the scope of this project. Finally, a more detailed design assignment will be shared including the most important criteria.

3.1. Synthesis of theoretical findings

The theoretical framework provides insight into how short track speed skaters interact with padding during a crash and which parameters influence this interaction. From the analysis of padding behavior, it was learned that foam deformation is governed by a combination of mass, velocity, and contact area and geometry. Foam exhibits strain-rate dependency, meaning that impact velocity must remain equal between real and simulated scenarios. Additionally, the contact area and contact geometry strongly influence the stress applied to the foam. Since foam deformation determines stopping distance and peak acceleration, maintaining similar stress conditions is essential. This leads to the requirement that the ratio between mass and contact area (m/A) should remain similar to that of a real short track speed skater.

The crash analysis shows that crashes in short track speed skating are complex and can be divided in five crash phases, including falling, sliding, impact, and post-impact motion. However, only the fourth crash phase directly determines how the padding responds as it directly revolves around short track speed skater padding interaction. Within this phase, a pattern emerges. Back-first impacts occur most frequently and represent the most typical crash scenario. These impacts involve a relatively large contact area and a distributed mass, resulting in a specific pressure distribution on the padding. Additionally, most short track crashes share similar parameters, with velocities above 40 km/h, impacts in the low region of padding and frequently at an angle between 35 and 55°. While crashes can occur in both single padding pieces or between two padding pieces, crashes in single padding pieces occur more frequently. Other aspects of crash dynamics are rotational acceleration and motion, and post-impact limb movement, which describe more about the biomechanical aspect of crashes.

Injury analysis indicates that both excessive linear and rotational acceleration are key factor in injury occurrences. Both deceleration possibilities can result in different injuries. Excessive linear deceleration tells more about mechanical interaction between the skater and padding. In contrast, rotational deceleration influences biomechanical aspects more during impact. Head-first crashes are indicated to be one of the most dangerous impact types, but its rarity does not make it a priority over common crashes as back-first impacts.

The scaling analysis demonstrates that maintaining a similar m/A ratio between the design and a real skater is essential to approximate realistic foam deformation. Current testing methods, such as the ISU drop test and the ICE-G1 projectile, do not satisfy this condition. Their relatively small contact area results in significantly higher stress levels on the padding, which likely leads to unrealistic deformation behavior and lower measured acceleration values compared to real crashes. This reveals a key limitation of the ICE-G1 projectile: it represents impact using a small, rigid, circular contact surface, which does not reflect the distributed geometry of a human body. As a result, the interaction between projectile and padding is not representative of the interaction between a short track speed skater and padding.

3.2. Definition of project scope

As mentioned previously, short track crashes involve both mechanical interaction and biomechanical responses. Mechanical interaction refers to the contact between the body and padding, the resulting force distribution and the deformation of foam. Biomechanical responses refers to deformation of the human body, joint motion and articulation and internal

injury mechanisms. While both aspects are important in crash dynamics, they cannot be addressed simultaneously in this project. As the mechanical interaction forms the basis for a good simulation of short track crashes, this is the primary factor considered for this project. After all, biomechanical responses cannot be measured accurately if the mechanical interaction between the projectile and padding does not resemble realistic scenarios.

As mechanical interaction is the primary concern of this project, the design should focus on the fourth crash phase, specifically the initial impact between short track speed skater and padding with a back-first impact type. Therefore, the design should encompass the contact geometry of a back-first crash to ensure a similar pressure distribution. In addition, the mass distribution should resemble a back-first crash in the design. Another aspect in the scope of the project is the m/A ratio similarity. Crash aspects true for most crashes are also included, which are launch velocity similarity because of strain-rate dependency of foam, crashes with impact angles around 45 degrees and lower region impact in single padding pieces, with the possibility of testing between two padding pieces. Finally, compatibility with the ICE-G1 launching mechanism plays an important role in the project in fits within the scope.

Biomechanical responses are outside the scope of this project. This includes rotational dynamics during sliding or impact with padding. Articulated body motion and post-impact limb movement also describe biomechanics and are therefore excluded. Internal injury mechanics are also outside the scope of this project, so this project will not include detailed reports about possible injuries after tests. Finally, additional crash types, such as head first crashes, will not be part of the initial design. These aspects are acknowledged as part of real crash dynamics but are excluded to maintain a focused and feasible design objective.

3.3. Refined design assignment

Current testing methods for short track speed skating padding, such as the ISU drop test and the ICE-G1 system, do not adequately represent the interaction between a short track speed skater and padding during a crash. The use of a small, flat impact surface leads to unrealistic pressure distributions and deformation behavior of foam, limiting the extent to which test results reflect real crash conditions.

The objective of this project is to develop a projectile that more accurately represents the mechanical interaction between a short track speed skater and padding during impact, while remaining compatible with the existing ICE-G1 launching system. The focus is on the initial impact phase of a back-first collision, as this is the most common and representative crash scenario in short track speed skating. The design assignment is therefore defined as follows: Design a projectile that captures the geometry and mass distribution of a short track speed skater during a back-first impact type, such that the resulting interaction with padding produces a more realistic pressure distribution and deformation response compared to the current ICE-G1 projectile.

To achieve this, the design must meet the following main criteria:

- Realistic contact geometry of the torso similar to a back-first impact type
- Representative mass distribution of a short track speed skater
- Preservation of a realistic mass-to-contact-area (m/A) ratio
- Compatibility with the ICE-G1 launching mechanism
- Repeatable measurements within 10% variance

The expected outcome of this project is a functional prototype that demonstrates an improved representation of the interaction between a short track speed skater and padding. This should result in measurement data that more closely reflects real crash conditions, enabling a more meaningful evaluation of padding performance. The full list of criteria can be found in Appendix B.

4

Design process

The next step is to design a new projectile within the project boundaries. This chapter describes the design process of the project. First, the design methodology will be explained, followed by an initial exploration of the solution space. After that, the ideation process will be shared, including form geometry exploration and ensuring compatibility with the ICE-G1 launching mechanism. Finally, three concepts will be shared, and the choice for the final concept will be explained.

4.1. Design methodology

The design phase consists of a divergent and a convergent phase, each with a distinct goal and approach. The divergent phase aims to broaden the perspective on the problem and to explore as many relevant solution directions as possible, as mentioned in Chapter 2, without prematurely limiting the outcome. In contrast, the convergent phase focuses on evaluating, refining, and narrowing down these possibilities until a single concept remains that best fits the design assignment.

During the divergent phase, multiple ideation techniques are employed, each serving a specific purpose within the process. Mind mapping is used to explore the breadth of the problem space and to ensure that no relevant aspects are overlooked. Form-related exploration is conducted using techniques such as brain sketching, and abstraction exercises, allowing rapid generation and comparison of back-first form geometries. To address the ICE-G1 infrastructure compatibility, the how-to method is applied, breaking the main challenge down into smaller, more manageable questions. The answers to these questions are structured in a morphological chart, which makes it possible to systematically combine partial solutions into complete ideas. The divergent phase ends once the solution space is sufficiently broad and all major directions have been explored.

The convergent phase then builds on this broad exploration by introducing structured decision-making. Ideas are evaluated and refined based on the core pillars of industrial design, which are viability, feasibility, and desirability, while progressively increasing the level of detail and strictness in evaluation. Harris profiles are used at multiple moments in the process to ensure that decisions are traceable and grounded in the requirements and wishes (Appendix B) derived from the theoretical framework. The chapter concludes with the final design choice.

4.2. Ideation process

The ideation phase begins with an exploration of the solution space using a mind map where the term "ICE-G1 projectile" is central. This exploration revealed five interesting directions to consider for the design process (Fig. 4.1). ICE-G1 compatibility and form and shape are most important directions to consider for the ideation phase. Visual look can help with decisions when detailing future concepts. Experimental validation helps with the definition of tests and the construction direction will provide insights when creating a prototype.

As the form and geometry of the design plays the most important role in simulating athlete padding interaction, this is chosen as the starting point. As the back-first impact type will be the simulated impact type by the design, the form geometry of the human back is explored by using a Dined model. Key anatomical characteristics of the back that could influence pressure distribution have been identified (Fig. 4.2). This includes the mass distribution of a short track speed skater for each body part, key characteristics of the general shape of the back and what body parts impact padding during a back-first impact. This detailed ideation revealed that a back-first impact includes the head, torso, slight part of the arms and a part of the hips of a short track speed skater. These characteristics have then been translated into the form geometry, measurements and mass distribution which should be used for the eventual design (Fig. 4.3.)

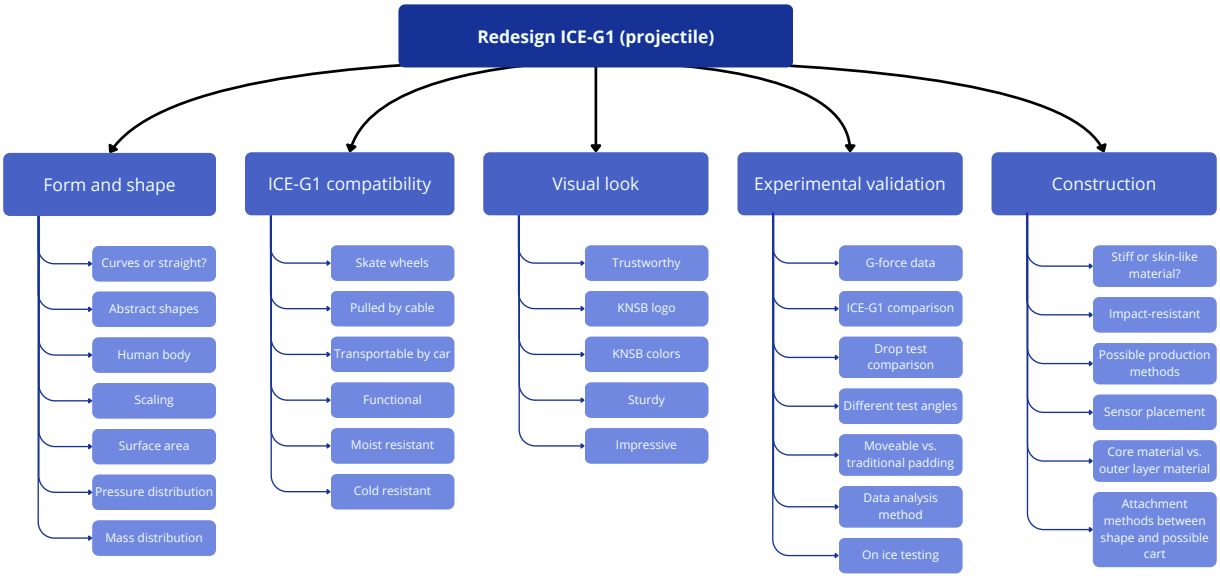

Figure 4.1: Summary of explored directions considered to be influential in decision making processes later in the design process

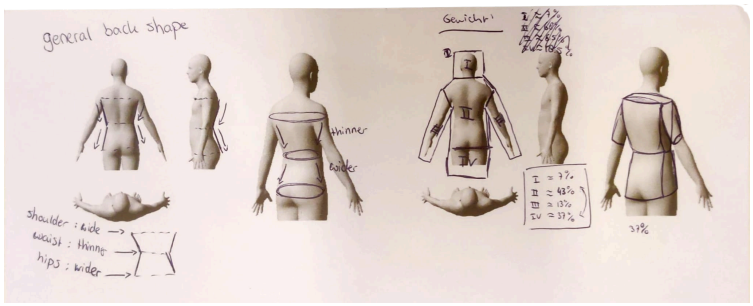

Figure 4.2: Exploration of key anatomical characteristics of a back-first impact type regarding mass distribution and general shapes and forms.

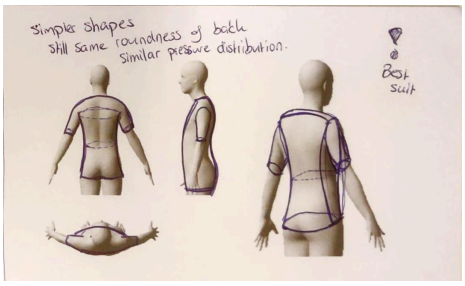

Figure 4.3: Insights combined into a form geometry estimated to provide accurate pressure distribution while remaining producible.

The next step in the ideation process is to make this form geometry compatible with the ICE-G1 launching mechanism. The main difference between the ICE-G1 projectile and a new design is the component that impacts the padding, which essentially means that a way must be found to attach this new and bigger form geometry on the existing cart basis. For this ideation, the how-to method has been applied to find solutions to smaller problems like attachment strategies and how to add mass to something. These smaller solutions have been placed in a morphological chart. By choosing different combinations of solutions for a singular problem, 36 ideas have been created, marking the end of the ideation process. From this ideation process, the most important aspect is found to be the connection between the form geometry and the ICE-G1 launching mechanism, and how to attach a realistic form to the cart basis for ICE-G1 compatibility.

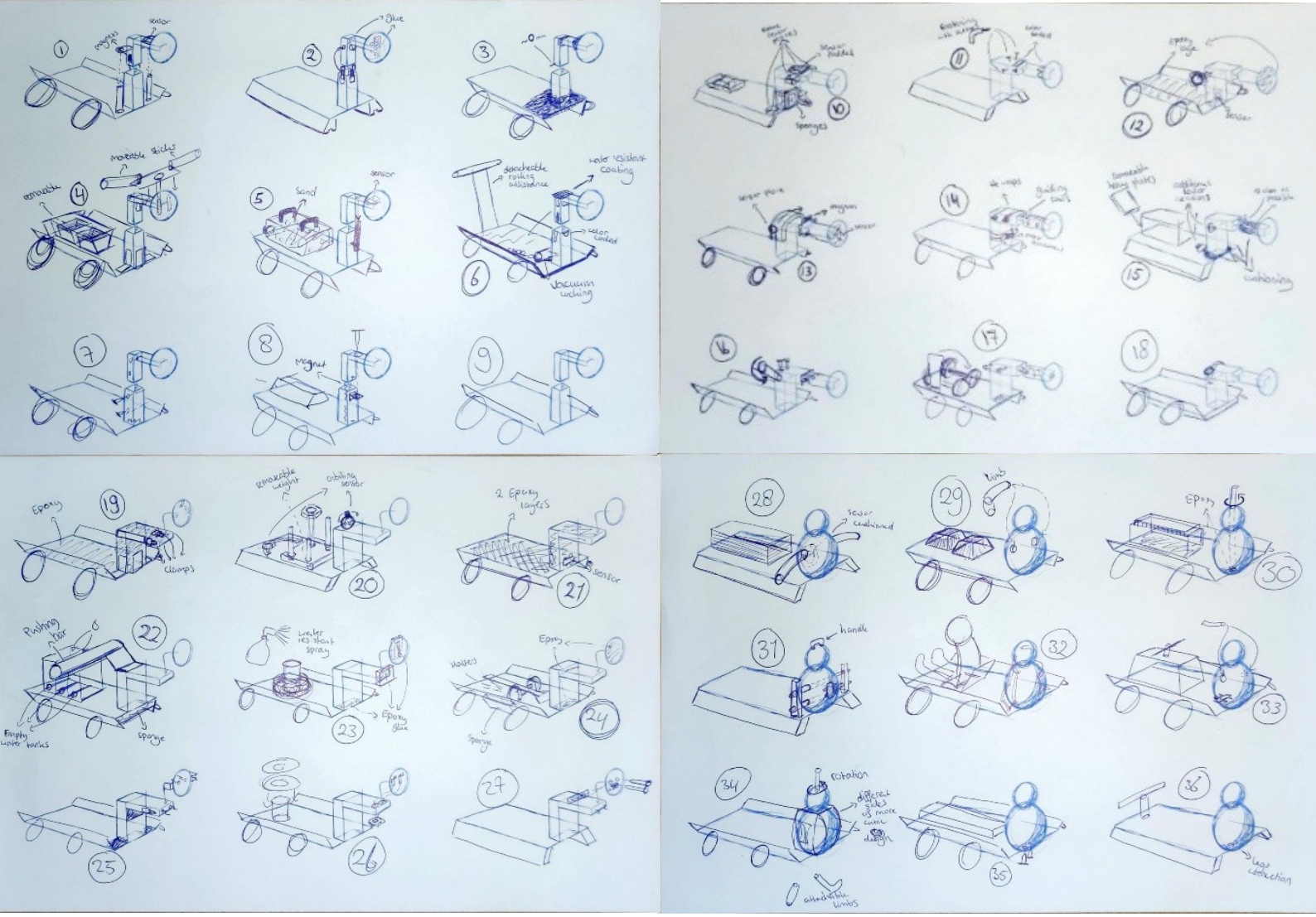

4.3. Conceptualization process

The next step in the design process is to detail the generated ideas into concepts. This conceptualization includes three major decision points. First, the 36 initial ideas will be cut into nine ideas. These ideas will be changed in more detailed concepts, after which another cut will be made to have three remaining concepts. These concepts will be finalized in poster format, after which the final concept will be chosen.

Each of the 36 ideas is evaluated and is given estimated scores on viability, feasibility, and desirability, based on how the form geometry and ICE-G1 compatibility are integrated. Viability includes the designs potential, feasibility includes the estimated method to combine the form geometry to a cart basis for ICE-G1 compatibility, and desirability includes the alignment with the project objective. Based on the received scores, nine ideas with the highest overall potential are selected for further development. The selected ideas are then developed into concepts by incorporating all not addressed categories of the morphological chart. A Harris profile of the most important criteria is then used to choose the three best concepts. Details can be found in Appendix E.

The first concept consists of a scaled dummy mounted on a cart base similar to the ICE-G1 system (Fig. 4.4). The design focuses on representing realistic mass distribution across the head, torso, and legs, while also providing a contact geometry that closely resembles a back-first human impact. The dummy is attached to the cart using four bolts located on the underside, which also form the primary interface for transport and installation. This makes the system relatively straightforward to mount and remove, but also introduces a potential weak point, as high impact loads are transferred through this connection. Perception feedback from other students is used to find that the concept aligns with the explored visual look (Fig. 4.1). In terms of use, the design allows direct measurement at specific body regions depending on sensor placement, supporting interpretation of localized impact behavior. However, due to the forward mass distribution, there is a risk of forward tilting during impact. In addition, the segmented structure introduces potential failure points, particularly at connections such as the neck, where parts could detach under high loading.

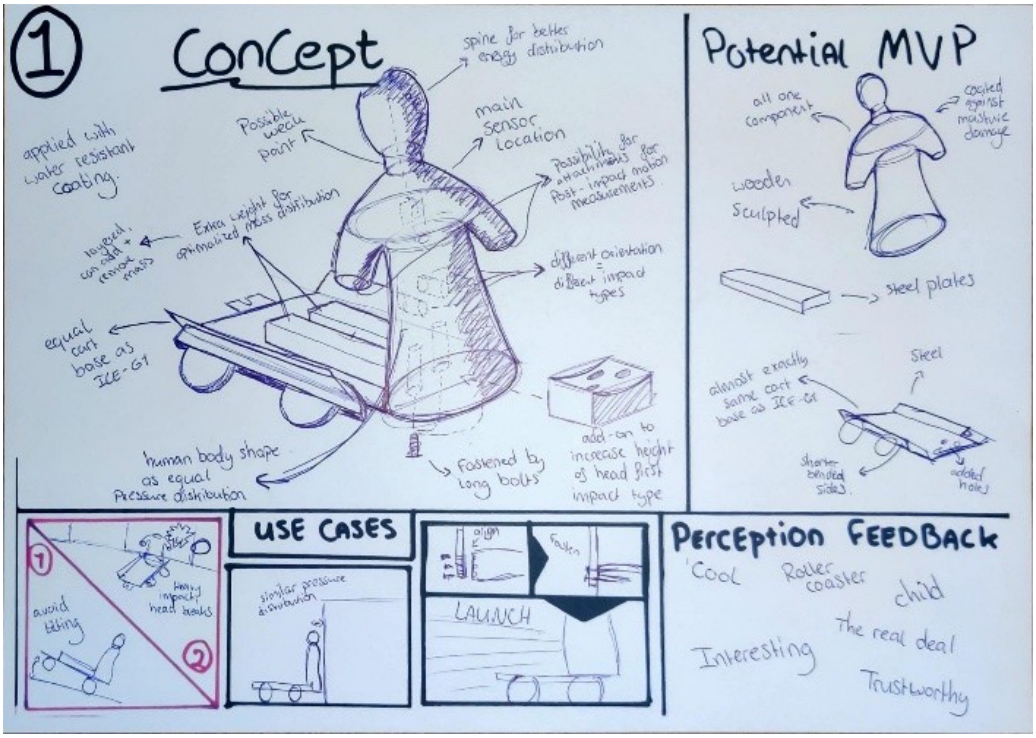

Figure 4.4: Concept 1: a dummy-like impact geometry attached to the ICE-G1 projectile's cart base.

The second concept consists of a square structure mounted on the front of the cart base, with each side representing a different impact geometry (Fig. 4.5). The square can be rotated to select the desired configuration, allowing multiple impact types to be tested within a single design. Rotation is achieved by manually repositioning the square and securing it using bolts located on the sides of the lower structure. This provides flexibility in use, as different crash scenarios can be simulated without changing the full setup. The perceived look does not totally align with the explored visual look (Fig. 4.1) The design also allows adjustments in mass distribution through additional weights on the cart. However, the off-center mass distribution can lead to forward tilting during impact. Another potential weak point is the central rod that supports and connects the square structure, which may be subjected to high bending loads and could fail under repeated impacts.

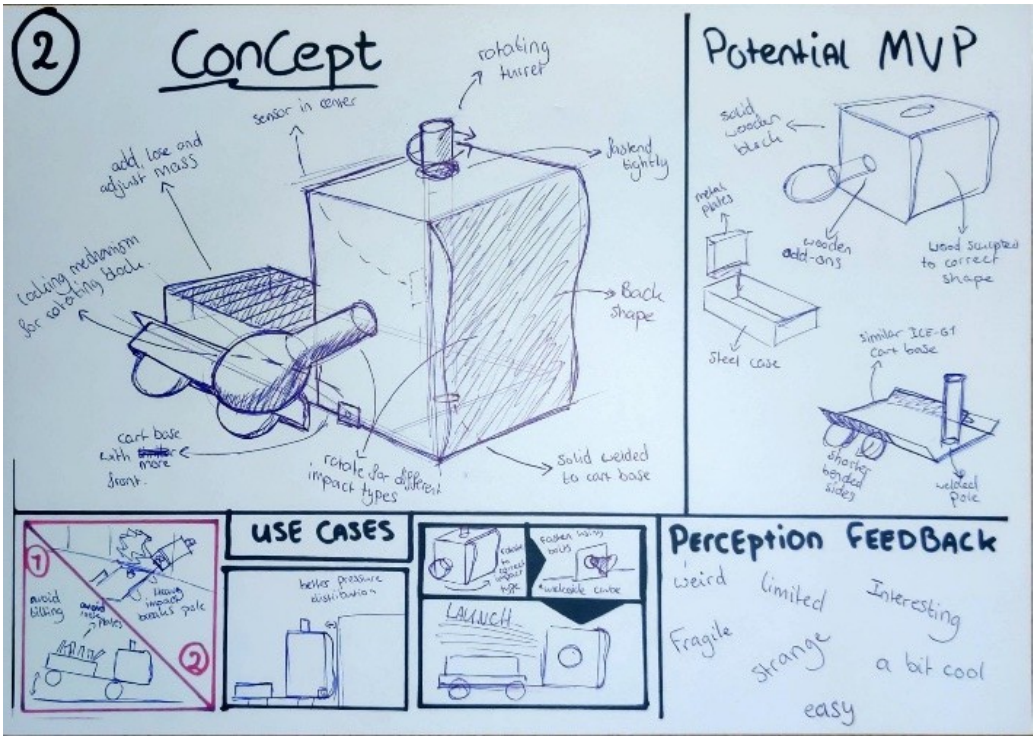

Figure 4.5: Concept 2: A square material attached to the ICE-G1 cart base. The main focus is on future application of multiple different impact type simulations, with the back first impact type as primary objective.

The third concept uses an interchangeable ram plate that can be mounted onto the cart base (Fig. 4.6). The plate is positioned using a bayonet connection, after which it is twisted into place. Magnets provide initial alignment and retention, and additional clasps are used to secure the plate during testing. This setup allows for quick swapping of different geometries, making it suitable for testing multiple configurations efficiently. Proper alignment during installation is essential to ensure consistent and reliable measurements. This concept aligns more with the explored visual look (Fig. 4.1) than the second concept, but aligns less with the wanted perception than concept 1. The main potential weak point of this design lies in the bayonet connection, which must withstand high impact forces. If not properly secured, there is a risk that the plate could loosen or detach during impact, making the locking and clamping mechanism a critical aspect of the design.

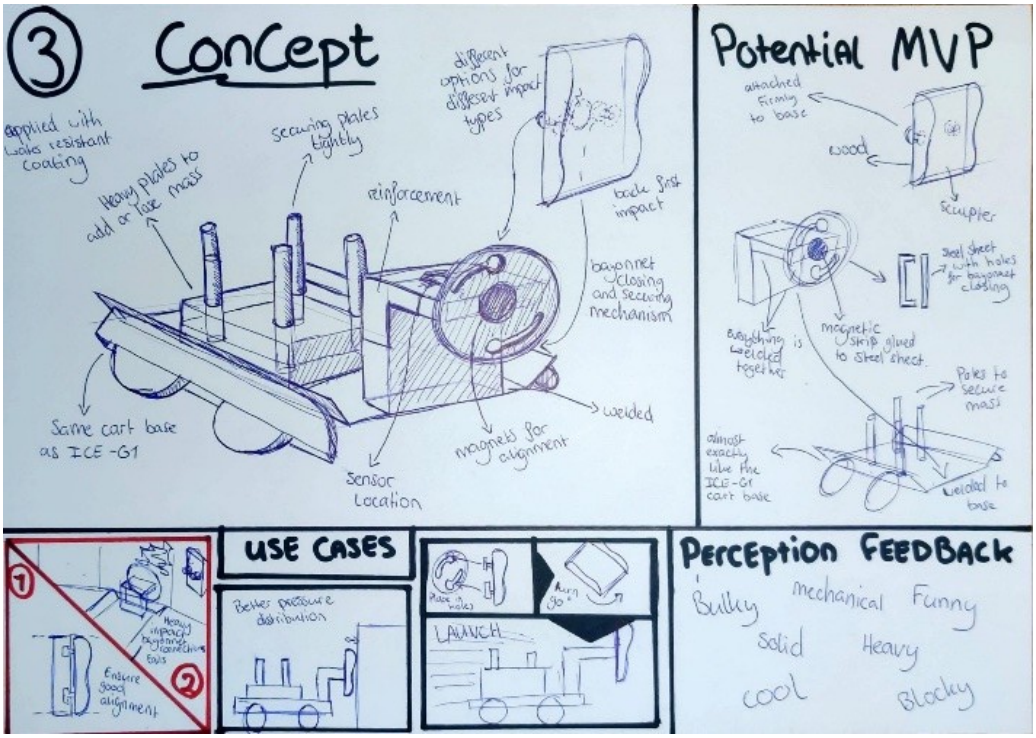

Figure 4.6: Concept 3: A more mechanical variant of the ICE-G1 projectile. The correct form geometry can be applied to the cart base with a bayonet mechanism.

To choose the final concept, the list of requirements has been used (Table 4.1). Based on a selection of the most important elements of this list regarding athlete – padding interaction and usability, which are findings from the theoretical framework and important requirements found by Beets et al. (2024), a Harris Profile has been created. This concluded that the first concept is the best concept, as it actually looks like a human and provides the estimated most accurate pressure distribution of all concepts. In addition, it is expected that data measurements are easier to interpret, as the human form allows users to immediately what body part experiences what forces, based on the sensor location.

Table 4.1: Harris profile for final concepts. Concept 1 is chosen as the best concept.

Requirement	Concept 1				Concept 2				Concept 3			
	–	-	+	++	–	-	+	++	–	-	+	++
The design must be able to simulate a back-first impact			■	■			■	■			■	■
The design must provide a better pressure distribution compared to the ICE-G1			■	■			■				■	
The design must apply more realistic stress to the padding compared to the ICE-G1			■	■			■	■			■	■
The design must result in more realistic foam deformation behavior than the ICE-G1			■			■	■				■	■
The design must result in a more realistic stopping distance compared to the ICE-G1			■	■			■	■			■	■
The design must be fully compatible with the existing ICE-G1 rail system			■	■		■	■			■	■	■
The design must be able to handle small imperfections when crossing rail sections	■					■				■	■	
The design must be able to withstand velocities up to 35 km/h			■	■		■				■	■	
The design must have a mass distribution similar to a short track skater			■	■		■	■		■	■		
The sensor must be located at a representative location on the design			■	■			■	■		■	■	
Measurements of the design must indicate interpretable safety risk			■	■			■			■	■	
The design must not have open sharp, hot or otherwise dangerous parts			■	■			■	■			■	■
The design must be resettable by two operators without lifting loads exceeding ergonomic limits	■	■			■	■				■	■	
The design must be able to be moved to the ice rink by two people		■				■					■	

5

Final concept

After considering multiple design choices, a final design has been chosen. In this chapter, the final design will be explained. First, a general overview of the final design will be shared. Then, a more detailed description of the design will be explained. Finally, a prototype of the final design will be shared and explained.

5.1. Concept overview

The final concept consists of a simplified anthropomorphic rigid crash dummy, called Harrie, mounted on a cart that is geometrically and mechanically identical to the cart used for the ICE-G1 projectile (Figure 5.1). Harrie is designed to simulate skater–padding interaction of a back-first impact type more realistically by introducing anatomically representative geometry of the body and mass distribution using the defined scaling factor, while remaining compatible with the existing ICE-G1 launching infrastructure.

Harrie directly addresses the project objective: to improve the athlete–padding interaction realism in impact testing of short track padding for the back-first impact type without requiring a complete redesign of the ICE-G1 system as a whole. By redesigning the projectile in this way, the system remains practical, comparable to previous measurements, and implementable within current operational constraints.

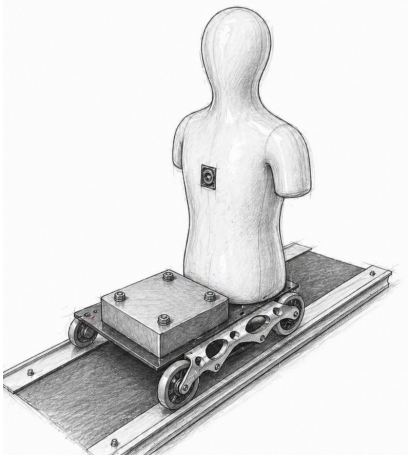

Figure 5.1: AI upscaled drawing of the scaled anthropomorphic rigid crash dummy Harrie, mounted on a cart almost identical to the cart used for the ICE-G1 projectile.

Harrie is a scaled representation of the torso of a short track speed skater, following the scaling principles as defined in Chapter 2. The geometry preserves the relationship between contact area and mass to ensure that acceleration levels during impact remain representative. In contrast to typical crash dummies, Harrie has no internal electronics and moveable parts. As the priority of this project revolves around the back-first impact type, Harrie consists of a solid torso and head structure with added mass attached on the cart close to the torso. This added mass is placed to achieve the correct mass distribution for a realistic impact simulation.

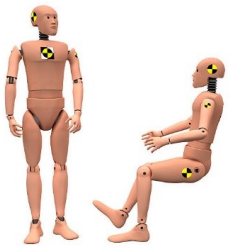

Figure 5.2: Typical crash dummies with electronics, sensors and moveable parts.

In essence, Harrie shifts the projectile from a flat, circular ram towards a distributed-mass body representation, thereby enabling more realistic interaction between the impacting object and foam padding. This transition ensures that the energy dissipation during impact is governed by the actual contact geometry of a skater, rather than the artificial surface of a standard test ram.

5.2. Harrie's design

Harrie forms the central element of the final concept, as it directly interacts with the padding and therefore determines the mechanical response of the foam during impact. Harrie deliberately focuses on one dominant factor: pressure distribution resulting from contact geometry and mass distribution. As established in Chapter 2, foam deformation behavior is primarily governed by local stress rather than total force alone. Local stress is determined by the ratio between mass and contact area and by how mass is distributed relative to the contact surface. Therefore, the design objective of Harrie was to reproduce the contact geometry and mass distribution of a back-first impact type in a scaled and controlled manner. Harrie is a scaled representation of a short track skaters torso and head, following the scaling factor and proportional mass distribution defined in Chapter 2 (Fig. 5.3). By preserving the relationship between mass and contact area (m/A), Harrie ensures that acceleration levels during impact remain representative under the constraints of the ICE-G1 system. This scaling strategy ensures that the foam experiences comparable stress levels to those generated by a real athlete, despite the reduced system size.

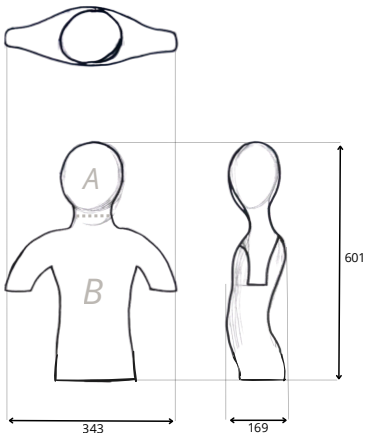

Figure 5.3: Detailed measurements and functional segments of the Harrie dummy, showing the division between the head (A) and torso (B). Measurements are in mm. A top view, front view, and side view are shown.

The body is divided into two functional segments: the head (A) and torso (B). The mass distribution follows the proportions defined earlier, resulting in approximately 2.1 kg for the head and 13.8 kg for the torso. This means that the lower body should have a mass of approximately 14.1 kg, which are represented by the cart structure and its added mass components. This ensures that the global mass distribution of the system mimics that of a human body without requiring fully articulated limbs. This distribution is achieved through a combination of structural mass and compact high-density steel elements, allowing precise control of the overall mass distribution without increasing geometric complexity (Fig. 5.3).

The internal structure consists of a solid load-bearing core manufactured from aluminum (AA6061-T6), selected for its high strength-to-weight ratio and stable mechanical behavior under dynamic loading (Callister & Rethwisch, 2018). The core incorporates spine-like reinforcement features that increase structural stiffness and distribute impact forces throughout the body, reducing local stress concentrations and preventing structural failure (Ashby, 2011). In addition, this rigid internal structure minimizes internal deformation, thereby preventing artificial vibration from influencing the measured acceleration signal. Surrounding the core, an outer shell made of polycarbonate (PC) defines the external geometry. Polycarbonate is selected due to its high impact resistance and ductility compared to more brittle thermoplastics (Harper, 2000). This ensures that the external shape and contact surface remain consistent under repeated impacts, while providing limited compliance without significantly affecting the global stiffness of the system. The torso is rigidly connected to the cart through bolted interfaces using steel fasteners and embedded threaded inserts in the aluminum core. Three connection points at the torso base ensure a stable and repeatable mechanical coupling. Steel mass components attached to the cart are fastened equally with four connection points. This rigid interface is essential, as relative motion between dummy and cart would introduce additional degrees of freedom, thereby distorting acceleration measurements and reducing interpretability (Budynas & Nisbett, 2020). More details can be found in Appendix F.

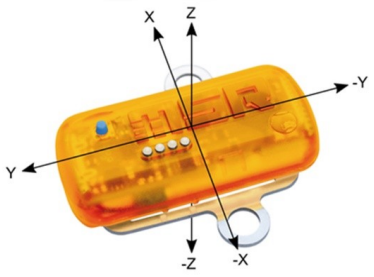

Figure 5.4: The MSR175 shock data logger used for high-frequency acceleration measurements. The sensor is oriented with the **Z-axis** in the horizontal impact direction, while the **Y-axis** and **X-axis** record vertical and lateral vibrations, respectively.

Harrie is equipped with a single primary acceleration sensor located at the chest region. In this design, the MSR175 transport data logger is used (Fig. 5.4) (MSR, 2025). The sensor is rigidly mounted within the internal structure to ensure that the measured signal accurately represents the global motion of the torso, avoiding local vibration effects (ISO 6487, 2015).

The device is capable of measuring accelerations up to ± 200 g at a sampling frequency of 6400 Hz. In addition, the use of a threshold-based recording system allows multiple impacts to be stored without requiring manual readout after each test, significantly improving experimental efficiency.

The cart geometry remains compatible with the ICE-G1 system (Fig. 5.5) and will be manufactured with stainless steel to protect the cart base from corrosion due to the humid and cold conditions at ice rinks. Its length and width are nearly identical to the original design, and the 30^o bent sections (D) position the wheels to align with the rail system. Maintaining this geometry ensures that launch dynamics remain unchanged. The main difference can be found at the front of the cart. As Harries width is greater than the carts width, the 30^o bent sections (D) have been shortened at the front. This change allows Harrie to be placed on the cart without interference. This cart design means that differences in impact behavior can be attributed to the dummy geometry rather than modifications in launch conditions. Together, the scaled geometry, controlled mass distribution, material selection, and rigid integration result in a system that is both physically robust and experimentally reliable, specifically optimized to improve pressure distribution realism while minimizing confounding variables. In Appendix FILLME, the designs measurements and material specifications are shown in more detail.

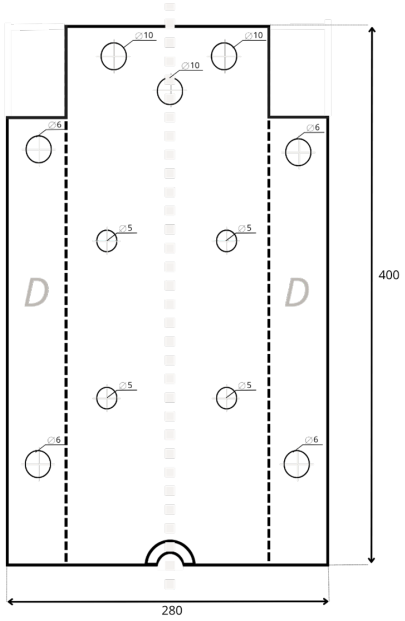

Figure 5.5: Measurements of the cart base (in mm) used tp be compatible with the ICE-G1 infrastructure, with a material thickness of 3mm.

5.3. Prototype

To test if Harries design does indeed have a more realistic interaction with padding, a prototype has been constructed to test the applied theory. This prototype is constructed using the same measurements and mass distribution as Harrie. The prototype is constructed by laser cutting shapes out of 9mm thick poplar plywood and glueing these shapes together with strong epoxy glue to create a 3D model (Fig. 5.6). Extensive sanding smoothened the connections between all plywood pieces (Fig. 5.7). Internal cavities have been created to add mass and a solid core by adding steel plates. This was done by using the density of poplar plywood to calculate the initial mass of each body segment. Then, steels density is used to calculate the necessary volume of the plywood that should be changed to steel in order to provide the correct mass for each body segment. The dummy is attached to the cart base with four M10 bolts 35 mm in length, which is estimated to be enough to able to withstand the forces during impact after discussions with the PMB personnel at the faculty of Industrial Design Engineering. A detailed description of the production and measurements can be found in Appendix G.

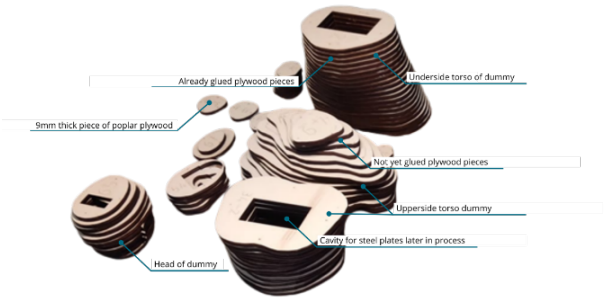

Figure 5.6: Base structure of the Harrie dummy constructed from high-quality plywood. The separate layers are glued together to create a 3D model.

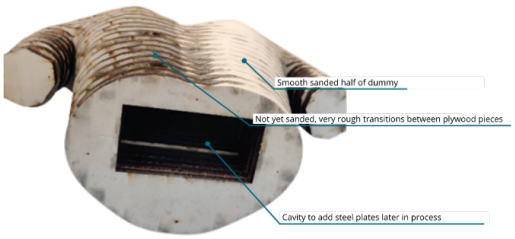

Figure 5.7: Detail of the sanding and finishing process to ensure smooth interaction with the padding.

During testing, an unforeseen failure occurred that led to significant structural damage to the prototype. The connection between the plywood components failed, and the attachment between the dummy and the cart was compromised as well. As a result, repairs and additional reinforcements were required. In particular, the repair of the connection between the dummy and the cart base introduced a metal plate at the bottom of the dummy. This plate was shaped to follow the curvature of the dummy as closely as possible. However, its presence may have altered the pressure distribution of the impacting surface (Fig. 5.8). While some influence on the measured results cannot be ruled out, it is expected that this effect is limited and does not invalidate the overall findings. Additional metal reinforcements were also applied to other parts of the structure. These were positioned in such a way that they do not affect the pressure distribution of the impacting shape (Fig. 5.9).

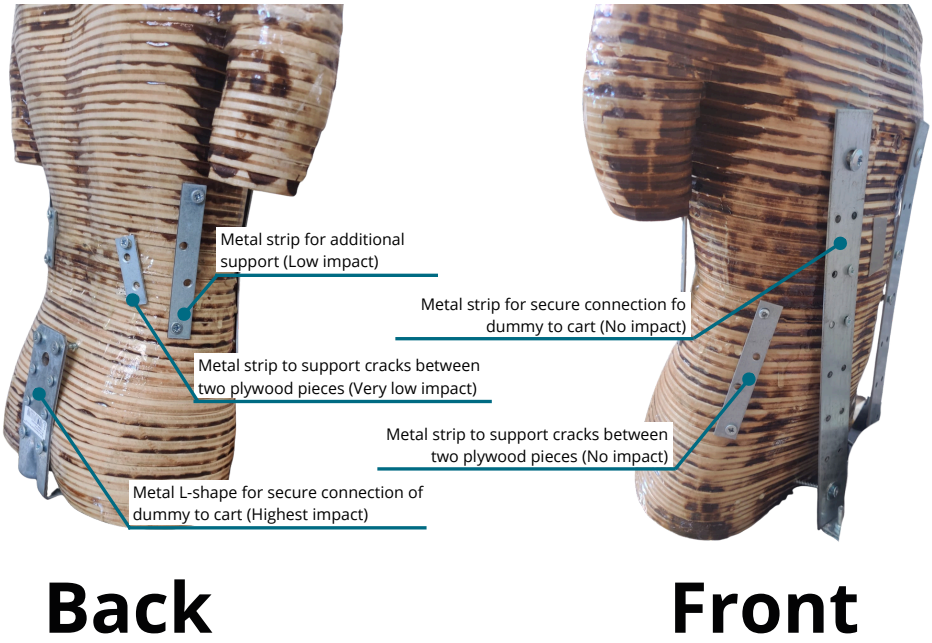

Figure 5.8: A compilation of repairs conducted to fix Harrie where needed. For each repair, the likelihood of altering test results is estimated, shown as the impact

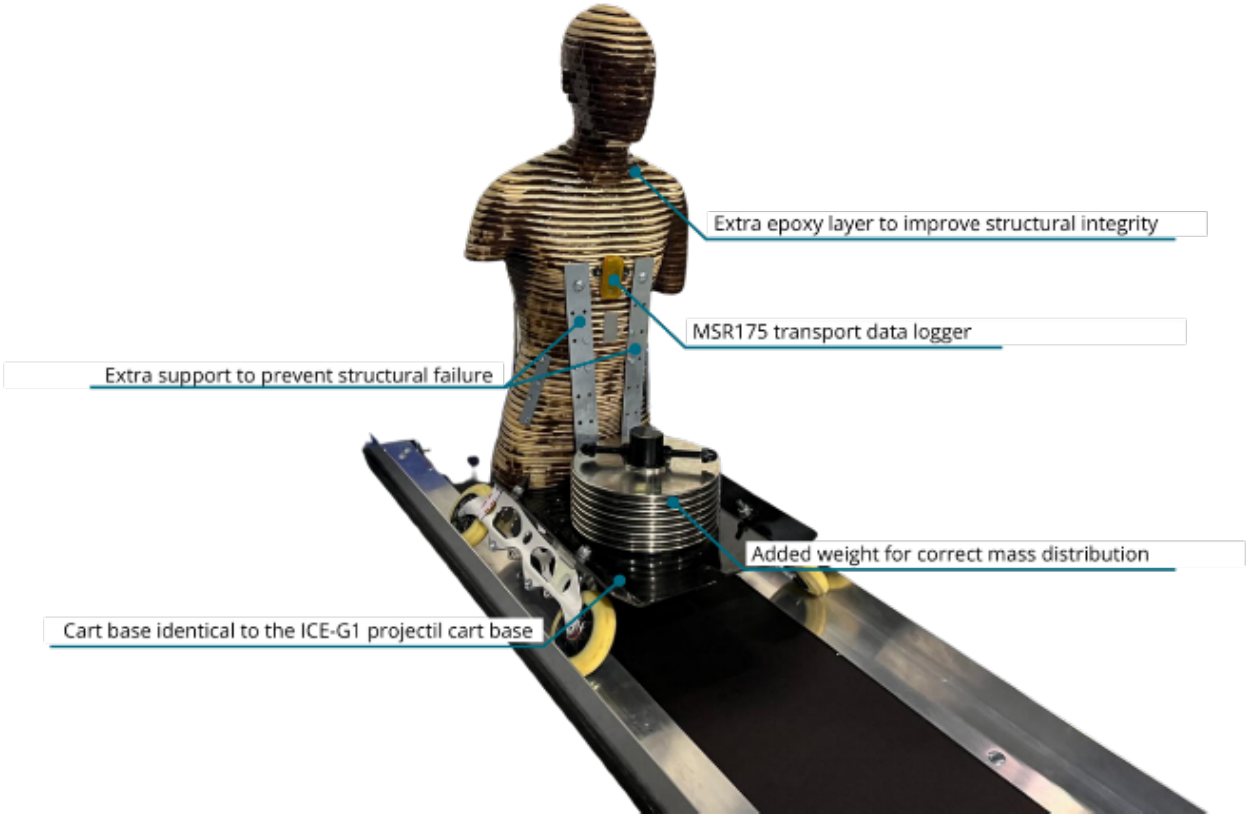

Figure 5.9: Finalized prototype of final design, standing on the pre-designed rails.

6

Experimental validation and testing

Experimental validation was carried out to determine whether the developed prototype meets the objectives defined in the refined design assignment. The main goal of this phase was to assess whether the prototype provides a more realistic simulation of the mechanical interaction between a short track speed skater and padding during impact, compared to existing methods such as the ICE-G1 projectile and the ISU drop test. The testing process consisted of three stages. First, pilot testing was conducted to verify system functionality and identify potential improvements. Second, on-ice testing was performed to evaluate the prototype under realistic crash conditions. Due to limitations encountered during these tests, additional off-ice experiments were carried out to further investigate repeatability and system behavior under controlled conditions.

6.1. Pilot testing and system verification

A pilot phase was conducted prior to formal testing to ensure that the measurement system and prototype functioned as intended. This phase focused on sensor reliability, structural integrity, and practical feasibility of the test setup. The sensor system was verified through controlled tests and showed consistent and stable behavior. This confirms that variations observed in later experiments can be attributed to differences in impact conditions rather than measurement inaccuracies.

During structural testing, a weakness was identified in the connection between the neck and torso of the prototype. Under impact loading, the head section continued moving after initial contact, resulting in excessive stress at the connection point. This issue was resolved by reinforcing the structure before continuing with further testing, but highlights the risk of structural failure in case of unforeseen loadings applied to the prototype. The connection between the plywood pieces of the prototype is found to be the weakest spot of the prototype.

An on-ice pilot test was then conducted following the original ICE-G1 setup configuration. This phase revealed three critical issues. First, high-frequency vibrations introduced substantial signal noise, complicating identification of the true impact peak. As a result, a low-pass filter was used during data processing in subsequent tests, and tests were performed with a lower measurement frequency to limit high-frequency noise. Another effect of this data noise was that it decreased the clarity of the data, increasing the difficulty to determine what measurement belonged to the impact and what could be attributed to data noise or vibrations of the system during launch. To improve synchronization between video and sensor data, a visible timer was introduced in the camera frame. Thirdly, fragile components in the ICE-G1 launch system were identified, requiring availability of spare parts during formal testing.

6.2. On-ice testing

The on-ice tests were designed to evaluate whether the prototype improves the representation of athlete-padding interaction under realistic conditions. In line with the project scope, the focus is on back-first impacts, which are the most common crash scenario in short track speed skating. The evaluation is based on three main aspects: the shape and development of the accelerationtime curve, the differences between padding systems, and the behavior of the prototype compared to existing test methods.

6.2.1. Test plan

Three test sessions were planned to investigate different aspects of impact behavior (Appendix H). In all tests, the sensor is configured with a measurement limit of ± 16 g, a sampling frequency of 1600 Hz, and a measurement threshold of 4 g. These settings were selected to capture the expected range of impact accelerations while minimizing noise.

The first session is planned to test straight impacts into traditional padding using both the prototype and the ICE-G1 projectile (Fig. 6.1). The purpose of this session is to compare the behavior of both systems under identical conditions and

to assess repeatability. In this session, both the prototype and ICE-G1 projectile are intended to measure fifteen successful launches at least.

The second session is conducted on a short track rink with moveable padding. Both straight and angled impacts are included in this session, but only with the prototype (Fig. 6.1). This setup reflects more realistic crash conditions and is intended to evaluate the differences between moveable and traditional padding. In addition, this test aims to find key differences between on-ice test results of the prototype and results of the official ISU drop test from the same padding. In this session, the aim is to launch the prototype at least twenty times angled and twenty times straight in padding.

The third session focuses on angled impacts in traditional padding, again comparing the prototype with the ICE-G1 projectile (Fig. 6.1). This session aims to assess how angled impacts affect the interaction between projectile and padding. Both the prototype and ICE-G1 projectile are aimed to measure at least fifteen successful launches.

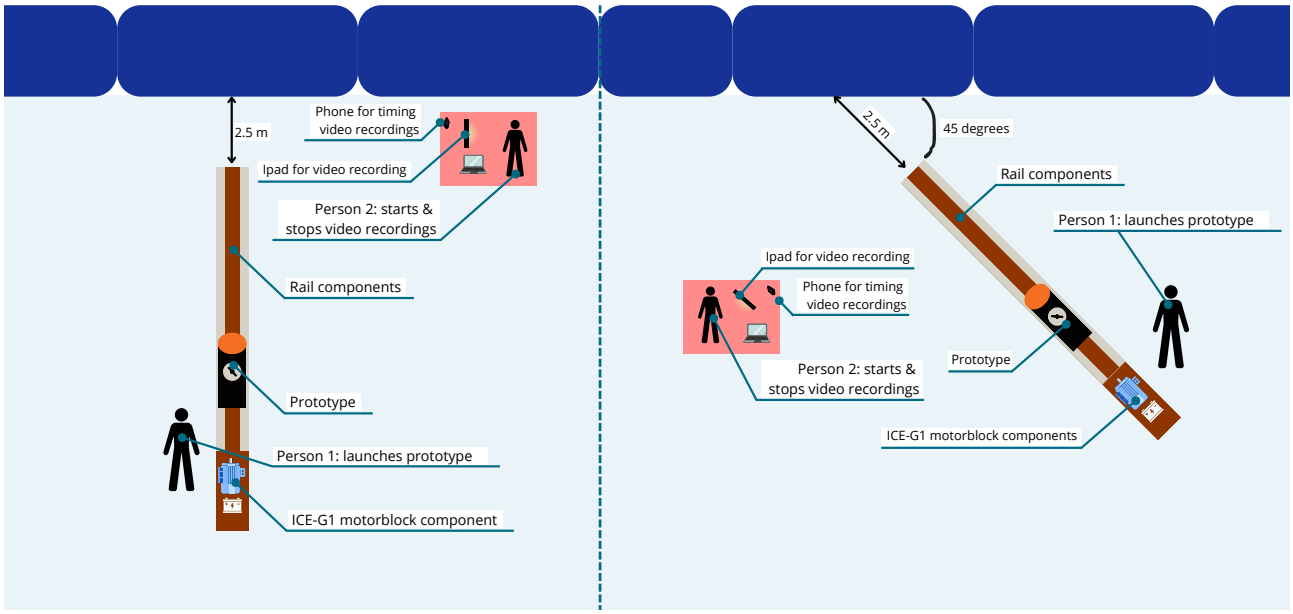

Figure 6.1: Test setup for straight impact (left) and angled impact (right) at 45°.

The collected data will be analyzed using a combination of sensor measurements and video analysis. Analysis will focus on peak acceleration, and time-based and kinematic indicators, including time to complete stop, stopping distance, rebound velocity, and duration above specific acceleration thresholds (e.g. 5 g). Accelerationtime graphs will be evaluated to assess the shape and development of the impact, including peak formation, decay behavior, and the presence of additional peaks. A low-pass filter will be applied to reduce the influence of noise. Results will be compared between padding types and projectile systems using the Intra Class Correlation (ICC) analysis to identify differences in impact dynamics and energy dissipation, with clear distinction between directly measurable results and observed trends requiring further validation.

6.2.2. Results

In practice, the original test plan could not be fully executed. During the first session, a rail connection failure caused the prototype to derail and cause extensive damage and required repairs (Fig. 5.8). As a result, this session was canceled. The time needed to repair the prototype reduced the available time for the second session by half, and the third session was adapted to include only straight impacts, as angled impacts were considered too risky for the damaged prototype. Furthermore, the analysis revealed that the sensor limit of 16 g was exceeded in all recorded impacts, which means that peak acceleration values could not be used for comparison. Despite these limitations, a total of 62 impacts have been recorded and analyzed.

The results show clear and consistent differences between impacts on moveable padding and traditional padding. These differences are most evident in the temporal development of the impact, the stopping distance, and the distribution of the acceleration over time. Impacts on moveable padding result in a significantly longer deceleration phase, with an average time to complete stop of approximately 167.7 ms, compared to 47.9 ms for traditional padding. In addition, the stopping distance is substantially larger for moveable padding (27.9 cm) than for traditional padding (15.7 cm). The duration of exposure to high acceleration levels also differs significantly. The time above 5 g is approximately 40 ms for moveable padding, compared to 80 ms for traditional padding. Similarly, the time above the sensor limit of 16 g is significantly shorter for moveable padding (4.4 ms) than for traditional padding (15.6 ms). Since these values are derived from video analysis rather than peak values, they can be considered reliable indicators of impact severity.

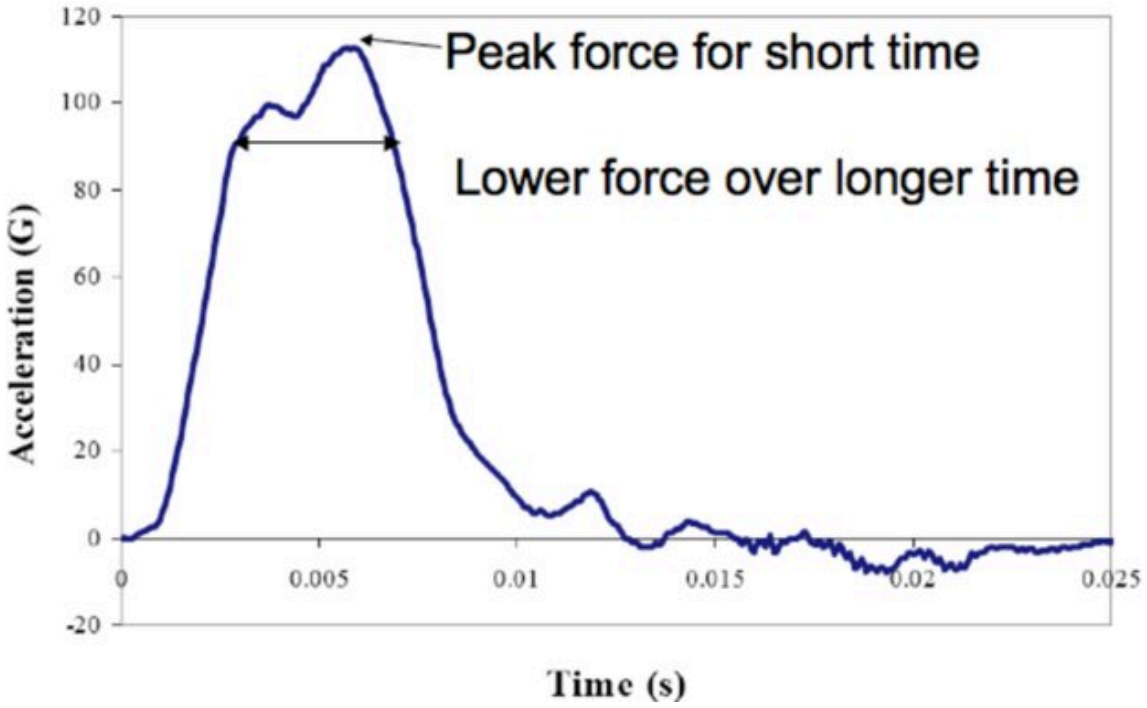

Figure 6.2: Example of the expected graph shape of measured acceleration data based on padded helmets (Blackman, 2007). Peak forces are not representable for tests in this project, but the general crash development should remain similar

Together, these results demonstrate that moveable padding distributes the impact over a longer time and distance, thereby reducing the duration of high acceleration exposure. This behavior is consistent with the theoretical expectation that increased deformation distance leads to lower average deceleration (Fig. 6.2). A strong indication, although not definitively proven due to sensor saturation, is that moveable padding also results in lower peak accelerations and improved energy absorption. This is supported by the observed rebound velocities, which are significantly lower for moveable padding (0.41 m/s) than for traditional padding (2.68 m/s) with similar impact velocities. Since rebound velocity reflects the amount of energy returned by the system, this suggests that moveable padding dissipates a larger portion of the impact energy. While this strongly implies reduced peak loading, the exact peak values cannot be confirmed.

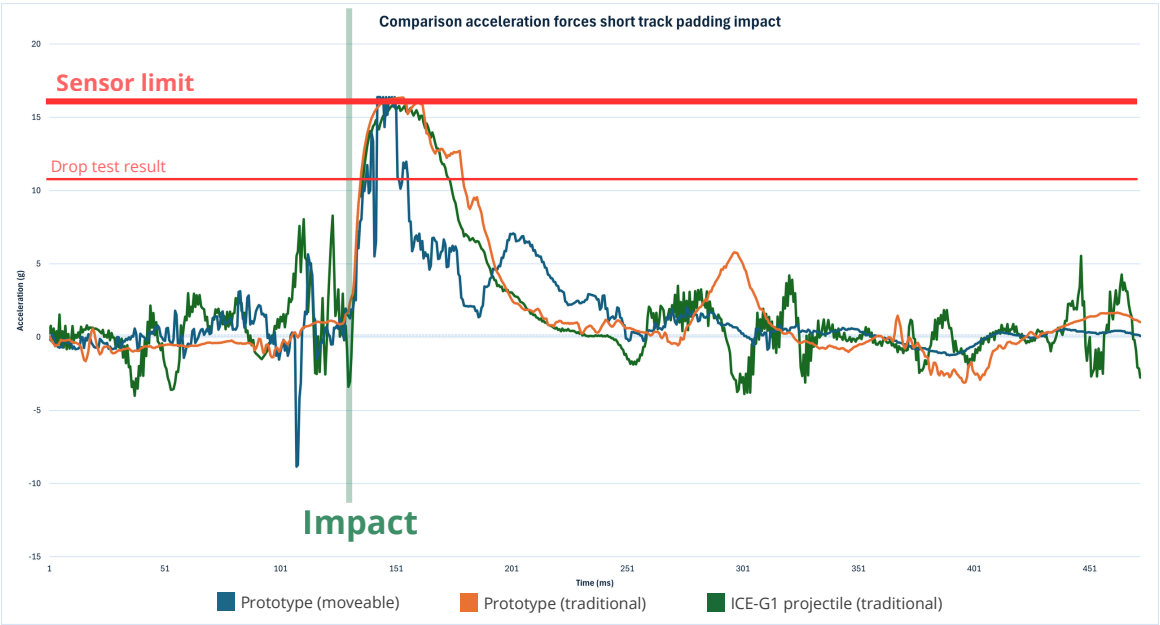

Figure 6.3: Graph showing average acceleration profiles of three tested scenarios. Blue is prototype on moveable padding, orange is prototype on traditional padding and green is ICE-G1 projectile on traditional padding. Sensor was capped on 16g. The green line highlights the first moment of contact between padding and projectile.

The acceleration-time graphs provide additional insight into the differences between impact scenarios and support the conclusions drawn from the numerical data. All measured impacts follow the expected general pattern of a padded collision, consisting of a rapid increase in acceleration, followed by a decay phase with oscillations and a smaller secondary response. However, the shape of the curves differs significantly between the two padding systems (Fig. 6.3). Impacts on moveable padding show a broader and more gradual peak, followed by a relatively smooth and extended decay phase. In contrast, impacts on traditional padding exhibit a sharper and more concentrated peak, with a faster decay and a more pronounced rebound phase. These differences in curve shape directly reflect the measured differences in stopping time and high-acceleration exposure. The broader curve of moveable padding corresponds to a longer deceleration phase and reduced time spent at high acceleration levels, while the sharper curve of traditional padding indicates a more impulsive load transfer.

A consistent feature in the prototype measurements is the presence of a secondary acceleration peak in the same direction as the initial impact. This behavior is observed in both padding configurations and is not present in the same form in the ICE-G1 data. It is unclear why this secondary peak can be observed exactly. It may be a result of the different mass distribution of the prototype compared to the ICE-G1 projectile. This could have introduced certain dynamics between the upper and lower body of the prototype, but more testing is required to find the exact cause.

A comparison with the ISU drop test reveals a clear and systematic discrepancy. The ISU test reports a peak acceleration of approximately 10.8 g for the same moveable padding, while the prototype measurements consistently exceed the 16 g sensor limit at comparable impact velocities. It can be stated with certainty that both test methods measure fundamentally different physical responses. The ISU test primarily measures local compression under high contact pressure, while the prototype captures global system behavior, including deformation, translation, and energy dissipation. The higher measured accelerations compared to theoretical values and the ISU drop test can be explained by how impact is modeled. Simple calculations (e.g., $a = \frac{\Delta v}{\Delta t}$) assume constant deceleration, while real impacts are highly non-linear, with short, sharp peaks that exceed the average deceleration. In addition, the ISU drop test mainly measures local foam compression under controlled conditions, whereas the prototype captures a more complex interaction, including distributed mass and system movement. This leads to different force distributions and can result in higher measured peak accelerations. As a result, the ISU drop test likely represents a simplified version of an impact and does not fully capture the dynamics of a realistic athletepadding collision.

A direct comparison between the prototype measurements and the standardized drop test highlights clear differences in how both methods represent an impact event. The drop test graph shows a relatively simple response: a single, well-defined acceleration peak followed by a short decay and a distinct secondary peak associated with the rebound of the cylindrical mass. This rebound phase, often referred to as bounce back, is a key parameter in the drop test, as it measures the time between the first and second impact. However, this behavior is inherently linked to the vertical nature of the test setup, where the mass loses contact with the padding and impacts it again due to gravity. In contrast, the prototype graph shows a more complex and continuous deceleration process. Instead of a discrete rebound, the prototype exhibits a prolonged decay phase with a smoother transition and, in some cases, a secondary peak within the same impact event. This indicates that the system remains in contact with the padding throughout the impact, allowing for continuous energy transfer rather than discrete impacts. These differences suggest that the two test methods capture fundamentally different aspects of padding behavior.

The drop test appears to isolate local material compression under controlled and highly repeatable conditions, resulting in a clean and consistent signal. However, this simplicity also implies that it represents a reduced version of a real crash, where factors such as distributed mass, horizontal motion, and interaction with the surrounding system are not included. The prototype, on the other hand, introduces these additional factors, resulting in a more complex signal that reflects a combination of deformation, translation, and internal mass dynamics. While this increased complexity makes the results less controlled and harder to interpret, it also suggests that the prototype may better approximate and simulate the nature of real athletepadding impacts. It is therefore reasonable to state that the prototype provides a more comprehensive representation of impact behavior, particularly in terms of how forces develop and dissipate over time. However, more validation is necessary to confirm if the additional dynamics of the prototype indeed correlate with padding performance during real crash events.

The comparison between the prototype and the ICE-G1 projectile provides additional insight into the origin of the observed differences with the ISU drop test. As the ICE-G1 has similar mass and contact geometry as the ISU drop test, but is launched similar to the prototype, the comparison between the prototype and the ICE-G1 projectile helps to distinguish the influence of the launch method from the influence of projectile design. Despite differences in geometry and mass distribution, both systems show a similar overall accelerationtime curve shape during the initial impact phase, characterized by a rapid rise to a peak followed by a decay. This similarity can be attributed to the shared horizontal launching method, suggesting that the general impact development is largely governed by how the projectile interacts dynamically with the padding during motion. However, differences become more apparent after the initial impact. The ICE-G1 signal shows more high-frequency oscillations and irregular behavior, whereas the prototype produces a smoother response with a clearer secondary peak. These differences are likely caused by the simplified geometry and rigid structure of the ICE-G1

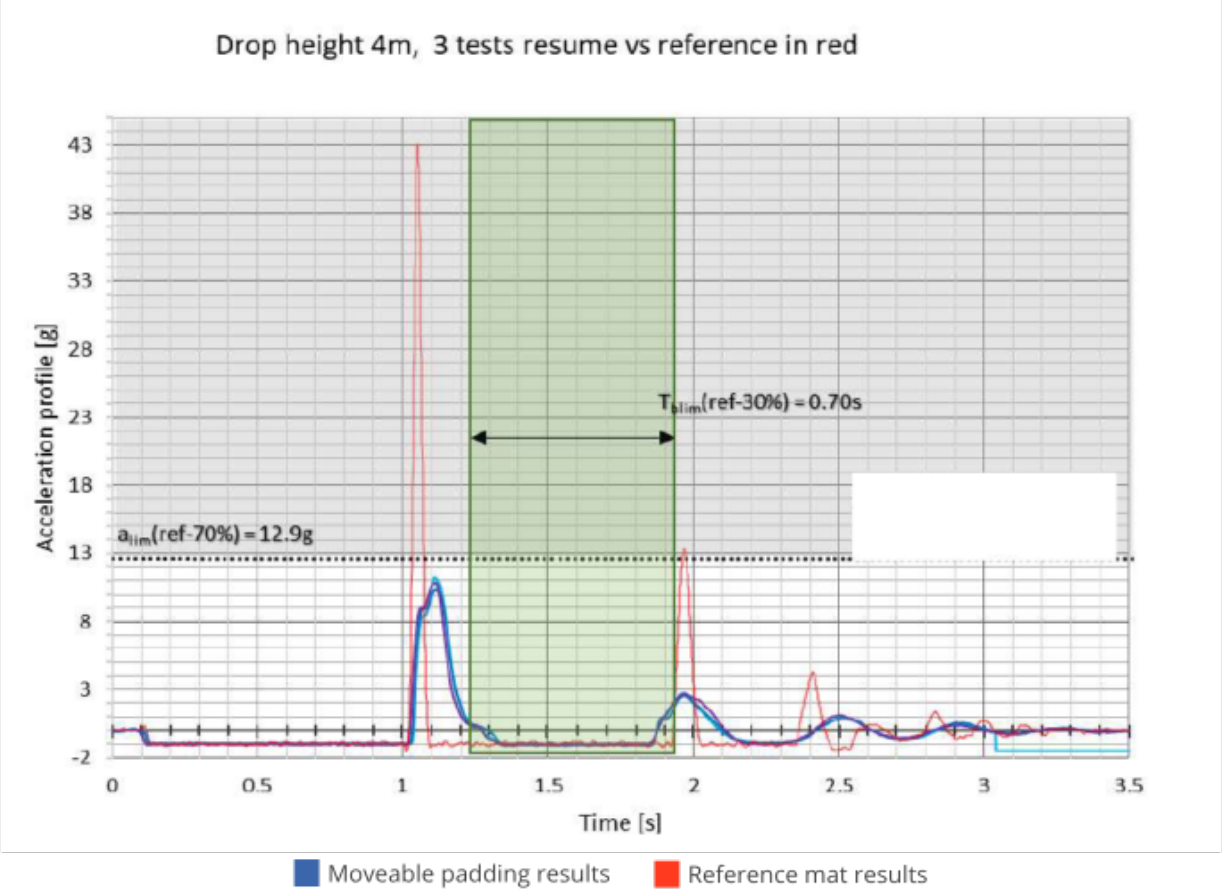

Figure 6.4: The ISU drop test results of the same moveable padding assessed by the prototype with similar velocities. The blue lines are results from the tested padding, the red line is the result from a reference mat, used to define the safety of new padding.

projectile, which introduce additional vibrations and more localized loading effects. While the overall shape of the impact is similar, indicating comparable global behavior, the magnitude and distribution of peak forces may differ significantly between both systems. Since both the prototype and ICE-G1 exceed the sensor limit, the exact peak values cannot be determined. As a result, it remains uncertain to what extent the observed differences are caused by projectile design rather than measurement limitations, and further research is required to quantify these effects.

6.3. Off-ice testing

Since the on-ice tests did not provide sufficient usable data, additional testing was carried out off the ice in Utrecht. The main goal of this testing was to evaluate repeatability and compare the prototype with the ICE-G1 projectile under controlled conditions.

6.3.1. Test plan

The off-ice tests are conducted using a simplified setup with a fixed padding configuration (Fig. 6.5). Only straight impacts are performed to ensure safety and consistency. This time, the configurations of the sensor were slightly altered. A measurement limit of $\pm$200 g was set, including a measurement threshold of 3 g, and a sampling frequency of 3200 Hz. The higher measurement limit allows accurate capture of peak accelerations, while the increased sampling frequency improves temporal resolution. The main objectives of this test are to compare peak acceleration between both projectiles and to evaluate the repeatability of the prototype.

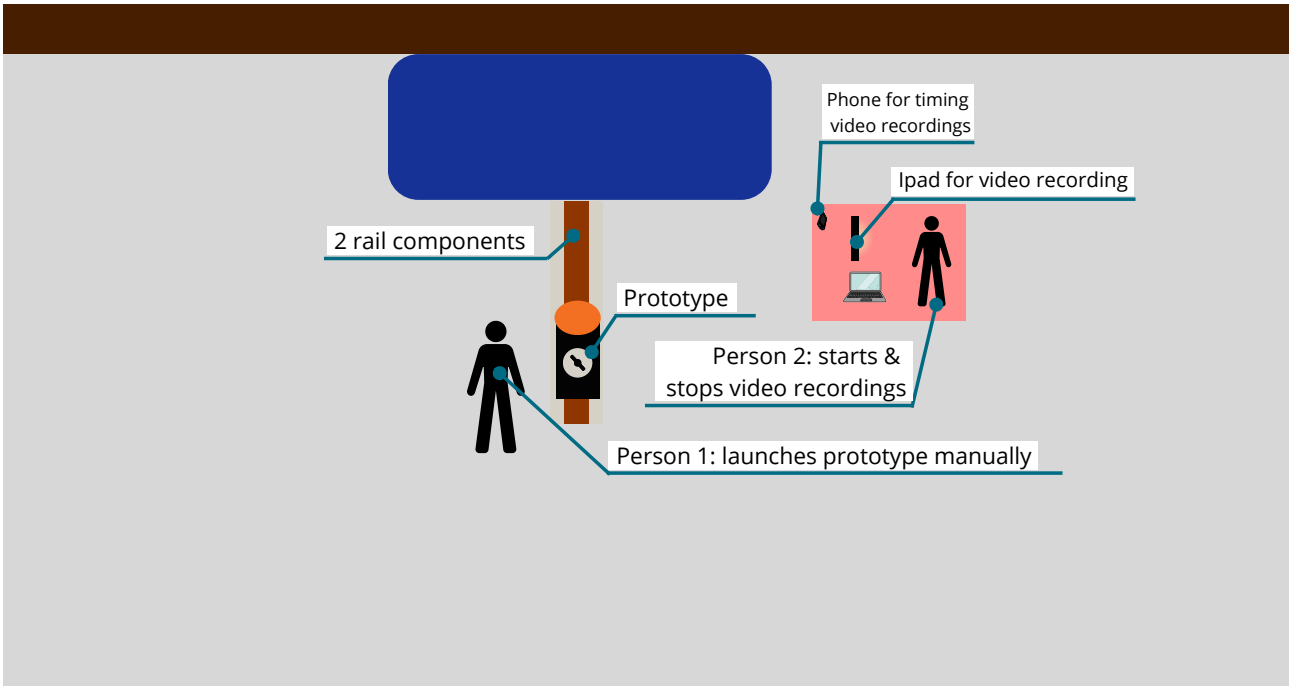

Figure 6.5: Test setup for off-ice testing. There are only two rail components instead of 6. Person 1 pushes the prototype manually. The blue block represents the piece of padding.

The off-ice data will be analyzed primarily using sensor measurements, as the increased measurement range allows reliable capture of peak accelerations. The analysis will focus on peak acceleration and repeatability. A low-pass filter will be applied to reduce noise and improve signal clarity for peak acceleration assessment. In addition, repeatability will be assessed statistically using measures such as coefficient of variation and intraclass correlation coefficient (ICC). Differences between both projectiles will be evaluated to determine whether variations in measured impact behavior are caused by the launching method or by differences in geometry and mass distribution, supporting interpretation of earlier on-ice results.

6.3.2. Results

A total of 36 valid impact trials were recorded for the prototype and 28 for the ICE-G1 projectile, with average impact velocities between 4 and 5 m/s. The increased sensor range ensured that peak accelerations were captured without saturation, allowing for a more reliable comparison between both systems.

The averaged accelerationtime graph shows clear differences in impact behavior between the prototype and the ICE-G1 projectile (Fig. 6.6). Both systems follow the expected general shape of a padded impact, with a rapid rise in acceleration after initial contact, followed by a decay phase. However, distinct differences are visible in both the peak development and the post-impact behavior. The prototype reaches a higher initial peak of approximately 5 g within the first 25 ms, followed by a gradual decrease and a clearly defined secondary peak around 75-85 ms. This secondary peak is consistent with earlier observations during on-ice testing. In contrast, the ICE-G1 projectile shows a lower and more distributed peak response of approximately 3 g, with multiple smaller peaks between 0 and 100 ms. This results in a less defined primary peak and a more irregular signal. The absence of a clear secondary peak and the presence of multiple oscillations indicate that the ICE-G1 response is influenced by structural vibrations and localized contact behavior, rather than representing a continuous mass interaction.

Regarding repeatability, both systems initially show moderate variability of approximately 20% in raw data (Table 6.1). After applying a low-pass filter, variability is reduced significantly. The prototype achieves a coefficient of variation of 6.9%, which satisfies the design requirement of remaining within 10% variation, confirming that the system produces consistent and repeatable measurements. The ICE-G1 projectile shows slightly lower variability at 5.5%, indicating marginally higher consistency. Statistical analysis shows that the results of both projectiles differ significantly (ICC between -0.227 and 0.002, $p < 0.05$), confirming that they do not measure the same physical interaction. Importantly, since both projectiles are tested using the same launching method in this setup, the observed differences in peak development, signal shape, and energy dissipation can be attributed primarily to differences in geometry, mass distribution, and contact behavior.

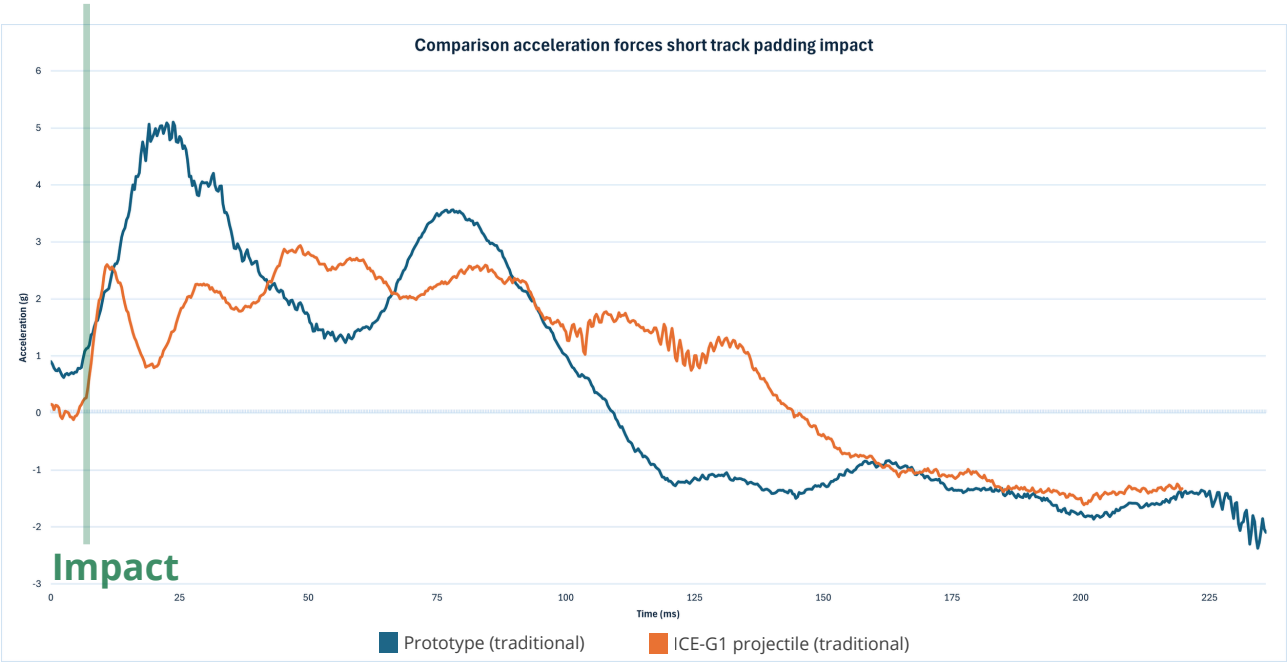

Figure 6.6: Graph showing average graphical display of acceleration forces during impact for both the prototype and ICE-G1 projectile

Table 6.1: Consistency and variance of both projectiles for raw data and data filtered with a low-pass filter.

Variable	Design	Mean acc. (g)	Std. Dev.	CoV	ICC	Notes
Raw data peak acceleration	Harrie	6,62	1,26	0,190	-0,277	Moderate variability
	ICE-G1	6,03	1,18	0,195	-0,277	Moderate variability
Low pass peak acceleration	Harrie	5,02	0,34	0,069	0,002	Low variability
	ICE-G1	2,95	0,16	0,055	0,002	Low variability

The off-ice results provide important context for interpreting the differences between the prototype and the ISU drop test. The ICE-G1 projectile shares key characteristics with the ISU test, such as mass (30 kg) and a small, flat contact area of similar size, but differs in its horizontal launching method. Since the ICE-G1 results show a similar global impact shape to the prototype but differ in peak development and signal behavior, this indicates that the launching method largely determines the overall shape of the impact, while the projectile design influences the magnitude and distribution of forces. This means that the discrepancy observed between the ISU drop test and the prototype cannot be attributed solely to the difference between vertical and horizontal impact. Instead, the results support the conclusion that both the test setup and the projectile design contribute to the observed differences in measured acceleration.

7

Conclusion

This project aimed to improve the simulation of the interaction between a short track speed skater and padding during impact. The central research question was how a projectile can be designed to simulate this interaction more realistically than current testing methods, while remaining compatible with the ICE-G1 system. To answer this, a theoretical framework on foam behavior and crash dynamics was established, followed by the design and experimental validation of a prototype.

The experimental results show that the prototype produces consistently higher peak accelerations than the ISU drop test. Based on the theoretical framework, this indicates a shorter stopping distance during impact, which directly supports the statement that the way load is applied to the padding strongly influences its deformation behavior. To interpret these results, a distinction must be made between effects caused by the test setup and those caused by the design of the impactor. The ISU drop test applies a vertical impact on a stationary piece of padding, while both the ICE-G1 projectile and the prototype apply a horizontal impact on padding positioned on ice. This change in boundary conditions influences how the padding deforms and displaces, meaning that part of the difference between the prototype and the ISU drop test is caused by the testing setup rather than the design itself. A more direct comparison is provided by the ICE-G1 projectile, which uses the same horizontal setup as the prototype but retains a localized impact geometry similar to the ISU drop test. The results show that the prototype produces higher peak accelerations than the ICE-G1 projectile as well. Since the setup is the same, this difference can be attributed to the design of the prototype, specifically the larger and more distributed contact area. In line with the theoretical framework, this leads to a different pressure distribution, reduced localized deformation, and a shorter stopping distance, reflected in higher peak accelerations. These findings show that the prototype changes the interaction between projectile and padding in a measurable and theoretically consistent way. In short, differences in the general impact development between the ISU drop test and the prototype are most likely caused by the change in test setup, while differences in magnitude and distribution of peak forces between both test methods can be attributed to the design differences of both impactors. However, due to the absence of real crash data and the lack of direct measurements of pressure distribution during testing, the exact extent of the improvement cannot be determined at this stage.

In addition, differences are observed between moveable and traditional padding. Although peak accelerations cannot be determined with high accuracy due to sensor limitations, the measured data indicates a consistent trend where moveable padding results in lower recorded accelerations compared to traditional padding. This trend is supported by other measurable aspects of the impact response, as impacts with moveable padding show a longer time from initial contact to full stop and increased stopping distance. According to the theoretical framework, this increase in stopping distance leads to a reduction in peak forces. Since moveable padding is able to translate and deform as a system, this behavior is consistent with expectations. However, due to the measurement limitations, the magnitude of this difference cannot be quantified with certainty. Combining the facts that moveable and traditional padding respond differently to impacts, and that the ISU drop test is unable to simulate impacts in moveable padding, it is clear that the ISU drop test is currently unable to provide a realistic safety assessment of moveable padding.

Overall, it can be stated with confidence that the prototype produces different impact responses than both the ISU drop test and the ICE-G1 projectile. Theory combined with test results support that the prototype likely impacts padding more like an average male short track speed skater than the current ISU drop test does. The prototype introduces a different load distribution that leads to higher peak accelerations and altered deformation behavior, while the consistent difference between moveable and traditional padding confirms the increased safety of moveable padding. Together, these results provide a more detailed understanding of padding behavior, while highlighting the need for further validation.

As a recommendation, the prototype should not yet replace the ISU drop test. Additional iterations and validation are required to better isolate the observed effects and confirm their relation to real crash conditions. However, if the new design is fit to be used regularly, both test methods should coexist, allowing results to be compared in parallel. In the

longer term, the new test method appears better suited to assess padding safety under more representative conditions, and is recommended as the primary way to test padding safety in the future. The ISU drop test can remain a simple and cost-effective initial screening method for manufacturers if this new test method will be implemented.

8

Limitations and recommendations

This chapter outlines the key limitations encountered during the project, including those defined at the outset and those identified during execution. It also provides recommendations based on experimental findings and theoretical insights for future development of the projectile, the ICE-G1 system, padding performance, and further research.

8.1. Limitations of the project

A major limitation within the project was the reliability of the ICE-G1 test assembly. Structural failures during testing, including severe damage to the dummy, required modifications that altered its physical properties and potentially influenced measurement accuracy. Furthermore, the prototype nature of the ICE-G1 launching system led to frequent mechanical failures, particularly in the cable, pulley, and winch systems, reducing testing efficiency and consistency. In some cases, tests had to be conducted manually. Sensor-related issues also affected the results. Misinterpretation of time synchronization between sensor data and video footage led to incorrect parameter settings and loss of testing time. Additionally, the limited durability of the system reduced the number and variety of tests that could be conducted. Despite these challenges, the project remained feasible, although the limitations likely slightly influenced the accuracy and completeness of the results.

8.2. Recommendations for projectile development

Before new projectile development is planned, it is recommended that additional testing is carried out with correct sensor settings to quantify the differences between the ISU drop test and the prototype. In addition, it is recommended that these tests include an extra sensor attached to the lower part of the prototype to measure differences in experienced acceleration between the top and bottom part of the prototype. Data acquired from these tests will most likely reveal the next step in the development of the new test method.

Additionally, it is recommended to add a pressure mat to the prototype to assess its effectiveness in simulating the correct pressure distribution. Comparing this to a pressure map of a real back-first short track speed skating crash can reveal how the dummy must be improved to create a more realistic simulation of a crash.

Next, it is recommended to keep the focus on the simulation of athlete padding interaction. While other factors such as rotational acceleration, post-impact limb movement and internal injury mechanics play a role in real crashes, the athlete - padding interaction remains a central factor in how realistically these other factors can be simulated as well. Therefore, it is recommended to only incorporate (some of) these factors when the basic simulation of athlete - padding interactions is proven to be similar to real crashes.

Finally, it is recommended to add functionality to switch what short track speed skater the projectile simulates. There could be many differences between male, female, senior and junior short track speed skaters. As it is currently not possible to assess how padding can handle each short track speed skater group, it is recommended to allow the projectile to change either mass or contact area size. This can provide important insights if padding works as intended for each short track speed skater.

8.3. Recommendations for launching system development

While a major overhaul of the ICE-G1 launching infrastructure is necessary, it is recommended that the current infrastructure is repaired to withstand at least four additional tests to help with the quantification of the difference between the prototype and ISU drop test.

After these tests, a major overhaul of all components is recommended. It is recommended to improve the motor used for launches to a more powerful, controllable and consistent variant. This will be essential to ensure repeatable and higher

launch velocities to be able to simulate impacts with higher velocities more consistently. As this puts more loads on the entire system, it is recommended to improve the rail sections, cable and pulleys with a focus on durability to prevent frequent failures. The length of the rails could be made shorter, but it is recommended to keep this equal, even with a stronger motor, as accelerating the prototype or a future iteration more rapidly can be dangerous and cause derailments or severe damages, as tests performed with current equipment already showed signs that this is a possibility.

8.4. Recommendations for padding improvement

Testing indicated that repeated impacts may weaken connections between padding elements, reducing their effectiveness. It is recommended to regularly inspect and maintain these connections after significant use. Preliminary observations suggest a slight decrease in energy absorption after repeated impacts, although further testing is required to confirm this effect. No additional immediate recommendations can be made to improve padding design based on the current data. It is recommended that padding is tested on a yearly basis to confirm if energy absorption capabilities decrease over time. In addition, it is recommended to test the effects of the cold and moist environment on moveable padding after a longer period without the padding being removed from the ice. Concerns have been expressed about the possibility of padding pieces potentially freezing to the ice, potentially reducing its ability to safely slow down a short track speed skater. It is recommended that this effect is tested in the future.

8.5. Recommendations for future research

Further research is needed to better understand injury mechanisms in short track speed skating. Developing a systematic method for collecting and analyzing injury data would provide valuable insights for safety improvements. Expanding video analysis to elite-level competitions may reveal differences in crash dynamics across performance levels. Additionally, acquiring real-world crash data from athletes would greatly enhance the validation of experimental models and improve the biomechanical relevance of testing systems. In this regard, acquiring pressure distribution maps of real short track speed skating crashes would greatly benefit the development of a new test method that can simulate athlete padding interaction more realistically. This could be combined with sensor data to assess the extent to which each test method can realistically simulate crashes and assess padding safety.

9

References

AAP. (2022, 7 februari). Skater Corey crashes out of short track - ESPN. ESPN.com. https://www.espn.com.au/olympics/story/_/id/33238084/beijing-olympics-skater-brendan-corey-crashes-short-track

Ashby, M. (2011). Materials Selection in Mechanical Design. In Elsevier eBooks (4th ed.). Elsevier. https://doi.org/10.1016/c2009-0-25539-5

Beets, E., De Klerk, J., Van Der Laan, M., Moonen, E., Otten, M., & Pel, F. (2024). ICE Design Mobile Testing System Final Report | Advanced Embodiment Design. Technische Universiteit Delft.

Bellis, M. (2024, June 7). A brief history of sports. ThoughtCo. https://www.thoughtco.com/history-of-sports-1992447

Blackman, E. G. (2007). Improving TBI Protection Measures and Standards for Combat Helmets. In E. G. Blackman, M. E. Hale, & S. H. Lisanby, Department Of Physics And Astronomy, University Of Rochester, Rochester, NY, 14627.

Budynas, R. G., & Nisbett, J. K. (2020). Shigleys mechanical engineering design (11th ed.). McGraw-Hill Education.

Callister, W. D., & Rethwisch, D. G. (2018). Materials science and engineering: An introduction (10th ed.). Wiley.

Chen, H. B., Yang, K. H., & Wang, Z. G. (2009). Biomechanics of whiplash injury. PubMed, 12(5), 305 314. https://pubmed.ncbi.nlm.nih.gov/19788851

Christensen, R. M. (1971). Theory of viscoelasticity: an introduction. http://www.sciencedirect.com/science/book/9780121742522

De Bruijn, O., Pepers, T., Van Andel, S., Van Ekeren, T., & Van de Kamp, E. (2023). Rapid curve innovators. Technical University of Delft.

De Leva, P. (1996). Adjustments to Zatsiorsky-Seluyanovs segment inertia parameters. Journal Of Biomechanics, 29(9), 12231230. https://doi.org/10.1016/0021-9290(95)00178-6

DINED. (n.d.). https://dined.io.tudelft.nl/en/database/tool

Engo GmbH. (z.d.). Engo offers a wide variety of accessories for ice rinks and stadiums. Engo. Geraadpleegd op 16 maart 2026, van https://www.engo.it/en/accessories/11-short-track-protection-mats.html#&gid=1&pid=3

Godesky, J. (2023, 17 mei). The Problem with the Double Diamond. Medium. Geraadpleegd op 19 maart 2026, van https://medium.com/design-bootcamp/the-problem-with-the-double-diamond-57ab03719ce0

Grilec, K., Mari, G., & Milo, K. (1970). Aluminium Foams in the Design of Transport Means. PROMET - Traffic&Transportation, 24(4), 295304. https://doi.org/10.7307/ptt.v24i4.437

Harper, C. A. (2000). Handbook of plastics technologies. McGraw-Hill.

Hendricks, M., Verhagen, E., & Van De Water, A. T. M. (2024). Epidemiology, etiology and prevention of injuries in competitive ice speed skatinglimited current evidence, multiple future priorities: A scoping review. Scandinavian

Journal of Medicine and Science in Sports, 34(4). https://doi.org/10.1111/sms.14614

Hillis, T. L. (2018). The incidence of injuries in development Short track speed skaters Part 1: On ice. Sports Injuries & Medicine, 4(4). https://doi.org/10.29011/2576-9596/100040

Hurdis, J. (1998). A brief history of indoor short track.

Idema T. (2023), Introduction to particle and continuum mechanics, TU Delft Open, doi 10.59490/tb.81

ISO 6487 International Organization for Standardization. (2015). ISO 6487:2015: Road vehiclesMeasurement techniques in impact testsInstrumentation. https://www.iso.org

Karton, C., Rousseau, P., Vassilyadi, M., & Hoshizaki, T. B. (2013). The evaluation of speed skating helmet performance through peak linear and rotational accelerations. British Journal Of Sports Medicine, 48(1), 4650. https://doi.org/10.1136/bjsports-2012-091583

KNSB. (2025). Shorttrack Communiqué 2B seizoen 2025-2026.

Maastricht UMC. (n.d.). Body composition. nutritionalassessment.mumc. Geraadpleegd op 20 februari 2026, van https://nutritionalassessment.mumc.nl/en/body-composition

Matyk, M., Raschka, C. (2012). Body composition and the somatotype of European top roller speed skaters. Papers On Anthropology, 20, 258. https://doi.org/10.12697/poa.2011.20.26

Maw, S., Johnston, C. (2010). The Design of Foam Crash Pads for Short Track Speed Skating on Boarded Rinks. In STARSS Conference, STARSS Conference.

Meaney, D. F., Smith, D. H., Department of Bioengineering, University of Pennsylvania, 240 Skirkanich Hall, 210 South 33rd Street, Philadelphia, PA 19104-6392, USA, Department of Neurosurgery, University of Pennsylvania, 105D Hayden Hall, 240 South 33rd Street, Philadelphia, PA 19104-6392, USA. (2011). Biomechanics of Concussion. In Clin Sports Med (Vols. 3030, pp. 1931). https://doi.org/10.1016/j.csm.2010.08.009

MSR. (2025, 18 november). Shock Data Logger for transport, shock and climate monitoring. EN MSR Data Loggers. Geraadpleegd op 25 maart 2026, van https://www.msr.ch/en/product/transportation-shock-data-logger-msr175/

Nayfeh, A. H., & Mook, D. T. (1995). Nonlinear oscillations. https://doi.org/10.1002/9783527617586

OWIA. (2025, 19 oktober). Short track speed skating: Corey opens season with strong performances in Montreal. Olympic Winter Institute Of Australia. Geraadpleegd op 16 maart 2026, van https://www.owia.org/individual-athletes-news/short-track-speed-skating-corey-opens-season-with-strong-performances-in-montreal

Palmer-Green, D., Brownlow, M., Hopkins, J., Eley, J., Jaques, R., & Hunter, G. (2014). EPIDEMIOLOGICAL STUDY OF INJURY AND ILLNESS IN GREAT BRITAIN SHORT-TRACK SPEED SKATING. British Journal Of Sports Medicine, 48(7), 649.3-650. https://doi.org/10.1136/bjsports2014-093494.238

Romeu-Mejia, R., Giza, C. C., & Goldman, J. T. (2019). Concussion Pathophysiology and Injury Biomechanics. Current Reviews in Musculoskeletal Medicine, 12(2), 105116. https://doi.org/10.1007/s12178-019-09536-8

Sovak, D., & Hawes, M. R. (1987). Anthropological status of international calibre speed skaters. Journal Of Sports Sciences, 5(3), 287304. https://doi.org/10.1080/02640418708729783

Sports injuries. (2025, 2 juni). Cleveland Clinic. https://my.clevelandclinic.org/health/diseases/22093-sports-injuries

Tremblay, R. (2012). Analysis on crash pad protection for short track on boarded rinks. https://www.isthq.com/wpcontent/uploads/2023/05/AnalysisoncrashpadProtectionforShorttraconboardedRinks.pdf

Van der Linden, B. (2017, 9 oktober). Veilige boarding bij shorttrack verplochten. AD. Geraadpleegd op 24 maart 2026, van https://www.ad.nl/andere-sporten/veilige-boarding-bij-shorttrack-verplichten a1cdebd4/?

A

Project Brief

TU Delft

IDE Master Graduation Project

Projectteam,procedural checks and PersonalProject Brief

In this document the agreements made between student and supervisory team about the student's IDE Master Graduation Project are set out. This document may also include involvement of an external client, however does not cover any legal matters student and client (might) agree upon. Next to that, this document facilitates the required procedural checks:

- Student defines the team, what the student is going to do/deliver and how that will come about
- Chair of the supervisory team signs, to formally approve the project's setup / Project brief
- SSC E&SA (Shared Service Centre, Education & Student Affairs) report on the student's registration and study progress
- IDE's Board of Examiners confirms the proposed supervisory team on their eligibility, and whether the student is allowed to start the Graduation Project

STUDENT DATA&MASTERPROGRAMME
Complete all fields and indicate which master(s) you are in

Family name	
Initials	
Given name	
Student number	

IDE master(s)	IPD ✓	DfI	SPD	
2nd non-IDE master				
Individual programme *(date of approval)*				
Medisign				
HPM				

SUPERVISORYTEAM
Fill in he required information of supervisory team members. If applicable, company mentor is added as 2nd mentor

Chair		dept./section	SDE
mentor		dept./section	HCD
2nd mentor			
client:	Innovatielab Thialf		
city:	Heerenveen	country:	Netherlands
optional comments			

! Ensure a heterogeneous team. In case you wish to include team members from the same section, explain why.

! Chair should request the IDE Board of Examiners for approval when a non-IDE mentor is proposed. Include CV and motivation letter.

! 2nd mentor only applies when a client is involved.

APPROVAL OF CHAIR on PROJECT PROPOSAL / PROJECT BRIEF -> to be filled in **by the Chair** of the supervisory team

Sign for approval (Chair)

Name _____ Date 6 Mar 2025 Signature _____

CHECK ON STUDY PROGRESS

To be filled in **by SSC E&SA** (Shared Service Centre, Education & Student Affairs), after approval of the project brief by the chair.
The study progress will be checked for a 2nd time just before the green light meeting.

Master electives no. of EC accumulated in total _____ EC

Of which, taking conditional requirements into account, can be part of the exam programme _____ EC

★	**YES**	all 1st year master courses passed
	NO	missing 1st year courses

Comments:

Sign for approval (SSC E&SA)

Name _____ Date 17 mrt 2025 Signature _____

APPROVAL OF BOARD OF EXAMINERS IDE on SUPERVISORY TEAM -> to be checked and filled in by IDE's Board of Examiners

Does the composition of the Supervisory Team comply with regulations?

YES	★	Supervisory Team approved
NO		Supervisory Team not approved

Comments:

Based on study progress, students is …

★	**ALLOWED** to start the graduation project
	NOT allowed to start the graduation project

Comments:

Sign for approval (BoEx)

Name _____ Date 17 Mar 2025 Signature _____

Personal Project Brief – IDE Master Graduation Project

Name student _____ **Student number** _____

PROJECTTITLE,INTRODUCTION,PROBLEMDEFINITIONand ASSIGNMENT
Complete all fields, keep information clear, specific and concise

Project title Design a new dummy-like projectile which better replicates real short track crash dynamics

Please state the title of your graduation project (above). Keep the title compact and simple. Do not use abbreviations. The remainder of this document allows you to define and clarify your graduation project.

Introduction

Describe the context of your project here; What is the domain in which your project takes place? Who are the main stakeholders and what interests are at stake? Describe the opportunities (and limitations) in this domain to better serve the stakeholder interests. (max 250 words)

Short track speed skating is a high-speed sport where crashes occur frequently, and injuries are a constant risk, as nearly two out of three short track speed skaters get injured during a season (Hendricks et al., 2024). Foam padding is placed around a short track speed skating ice rink to protect short track speed skaters during a crash. Because short track speed skaters collide with the padding during falls, effective impact absorption is crucial to prevent injuries (Tremblay, 2012). However, if padding is not tested under realistic conditions, its true protective capabilities remain uncertain. The KNSB developed a testing setup, the Impact & Crash Evaluator (ICE-G1), to simulate crashes by launching a sled with a rigid ram into the padding and measuring impact forces.

Yet, because this sled with a rigid ram behaves like an inanimate object, it fails to replicate the complex biomechanics of an actual human body during a crash. As a result, the impact forces measured do not fully capture how a short track speed skater's body would deform or react, leading to potentially misleading conclusions about the padding's performance, making this current approach insufficient.

Therefore, developing a new design that can be launched in padding is necessary. By transforming it from "something" into "someone" – that is, creating a dummy-like design that more closely mimics human biomechanics – data can be obtained that truly reflects real crash scenarios. This improved simulation will provide a better assessment of padding, ensuring that safety measures and choices are based on realistic and reliable results.

Hendricks, M., Verhagen, E., & Van de Water, A. T. M. (2024). Epidemiology, etiology and prevention of injuries in competitive ice speed skating—limited current evidence, multiple future priorities: A scoping review. Scandinavian Journal Of Medicine And Science in Sports, 34(4). https://doi.org/10.1111/sms.14614

Tremblay, R. (2012). Analysis on crash pad protection for short track on boarded rinks. https://www.isthq.com/wp-content/uploads/2023/05/AnalysisoncrashpadProtectionforShorttraconboardedRinks.pdf

→ *space available for images / figures on next page*

introduction (continued): space for images

image / figure 1 Padding around a short track ice rink

image / figure 2 The sled with a rigid ram of the ICE-G1

Problem Definition

What problem do you want to solve in the context described in the introduction, and within the available time frame of 100 working days? (= Master Graduation Project of 30 EC). What opportunities do you see to create added value for the described stakeholders? Substantiate your choice.
(max 200 words)

The current ICE-G1 testing setup does not realistically mimic the biomechanics of short track speed skaters during a crash. This is because the sled with a rigid ram behaves like a solid object rather than a human body. As a result, the forces measured do not accurately reflect how a short track speed skater's body would deform, rotate, or distribute impact forces, leading to unrealistic crash simulations.
In an ideal scenario, a real short track speed skater would be launched into the padding to test its effectiveness, as this would provide the most accurate data. However, this approach is unethical and impractical due to various reasons. Because of this, the ICE-G1 test setup is on one extreme of a spectrum—predictable but unrealistic—while a real skater represents the other extreme—realistic but unpredictable.
To bridge this gap, a new dummy-like design must be developed that balances realism with predictability, somewhere in the middle of the aforementioned spectrum. This dummy should allow controlled variations in crash behavior while still mimicking human biomechanics as closely as possible. By achieving this, the test results will better represent real-life crash dynamics, leading to more accurate padding assessments and ultimately improving short track speed skater safety.

Assignment

This is the most important part of the project brief because it will give a clear direction of what you are heading for. Formulate an assignment to yourself regarding what you expect to deliver as result at the end of your project. (1 sentence) As you graduate as an industrial design engineer, your assignment will start with a verb (Design/Investigate/Validate/Create), and you may use the green text format*:*

Design a new dummy-like product that can be launched in padding using the same launching mechanism which better replicates real short track crash dynamics

Then explain your project approach to carrying out your graduation project and what research and design methods you plan to use to generate your design solution (max 150 words)

This project will start with an analysis phase, where the current sled with a rigid ram will be analyzed, as well as biomechanics of short track speed skaters during crashes. In this phase, field research, like going to ice rinks, will take place and interviews will be held with short track speed skaters about their experiences.
After this phase, an ideation phase starts, where knowledge gained will be used to create initial ideas. Low-fidelity prototypes will be used to test certain ideas or assumptions, ultimately leading to a well thought-out design direction.
Inthe conceptualisation phase, this design direction will be explored, and more elaborate prototypes will be developed. This phase ends with the design of a final concept.
Inthe final phase, this concept will be developed and tested. Results will then be analyzed and presented in a clear manner.

Project planning and key moments
*To make visible how you plan to spend your time, you must make a planning for the full project. You are advised to use a Gantt chart format to show the different phases of your project, deliverables you have in mind, meetings and in-between deadlines. Keep in mind that all activities should fit within the given run time of 100 working days. Your planning should include a **kick-off meeting**, **mid-term evaluation meeting**, **green light meeting** and **graduation ceremony**. Please indicate periods of part-time activities and/or periods of not spending time on your graduation project, if any (for instance because of holidays or parallel course activities).*

Make sure to attach the full plan to this project brief.
The four key moment dates must be filled in below

Kick off meeting	6 mrt 2025
Mid-term evaluation	9 mei 2025
Green light meeting	15 juli 2025
Graduation ceremony	26 aug 2025

In exceptional cases (part of) the Graduation Project may need to be scheduled part-time. Indicate here if such applies to your project

Part of project scheduled part-time	
For how many project weeks	
Number of project days per week	

Comments:

Motivation and personal ambitions
Explain why you wish to start this project, what competencies you want to prove or develop (e.g. competencies acquired in your MSc programme, electives, extra-curricular activities or other).

Optionally, describe whether you have some personal learning ambitions which you explicitly want to address in this project, on top of the learning objectives of the Graduation Project itself. You might think of e.g. acquiring in depth knowledge on a specific subject, broadening your competencies or experimenting with a specific tool or methodology. Personal learning ambitions are limited to a maximum number of five.
(200 words max)

I've always been interested in sports, and ice skating in particular. While I have not practiced the sport myself, I've watched a lot of ice skating, with short track being the discipline I am most interested in. This is a relatively young sport, and thus has many design opportunities.

During a course in my master's degree, I've already worked on the initial testing system, which positively surprised me by its depth and creative freedom. I was keen on continuing working on this project, and wanted to design for the parts I was least involved in during initial development.

My specific goals are to learn how to include the human aspect in such a technical product, to get more experience with stakeholder management, to get more experience being owner and planner of my own project and to learn new prototyping skills in the process.

During this project, I want myself to be more proactive and confident. I will learn how to design effectively, trying to combine thinking (theoretical) and making (practical) more effectively to reach my goals, and to be bolder, to not be afraid to reach out to other companies for example, and just to do things I'm not sure about, instead of postponing these things.

B

List of requirements and wishes

The requirements of this project are based on findings in the theoretical framework and observations during testing. All requirements fit within the project scope. The wishes present aspects and additional factors which are relevant for evaluating crash dynamics, but which fall outside the scope of this project. They can form a starting point for future iterations or additional projects, but are not used in the scoping and decision making of this project.

Requirements

Subject	Aspect	Requirement #	Requirement	Origin
1. System compatibility & integration	1.1. Ice-G1 compatibility	*1.1.1.*	*The design must be fully compatible with the existing ICE-G1 rail system, motor assembly and launch mechanism*	Project brief
		1.1.2.	*No modifications to components other than the projectile shall be required*	Project brief
	1.2. Launch interface compatibility	*1.2.1.*	*The design must be able to integrate with the existing cable release mechanism*	Project brief
		1.2.2.	*The design must be able to handle small imperfections when crossing rail sections*	Pilot test
		1.2.3.	*The design must be able to withstand velocities up to 35 km/h without structural failure*	Beets et al. (2024)
2. Impact velocity & energy representation	2.1. Representative impact velocity	*2.1.1.*	*The design must be able to impact padding with a velocity of 35 km/h*	Beets et al. (2024)
	2.2. Velocity accuracy	*2.2.1.*	*The design must allow controlled impacts between the range of 25 and 35 km/h*	Beets et al. (2024)
		2.2.2.	*Under identical launch conditions, impact velocity must not vary more than 5% over 5 consecutive tests*	Beets et al. (2024)
3. Mass & Inertial properties	3.1. Mass representation	*3.1.1.*	*The design must represent a 72 kg average male short track speed skater*	Chapter 2.4
		3.1.2.	*The design must justify its equivalent mass based on physics if the mass is lower than 72 kg*	Chapter 2.4
	3.2. Mass distribution	*3.2.1.*	*The design must have a mass distribution similar to the distribution of a short track speed skater*	Chapter 2.1
4. Biomechanical representation	4.1. Contact area representation	*4.1.1.*	*The design must be able to simulate a back-first impact*	Chapter 2.2
		4.1.3.	*The design must provide a better pressure distribution compared to the ICE-G1's projectile*	Chapter 2.1
		4.1.4.	*The design must apply more realistic stress to the padding compared to the ICE-G1's projectile*	Chapter 2.1
		4.1.5.	*The design mus result in more realistic foam deformation behavior than the ICE-G1's projectile*	Chapter 2.1
		4.1.6.	*The design must avoid unrealistically high or low pressure put on the padding*	Chapter 2.1
		4.1.7.	*The design must result in a more realistic stopping distance compared to the ICE-G1's projectile*	Chapter 2.4
	4.2. Padding impact	*4.2.1.*	*The design must impact padding at the lower third of the padding*	Chapter 2.2
		4.2.2.	*The design must be able to test straight (90 degree) impacts*	Chapter 2.2
		4.2.3.	*The design must be able to test impacts with an angle between 35 and 55 degrees*	Chapter 2.2
		4.2.4.	*The design must be abe to test all padding types*	Project brief
		4.2.5.	*The design must be able to test single padding impact*	Chapter 2.2
		4.2.6.	*The design must be able to test between padding impact*	Chapter 2.2
		4.2.7.	*The design must be able to activate all necessary layers of foam in padding*	Chapter 2.1
5. Measurement & data acquisition	5.1. Sensor settings	*5.1.1.*	*The sensor must be able to measure impacts without being capped at a limit*	On-ice testing
		5.1.2.	*The sensor must be able to measure with a sampling frequency of at least 1000 Hz*	Beets et al. (2024)
		5.1.3.	*The sensor must not run out of charge during a test*	Beets et al. (2024)
	5.2. Sensor placement	*5.2.1.*	*The sensor must be located at a representative location on the design*	Chapter 2.3
		5.2.2.	*The sensor must be placed with one measurement direction directly towards the impact direction*	Beets et al. (2024)
		5.2.3.	*The sensor's placement must reduce data noise compared to the ICE-G1 projectile*	Pilot test
	5.3. Measurements & repeatability	*5.3.1.*	*The design must be able to measure acceleration forces*	Project brief
		5.3.2.	*The data must be able to be compared to both ISU drop test measurements and ICE-G1 test measurements*	Project brief
		5.3.3.	*The design must be able to measure impact velocity*	Beets et al. (2024)
		5.3.4.	*The design must be able to measure the stopping distance*	Beets et al. (2024)
		5.3.5.	*Measurements of the design must not vary by more than 10% over 5 consecutive tests*	
		5.3.6.	*Measurements of the design must indicate interpretable safety risk for short track speed skaters*	Chapter 2.3
6. Structural integrity & safety	6.1. Structural safety	*6.1.1.*	*The design must not structurally fail during tests with velocities of 35 km/h*	Beets et al. (2024)
		6.1.2.	*The design shall not harm the operators with loose parts before, during and after impact*	Beets et al. (2024)
		6.1.3.	*The design must not have open sharp, hot or otherwise dangerous parts which could harm operators*	Beets et al. (2024)
		6.1.4.	*Internal masses in the design must be fixed in place and secured during impact*	Chapter 4.3
	6.2. Operator safety	*6.2.1.*	*Parts of the design must not exceed 40 kg*	Beets et al. (2024)
		6.2.2.	*The design must consist of modular parts*	Beets et al. (2024)
		6.2.3.	*Operators must be able to have a safe distance compared to padding during tests with the design*	Beets et al. (2024)
		6.2.4.	*Operators must understand the risks of carrying out the test and working with the design*	Beets et al. (2024)
		6.2.5.	*The design must be resettable by two operators without lifting loads exceeding ergonomic safety*	Beets et al. (2024)
7. General constraints	7.1. Environment	*7.1.1.*	*The design must be able to operate at temperatures of -6 degrees celsius*	Beets et al. (2024)
		7.1.2.	*The design must not lose structural integrity due to the humid conditions*	Beets et al. (2024)
		7.1.3.	*The design must be protected against moisture*	Beets et al. (2024)
		7.1.4.	*The design must not sink in ice*	Beets et al. (2024)
		7.1.5.	*The design must not melt the ice*	Beets et al. (2024)
	7.2. Durability	*7.2.1.*	*The design must consists of replaceable parts in case of damage*	On-ice testing
		7.2.2.	*The design must be able to withstand at least 250 crashes before parts need replacements*	Beets et al. (2024)
	7.3. Budget	*7.3.1.*	*The prototype for the design must not exceed €2000*	Project brief
		7.3.2.	*The design must not cost more than €40.000*	Beets et al. (2024)
	7.4. Transportability	*7.4.1.*	*The design must be able to be placed in an average family car*	Beets et al. (2024)
		7.4.2.	*The design must fit with all other ICE-G1 components in an average family car*	Beets et al. (2024)
		7.4.3.	*The design must be able to be moved to the ice rink by two people*	Beets et al. (2024)

Wishes

Subject	Aspect	Wish #	Wish	Origin
1. System compatibility & integration	1.1. Ice-G1 compatibility	*1.1.1.*	*The design should be able to adapt to future changes of the launching mechanism*	Recommendations
	1.2. Launch interface compatibility	*1.2.1.*	*The design should be able to withstand velocities up to 60 km/h without structural failure*	Chapter 2.1
2. Impact velocity & energy representation	2.1. Representative impact velocity	*2.1.1.*	*The design should be able to impact padding with a velocity of 60 km/h*	Chapter 2.1
	2.2. Velocity accuracy	*2.2.1.*	*The design should allow controlled impacts between the range of 50 and 60 km/h*	Chapter 2.2
		2.2.2.	*The design should be able to be launched with exactly the same velocity every time*	Beets et al. (2024)
3. Mass & Inertial properties	3.1. Mass representation	*3.1.1.*	*The design should allow mass changes to represent heavier skaters*	Beets et al. (2024)
		3.1.2.	*The design should allow mass changes to represent lighter skaters*	Beets et al. (2024)
	3.2. Mass distribution	*3.2.1.*	*The design should allow the mass distribution to be altered*	Chapter 2.4
4. Biomechanical representation	4.1. Contact area representation	*4.1.1.*	*The design should enable the possibility to simulate head-first impacts*	Chapter 2.2
		4.1.2.	*The design should enable the possibility to simulate hips-first impacts*	Chapter 2.2
		4.1.3.	*The design should enable the possibility to simulate legs-first impacts*	Chapter 2.2
		4.1.4.	*The design should enable the possibility to simulate legs-up bottom-first impacts*	Chapter 2.2
		4.1.5.	*The design's pressure distribution should be exactly like the distribution of a short track speed skater*	Chapter 2.1
		4.1.6.	*The design should apply the exact amount of stress on the padding as a short track speed skater would*	Chapter 2.1
		4.1.7.	*The design should provoke a similar reaction from foam as a short track speed skater would*	Chapter 2.1
		4.1.8.	*The design should have the exact stopping distance as a short track speed skater would have*	Chapter 2.4
		4.1.9.	*The design should be made of a softer tissue material resembling skin tissue*	Chapter 2.3
5. Measurement & data acquisition	5.1. Sensor settings	*5.1.1.*	*The sensor should have a sampling frequency of at least 3000 Hz*	On-ice testing
		5.1.2.	*The design should use more than a single sensor*	On-ice testing
		5.1.3.	*Sensor noise should be completely eliminated*	Pilot testing
	5.2. Sensor placement	*5.2.1.*	*The design should allow the sensor to be swapped to different locations*	Chapter 2.3
		5.2.2.	*The locations of the sensor should provide information about fragile body parts with risk of injury*	Chapter 2.3
	5.3. Measurements & repeatability	*5.3.1.*	*The design should be able to measure rotational acceleration*	Chapter 2.2
		5.3.2.	*The design should provide insight into segmental deceleration differences of a short track speed skater*	Chapter 2.3
		5.3.3.	*Measurements of the design should not vary by more than 5% over 5 consecutive tests*	
6. Structural integrity & safety	6.1. Structural safety	*6.1.1.*	*The design should not structurally fail during tests with velocities of 60 km/h*	Chapter 2.1
		6.1.2.	*Internal masses in the design should not be able to move*	Chapter 4.3
	6.2. Operator safety	*6.2.1.*	*The design should not be able to harm operators in case of unforseen derailment*	On-ice testing
		6.2.2.	*The design should provoke a feeling of trust and safety*	Beets et al. (2024)
		6.2.3.	*All individual parts of the design should be able to be carried by a single operator without exceeding ergonomic safety*	Beets et al. (2024)
		6.2.4.	*Operators should not require special safety gear in order to use the design*	Beets et al. (2024)
		6.2.5.	*Operators should be allowed to leave the ice while still being able to start the launch sequence*	On-ice testing
7. General constraints	7.1. Environment	*7.1.1.*	*Water should not be able to damage or wear the design*	Beets et al. (2024)
		7.1.3.	*The design should not damage the ice or padding in case of an unforseen bad launch*	On-ice testing
	7.2. Durability	*7.2.1.*	*All parts that are designed to wear down should be able to be easily replaced within 10 minutes*	On-ice testing
		7.2.3.	*Every part of the design should be recyclable*	Beets et al. (2024)
	7.3. Transportability	*7.3.1.*	*The design should be able to be transported in a small family car*	Beets et al. (2024)
		7.3.2.	*All parts of the design should be able to be moved to the ice rink by a singular person*	Beets et al. (2024)

C

ICE-G1 details

This chapter describes the Impact and Crash Evaluator 1st Generation (ICE-G1) testing method in detail. The goal of this chapter is to provide a clear and complete understanding of what the ICE-G1 is, how it functions, and how its components are integrated into a single testing system. This chapter does not yet evaluate the ICE-G1 or compare it to real crash dynamics. Instead, it establishes a shared technical and conceptual reference that will be used throughout the remainder of the report. First, the purpose and intended testing philosophy of the ICE-G1 are explained. Next, the main components of the system are described in detail, including their function within the overall test setup. Finally, a synthesis summarizes the ICE-G1 as a testing method and explicitly positions the component that is central to this project.

C.1. Purpose and context of the ICE-G1 method

The ICE-G1 test method was developed to improve upon the existing industry standard padding safety test prescribed by the ISU, commonly referred to as the ISU drop test. While the drop test offers a highly controlled and repeatable method, it is limited to vertical impacts on individual padding elements and does not allow testing under more realistic, on site conditions. The original design assignment for the ICE-G1 was to create a portable testing system that could be transported using a standard passenger vehicle and deployed directly at ice rinks. In the long term, the system was envisioned to function both as a development tool for evaluating new padding systems and as a recurring inspection tool to assess the condition and safety performance of padding currently in use.

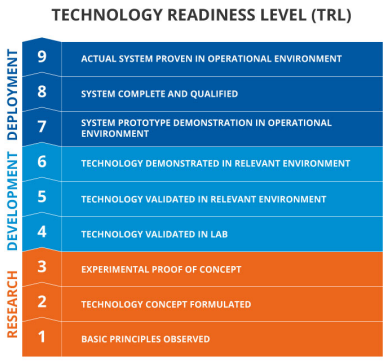

The ICE-G1 was developed over a period of approximately 20 weeks by a team of six masters students from the Industrial Design Engineering faculty at Delft University of Technology. The outcome of this project was a functional prototype intended to validate core design assumptions and demonstrate feasibility, rather than a finalized, fully operational testing product. In terms of Technological Readiness Levels (TRL), the ICE-G1 can be classified primarily at TRL 3, indicating experimental proof of concept validation.

From a testing philosophy perspective, the ICE-G1 was designed to simulate a highly controlled crash scenario: a linear, back first impact of a heavy short track speed skater against rink padding. All major system parameters were selected to represent a p90 male short track speed skater impacting the padding at a velocity of approximately 60 km/h, without rotational motion. The focus on this specific crash configuration reflects an intention to capture a common and severe loading case while maintaining comparability with the ISU drop test.

The ICE-G1 measures acceleration during impact using an accelerometer integrated into the projectile, and peak acceleration values are used as the primary safety metric. By collecting data similar in nature to the ISU drop test while enabling on site testing and horizontal impact motion, the ICE-G1 establishes a methodological bridge between existing standardized testing and more realistic crash representation.

TEST PARAMETERS:

Mass projectile: 30 kg
Velocity: 20-35 km/h
Area of impact: 0,0314 m^2
Angle of impact: 90°
Location of impact: bottom center

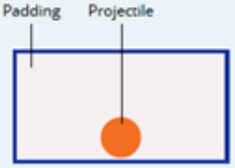

C.2. Test components in detail

The ICE-G1 testing system consists of three primary subsystems: the motor assembly, the rail system, and the projectile. These components are mechanically integrated into a single launch and impact system. During a test, the system accelerates a projectile along a straight rail track toward the rink padding, reaching velocities of up to approximately 35 km/h. Acceleration is achieved by winding a nylon cable around a rear mounted winch driven by an electric motor. The cable is routed from the rear winch to the front of the rail system, around a front pulley, and back toward the rear, where it is connected to the projectile . When the motor is activated, the cable pulls the projectile forward along the rails. Once the projectile passes over the front pulley, the cable automatically detaches, allowing the projectile to leave the rails and impact the padding freely. After impact, the system is reset for subsequent tests.

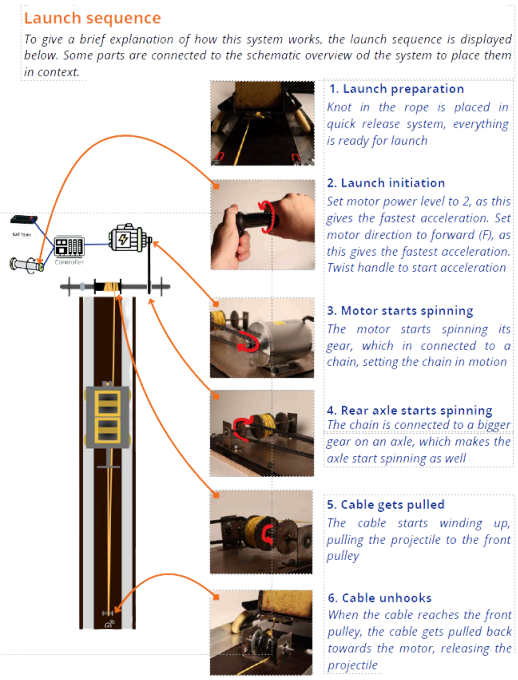

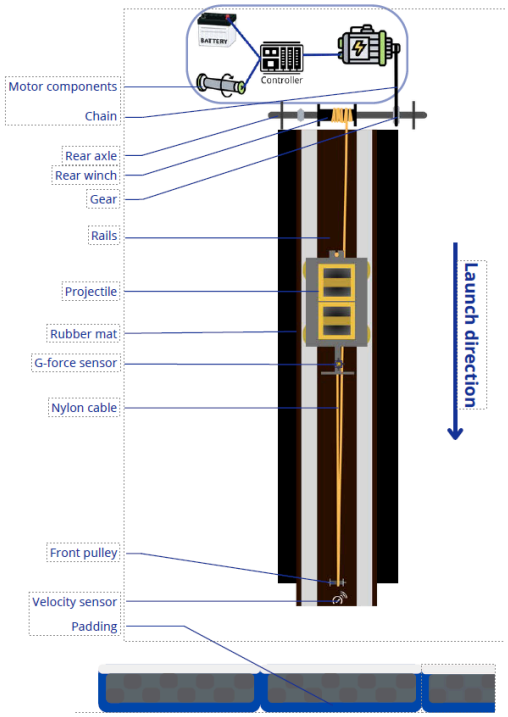

The propulsion system of the ICE-G1 is based on a VEVOR 3 kW, 72 V brushless DC motor. The motor is powered by a 72 V battery pack consisting of five batteries connected in series. System control is provided through a throttle interface, allowing the operator to regulate motor speed manually. As a result, the exact launch velocity varies slightly between tests. For safety and usability, the system includes an electronic lock that allows the user to shut down the system when needed. The motor is connected to the rear winch via a chain with a 1:2 gear ratio, translating motor torque into cable tension sufficient to accelerate the projectile along the rails to the intended velocity.

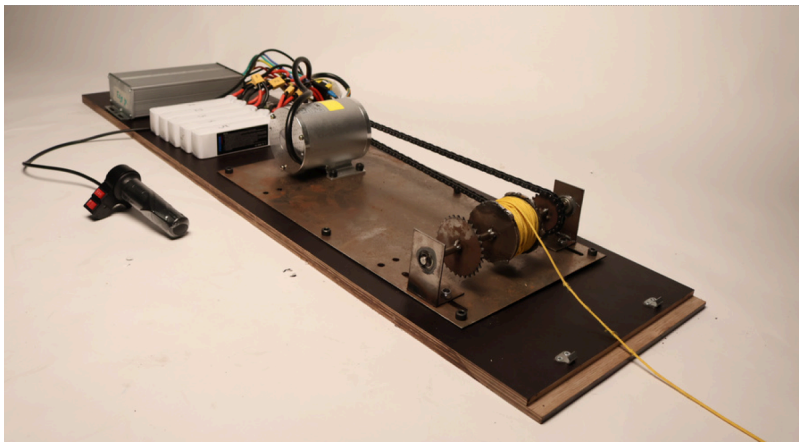

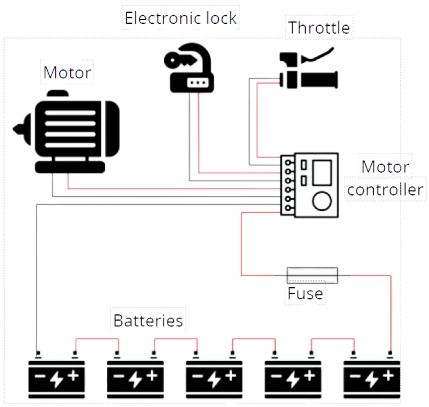

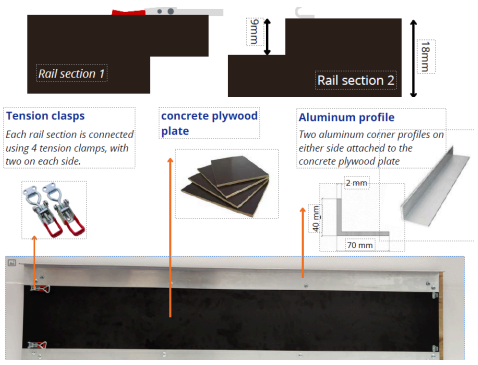

The rail system provides guidance and support for the projectile during acceleration. It consists of six modular rail sections, each 1.5 meters in length, resulting in a total rail length of 9 meters. An additional rear rail section houses the motor and drive components and is not included in the 9 meter measurement.
Each rail section is 400 mm wide and 18 mm thick and is constructed from a concrete plywood base with two L-shaped aluminum profiles mounted along the sides. These aluminum profiles serve as guide rails for the projectile wheels. Rail sections are connected using overlapping ends and secured with tension clasps, with two clasps positioned on each side of the rails. Alignment between rail sections is performed manually, without dedicated alignment tools, which may introduce small geometric deviations along the rail length.

The projectile is the component that directly interacts with the padding and is therefore central to the ICE-G1 test method. The projectile has overall dimensions of $400 \times 270 \times 145$ mm and is mounted on wheels of inline skates to minimize rolling resistance along the rails. On top of the main projectile structure, an open container (300 Œ 150 mm) houses two removable weights with a combined mass of approximately 24 kg. At the rear of the projectile, a quick release mechanism enables automatic detachment of the cable at the end of the launch phase. The front of the projectile features a circular ram with a diameter of 200 mm. This geometry was selected to approximate a back first human body impact and to ensure consistent contact with the padding. The ram is positioned approximately 250 mm ahead of the main projectile body, ensuring that only the ram makes contact with the padding during impact. An accelerometer is mounted directly behind the ram to measure impact acceleration while remaining protected from direct contact forces.

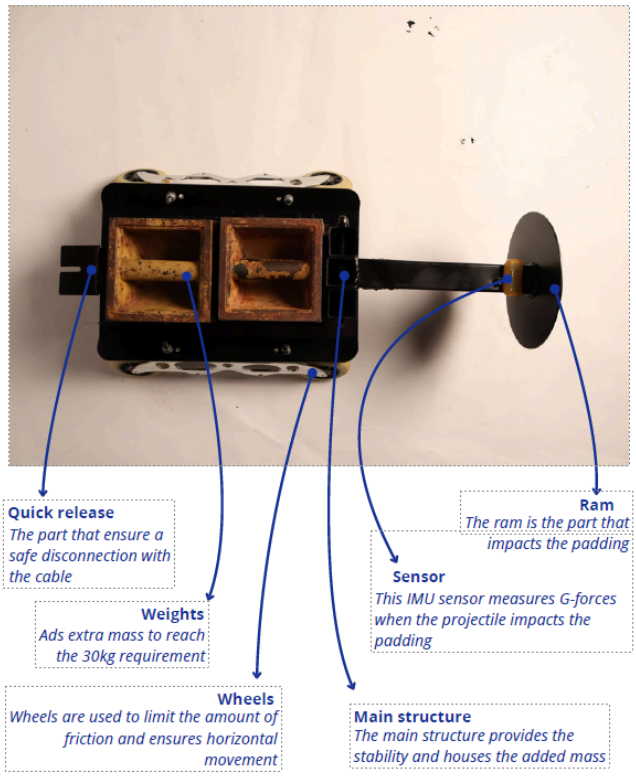

D

MCA analysis

To uncover relationships between variable in crash dynamics, a Multiple Correspondence Analysis (MCA) was performed. The MCA identifies dimensions, each of which represents a dominant pattern of difference in the dataset. Importantly, a dimension should not be interpreted as a single variable, but as a contrast between two groups of variables that tend to co-occur. Each dimension can therefore be understood as a continuum with two opposing sides: Variables located on the same side of a dimension tend to occur together and variables on opposite sides of a dimension rarely co-occur. The meaning of a dimension emerges from the combined interpretation of the variables defining its two ends. A key consequence is that a variable may appear close to another variable in one dimension, but can appear unrelated or even opposed to that same variable in another dimension. This does not indicate a contradiction, but rather that crash behavior is multi-dimensional: different mechanisms dominate different aspects of the crash. Only variables that contribute meaningfully to a dimension are shown in the plots, which are calculated values after performing the MCA. Variables close to the center have little explanatory power and are omitted. Variables further from the center have stronger interpretative value. The first four dimensions were analyzed, together explaining approximately 60

Phase 1		Phase 2		Phase 3		Phase 4		Phase 5	
Abbr.	**Correspondence**	**Abbr.**	**Correspondence**	**Abbr.**	**Correspondence**	**Abbr.**	**Correspondence**	**Abbr.**	**Correspondence**
poa	Push other athlete	sitting	Sitting on ice	str	Straight impact (90-81 degrees)	baf	Back-first impact	hea	Head post-impact movement
iba	Ice breaking away	lying	Lying on hips	tff	Angled impact (55-35 degrees)	shf	Shoulder-first impact	no	No post-impact movement
coa	Collision other athlete	towards	Towards padding	thi	30-40 km/h	hif	Hips-first impact	leg	Legs post-impact movement
fsi	Front skate in ice	away	Away from padding	fou	40-50 km/h	lub	Legs-up bottom-first impact		
soi	Shoe on ice	side	Parallel to padding	low	Lowest region of padding				
lob	Loss of balance			red	Main crash zone 1				
				blu	Main crash zone 2				

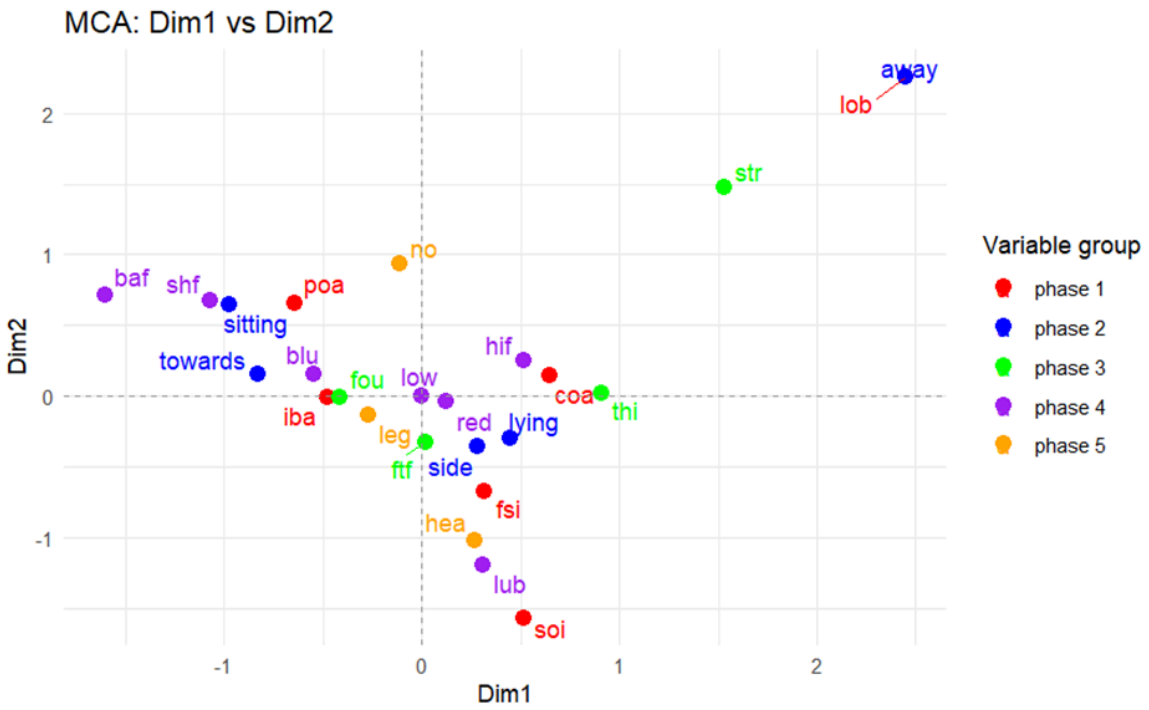

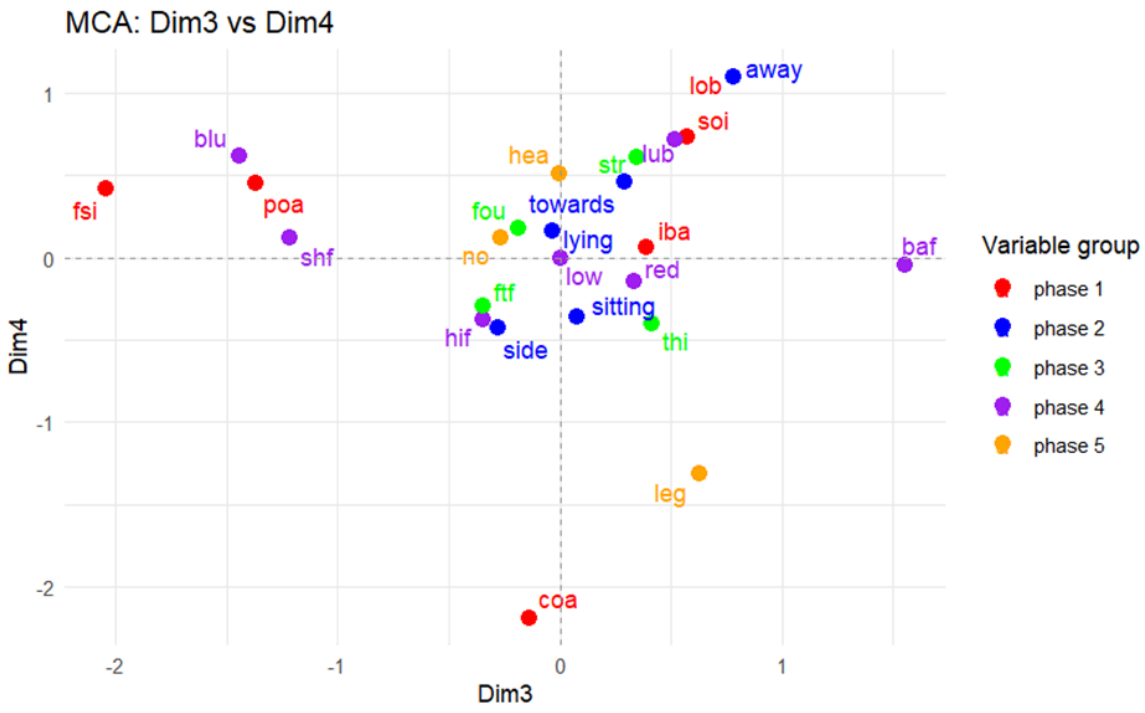
MCA: Dim3 vs Dim4
Dim4
Dim3
1
0
-1
-2
-2
-1
0
1
away
lob
soi
blu
hea
str
lub
fsi
poa
towards
fou
lying
iba
baf
shf
no
low
red
ftf
sitting
hif
side
thi
leg
coa
Variable group
phase 1
phase 2
phase 3
phase 4
phase 5

E

Design process specifics

In the design process, the back-first shape has been explored. The next step to attach such a shape to the cart base is the start of this appendix. Initially, the ideation proceeded with an extra requirement that the projectile should be able to change between the back-first impact type and the head-first impact type. This is what was explored first in the ideation phase. Later, after conversations with supervisors and careful considerations, this requirement was dropped. The final design was chosen without this requirement, but earlier ideation still revolved around the idea of changing impact types between launches. The start of ideation revealed four techniques that could be used to attach a shape to a cart base which is compatible with the ICE-G1 launching infrastructure. This is important, as it allows the ramming component and cart to be transported separately, and to make sure two people would be able to transport all components to the ice rink without exceeding the ergonomic lifting limits. These four techniques have been drawn, and form the basis of the next ideation technique. Four models have also been created to see how each technique could function.

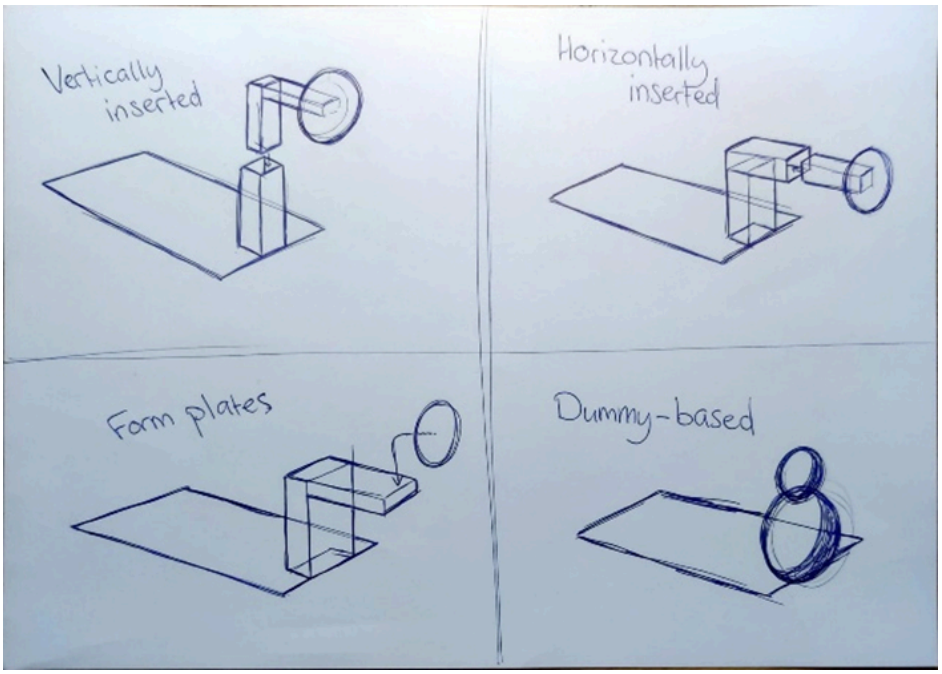

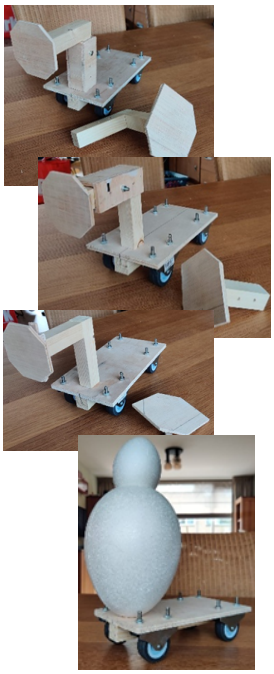

Based on the insights gathered from the physical models and other main questions that arose, multiple questions have been formulated with the aim to provide a solution to a single small problem of the design, such as how to add/remove mass and how to lock the shape securely in place. Answers to these questions have been put in a chart, which is the basis for the subsequent sketching phase.

For each shape-attachment technique, nine sketches have been made based on 3 to 5 solutions in the chart. Three of these sketches have been made based on my own thoughts and expectations of what would result in good ideas. Six of these sketches used random answers generated by a randomizer. This would result in ideas that I personally liked, but also forced me to think creatively and find solutions that I did not think of.

Idea #	Main direction	Sol. 1	Sol. 2	Sol. 3	Sol. 4	Sol. 5
1	Vertical inserted	H-1	I-1	C-4	-	-
2	Vertical inserted	B-8	G-3	C-6	-	-
3	Vertical inserted	E-3	G-2	C-3	-	-
4	Vertical inserted	J-2	C-1	F-4	B-6	-
5	Vertical inserted	C-4	D-1	J-4	I-5	-
6	Vertical inserted	H-5	B-4	J-3	D-7	E-1
7	Vertical inserted	C-6	H-2	G-1	-	-
8	Vertical inserted	D-6	H-1	C-1	B-5	-
9	Vertical inserted	C-2	H-3	J-1	-	-
10	Horizontal inserted	I-1	E-5	F-3	-	-
11	Horizontal inserted	G-3	H-5	B-2	-	-
12	Horizontal inserted	I-4	E-2	F-2	-	-
13	Horizontal inserted	G-2	I-2	H-1	F-2	-
14	Horizontal inserted	B-7	G-2	F-2	H-3	-
15	Horizontal inserted	E-3	F-3	C-3	G-3	J-2
16	Horizontal inserted	F-4	B-2	H-3	-	-
17	Horizontal inserted	D-4	G-2	B-2	-	-
18	Horizontal inserted	E-3	F-2	I-5	-	-
19	Form plates	C-1	E-2	B-8	-	-
20	Form plates	G-3	F-2	J-2	-	-
21	Form plates	C-2	I-5	E-2	-	-
22	Form plates	J-3	E-5	D-2	G-2	-
23	Form plates	E-1	H-3	C-2	D-5	-
24	Form plates	E-5	C-2	D-4	G-1	J-1
25	Form plates	B-8	C-3	H-1	I-1	-
26	Form plates	D-5	B-5	I-3	-	-
27	Form plates	B-1	G-3	F-3	-	-
28	Dummy	D-5	I-1	F-4	-	-
29	Dummy	F-1	D-6	G-2	-	-
30	Dummy	E-2	C-4	D-5	-	-
31	Dummy	I-2	C-4	J-4	G-3	-
32	Dummy	D-3	G-1	B-6	I-2	-
33	Dummy	I-3	J-2	G-1	F-1	D-4
34	Dummy	F-1	B-8	C-4	E-2	-
35	Dummy	D-6	B-2	I-4	-	-
36	Dummy	J-4	G-3	B-9	-	-

The 36 sketches that resulted from this process have been scored on feasibility, viability and desirability based on personal assessment. Nine ideas were scored best. These ideas were worked out further by incorporating solutions which were not yet incorporated in the design.

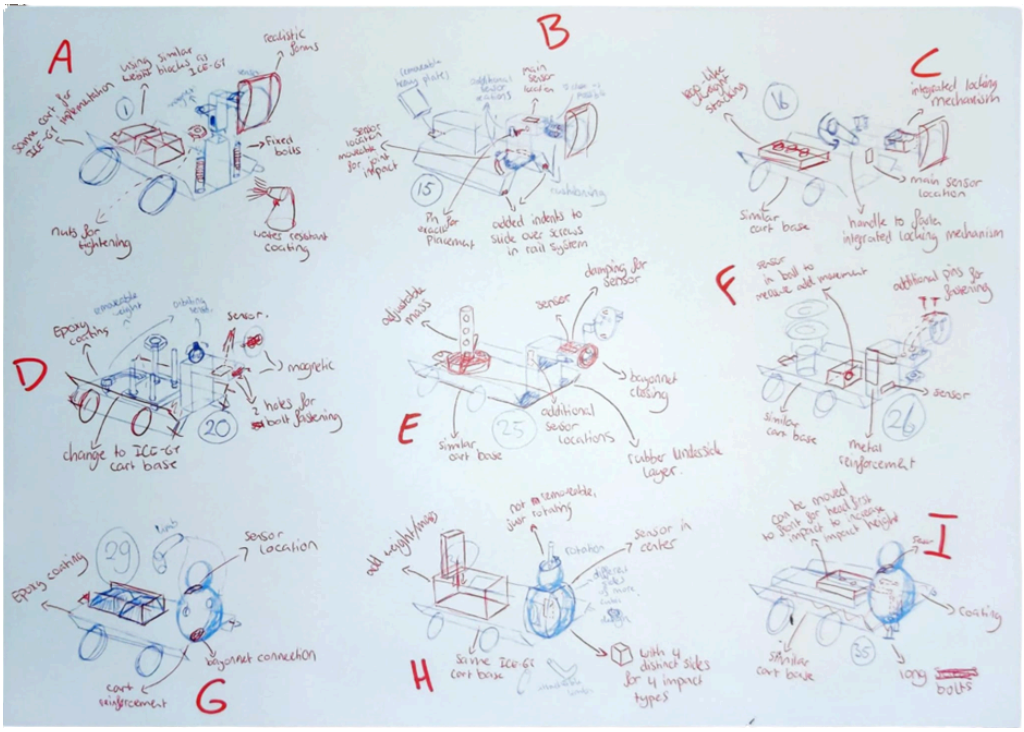

Category	SOLUTIONS								
Main direction	Vertical inserted	Horizontal inserted	Form plates	Dummy					
Locking mechanism	Magnets	Screws	Bayonnet connection	Vacuum	Bolts and nuts	Rope	Tie-wraps	Clamps	Glue
Improving impact resistance	Metal plates	Epoxy layer	Cushioning	Spinal features	Layered material	Glue			
Adding mass	Sand	Water	Actual human being	Halters	Heavy plates	Heavy solid object	Thicker material use		
Make moist resistant	Spray	Epoxy layer	Tight fastening	Rubber layer	Sponges				
Post-impact movement possibility	Attachable limbs	Orbiting sensor	Extra sensor joint locations	bendy sticks					
ICE-G1 compatibility	Same cart	Reversed cart	Sliding base						
Ensuring similar impacts during testing	Magnets	Pins	Guiding rails	Sensors	Color coded	Legos			
Sensor placement	Cushioned behind contact area	In front contact area	At joint location	Center of mass	Right behind contact area				
Ensuring handability by two operators	Removable parts	Removable mass	Easy to roll forwards	Grippy handles					

Legend

- Idea A
- Idea B
- Idea C
- Idea D
- Idea E
- Idea F
- Idea G
- Idea H
- Idea I

These ideas have been scored based on a selection of requirements, which revealed three main concepts that should be refined further, which are concepts G and I combined, concept H and concepts D and E combined. These have been detailed more in a poster format, after which the final choice has been made based on important requirements defined in chapter 3.

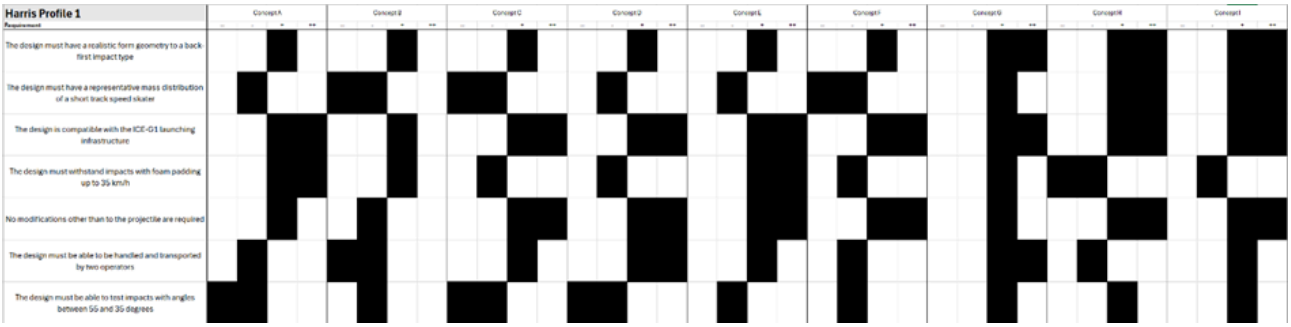
Harris Profile 1
Requirement
Concept A
Concept B
Concept C
Concept D
Concept E
Concept F
Concept G
Concept H
Concept I
The design must have a realistic form geometry to a back first impact type
The design must have a representative mass distribution of a short track speed skater
The design is compatible with the ICE-G1 launching infrastructure
The design must withstand impacts with foam padding up to 35 km/h
No modifications other than to the projectile are required
The design must be able to be handled and transported by two operators
The design must be able to test impacts with angles between 55 and 35 degrees

F

Material and manufacturing substantiation

Harrie consists of a rigid internal load-bearing core, an outer shell defining the contact geometry, and additional mass elements to achieve the required mass distribution. The internal core is manufactured from aluminium alloy (AA6061-T6), selected for its combination of high stiffness, relatively low density (2700 kg/mş), and stable behaviour under dynamic loading. This ensures that the structure remains effectively rigid during impact, preventing internal deformation that could influence the measured acceleration signal. The core incorporates spine-like reinforcement features that increase the second moment of area, thereby improving bending stiffness and distributing impact loads over a larger volume. This reduces local stress concentrations and ensures that the structure behaves as a single load-bearing body. The outer shell is manufactured from polycarbonate (PC) with an approximate thickness of 35 mm. This shell defines the external geometry and contact surface, and is sufficiently impact-resistant and ductile to withstand repeated impacts without cracking or permanent deformation. The global mass distribution is achieved through a combination of the aluminium core and additional steel mass elements. Due to its high density (7850 kg/mş), steel allows compact integration of mass, enabling precise positioning of the centre of mass relative to the contact surface without increasing the overall geometry.

The torso and legs are rigidly connected to the cart through bolted interfaces using steel fasteners (e.g. M6M8) in combination with threaded inserts embedded in the aluminium core. The inserts ensure load transfer into the core material without local thread failure, while the use of multiple connection points prevents rotation and relative motion between components. This rigid coupling is required to ensure that the dummy and cart behave as a single rigid body during impact, eliminating additional degrees of freedom that could affect measurement repeatability. The acceleration sensor is mounted in the chest region within a rigid housing that is directly coupled to the internal core. This mounting configuration ensures that the measured signal represents the global deceleration of the torso rather than local structural vibrations or compliance. The positioning of the sensor near the primary impact region further ensures that peak accelerations are captured accurately.

The internal core is manufactured using CNC machining from a solid aluminium block, allowing precise control over geometry, mass distribution, and integration of internal features such as reinforcement ribs and insert locations. This method ensures high dimensional accuracy and repeatability between prototypes. The outer shell can be manufactured using thermoforming or additive manufacturing, depending on required surface quality and production constraints. Thermoforming provides a smooth and continuous surface with uniform thickness, while additive manufacturing allows rapid iteration and integration of geometric features during development. Steel mass elements are manufactured as prismatic blocks and attached using bolted connections, allowing straightforward adjustment of mass distribution during calibration. The modular design enables disassembly and replacement of individual components, facilitating maintenance and iterative refinement without requiring complete reconstruction of the system.

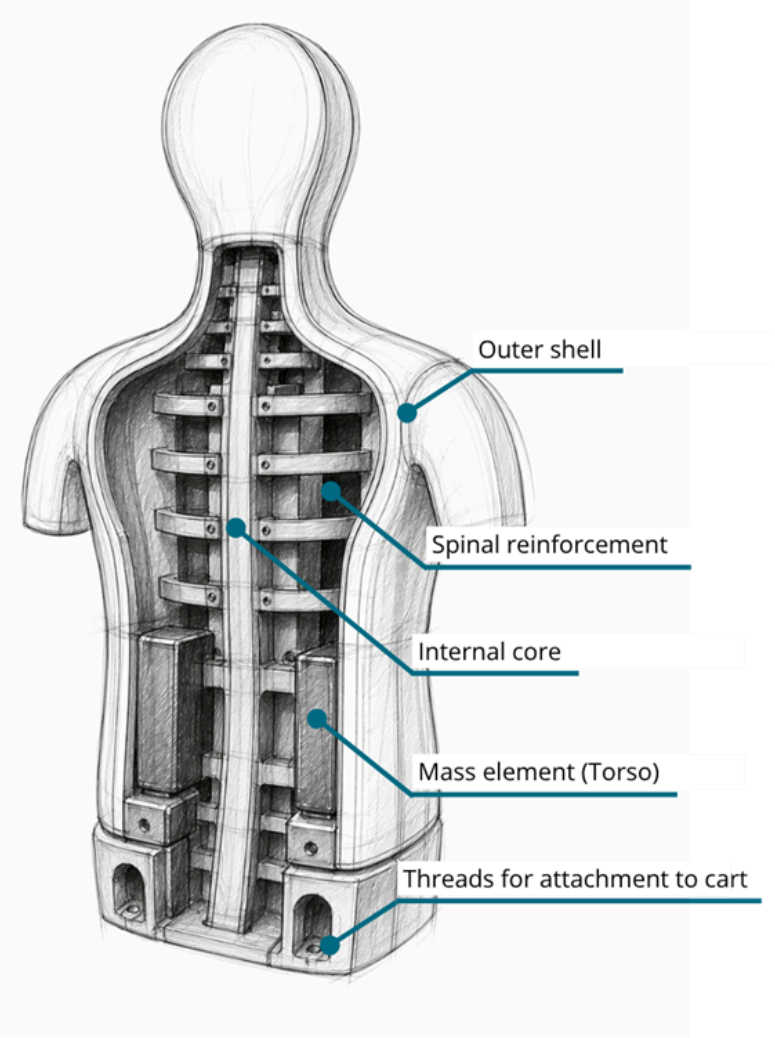

Component	Material	Key Properties	Function	Manufacturing Method
Internal core	Aluminium (AA6061-T6)	High stiffness, low density	Load-bearing structure	CNC machining
Spinal reinforcement	Aluminium (integrated)	Increased second moment of area	Load distribution and stiffness increase	CNC machining
Outer shell	Polycarbonate (PC)	Impact resistant, ductile	Defines contact geometry	Thermoforming / 3D printing
Mass elements (torso)	Steel	High density (7850 kg/mş)	Local mass distribution	Machining / standard stock
Mass elements (cart)	Steel	High density, robust	Global mass distribution	Machining
Fasteners & inserts	Steel	High strength, wear resistant	Structural connections	Standard components
Sensor housing	Aluminium / polymer	Stiff, dimensionally stable	Sensor fixation	CNC / 3D printing

G

Prototype development and measurements

The central objective of the prototype is to mimic the form geometry and mass distribution of the final design. Its manufacturing methods and material choices differ, as the prototype is not expected to be used regularly, but rather to test the hypothesis if the theory is applied correctly. As the final design is made to mimic the upper body of short track speed skaters, a 3d model has been created which should represent the average male short track speed skater.

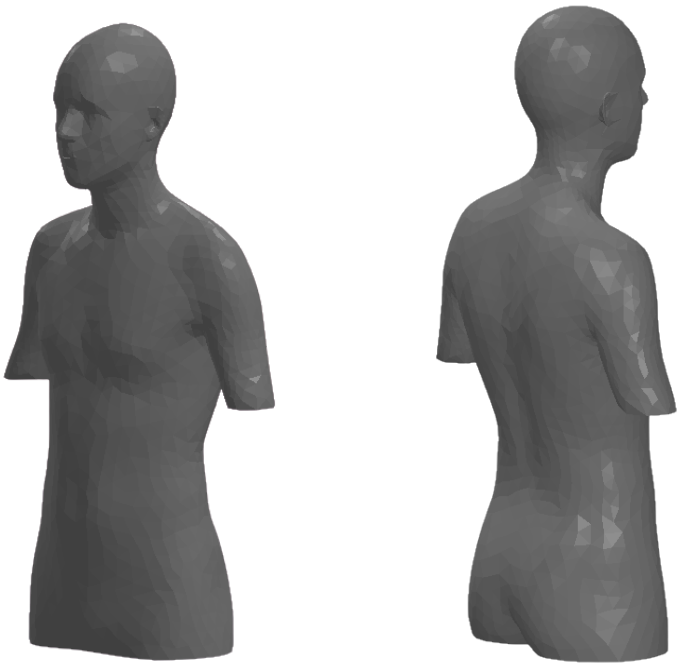

This model is based on the measurements and scaling factor defined in chapter 5. Below, a more detailed figure describes the mates and measurements in more detail.

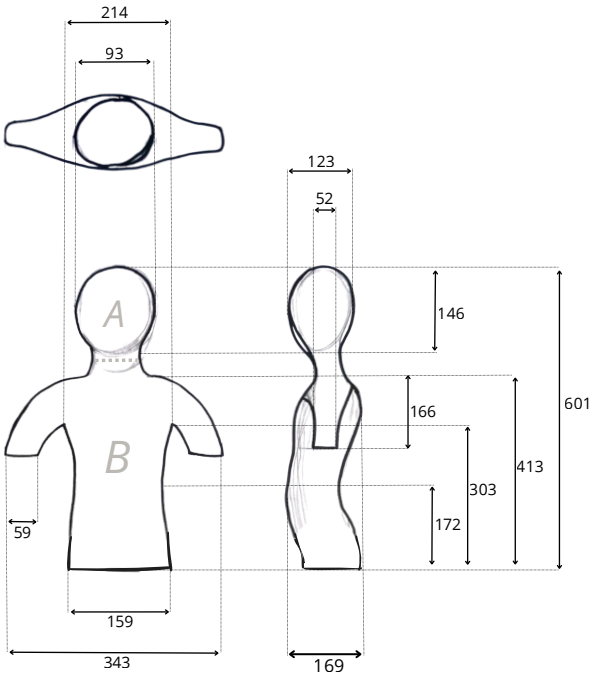

As the prototype is constructed from poplar plywood, additional mass needs to be added. Poplar plywoods density means that constructing the dummy from just plywood would result in a mass which is considered too low. To get a mass of 30 kg, internal cavities have been added which will be filled with steel plates. These plates will subsequently also function as the spinal reinforcement of the prototype. The volume of the cavities have been calculated using the difference in density between poplar plywood and steel, to calculate how much plywood must be changed to steel in order to get the designed mass distribution. This leads to the following cavities in the prototype.

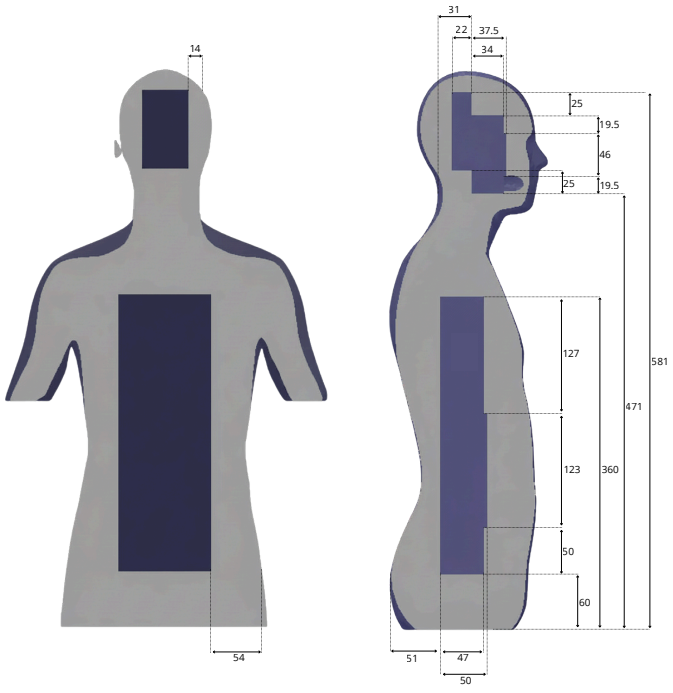

After finalizing the 3d model with its cavities, a file has been created to execute the laser cutting method to create plywood pieces with 9mm thickness. Based on poplar plywood plates with dimensions of 1200 x 700 x 9 mm, three plates are needed to be able to cut all necessary pieces.

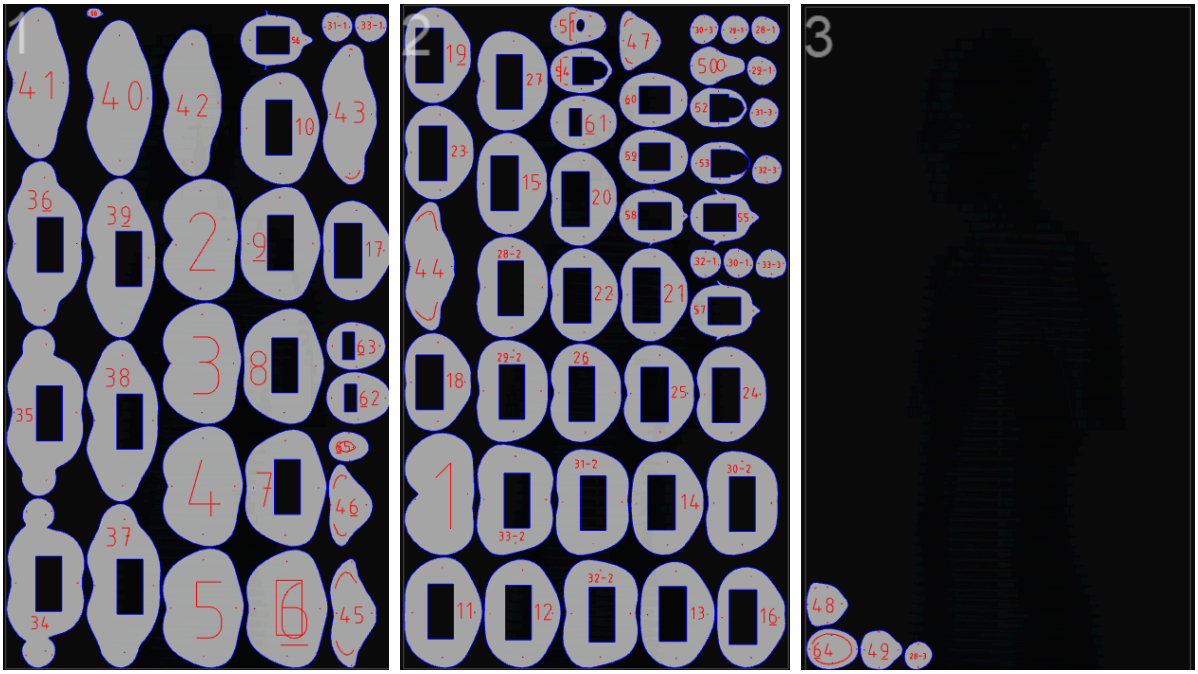

These pieces are assembled in the correct order, and steel plates are inserted before finalizing the construction of the prototype. Sanding is required, especially at the back, to smoothen the connection between the plywood pieces. It is estimated that the mass lost because of this sanding is minimal, and does not effect the test results in a meaningful way. Adding weights as additional mass to the cart finalizes the prototype, and its ready for use. A neck gaiter from the KNSB is used to dress up the prototype during testing.

H

Detailed test plan and analysis strategy

H.1. Test objectives

During the two planned test days, several aspects of the dummy will be evaluated. The primary goal of these tests is to assess whether the dummy functions as intended and whether it provides reliable and meaningful results under realistic conditions.

- **G1 Simulation accuracy**
  - G1.1 Determine whether the deceleration curve matches expectations
  - G1.2 Evaluate whether measured g-forces fall within the expected range
  - G1.3 Assess whether the penetration depth into the padding matches expectations
- **G2 Measurement repeatability**
  - G2.1 Analyse variation between repeated measurements
  - G2.2 Determine differences between padding elements of the same type
- **G3 Identification of weaknesses**
  - G3.1 Assess whether structural failure occurs
  - G3.2 Identify where and why damage appears on the dummy
  - G3.3 Evaluate whether the dummy causes damage to the padding or ice

Overall, these objectives focus on evaluating the functionality and reliability of the dummy, validating design assumptions, and identifying areas for improvement in future iterations.

H.2. Test approach

All tests are performed using a back-first impact configuration. By limiting the experiments to a single type of crash scenario, variability between tests is reduced, improving reliability and comparability.

The first test block takes place on Wednesday between 12:00 and 14:30 on the ice hockey rink. During this session, the focus is on collecting a large dataset of repeated straight impacts into the padding. The setup phase takes approximately 20 minutes, after which multiple sets of launches are performed. Each set consists of approximately ten launches, followed by reading and storing the sensor data. If time allows, additional launches are carried out. Throughout the test, multiple cameras record the impacts from different angles, and both the time and velocity of each launch are documented.

The second test block is conducted later on Wednesday on the short track rink. This test follows a similar procedure but is performed using movable padding. The available time is uncertain, but the aim is to perform at least twenty launches. In addition to evaluating the same objectives as the first test, this block provides insight into differences between traditional and movable padding systems.

The third test block takes place on Thursday between 12:00 and 16:00. The first part focuses on analysing variations between different pieces of padding of the same type by performing multiple launches per padding section. The second part introduces impacts under an angle of 45 degrees, allowing evaluation of more realistic crash scenarios. The final part of this block involves testing the original projectile to enable direct comparison with the new design.

H.3. Expected results

Based on the design and prior assumptions, the deceleration curve is expected to show a single clear peak. The measured g-forces are expected to be slightly higher than those observed in the ISU drop test due to differences in energy distribution and penetration depth. The dummy is expected to penetrate the padding less deeply than the ISU test cylinder but similarly to a real skater.

In terms of repeatability, measurements are expected to vary within approximately 10% of the average value, excluding outliers. Only minimal differences are expected between different pieces of padding of the same type.

Regarding structural performance, no major failures are expected. The dummy should remain intact, with only minor cosmetic damage such as small dents. No damage to the padding or ice is expected.

H.4. Required equipment

- ICE-G1 launch system
- Newly designed projectile
- Sensor system
- Laptop with charger
- Two cameras capable of slow-motion recording
- Tripods for camera positioning
- Measuring tools (e.g. tape measure)
- Tools for adjustments and repairs
- Ice rink
- Multiple padding elements
- Markers (e.g. stickers) for visual tracking

H.5. Pilot test

Prior to the main testing sessions, a pilot test is conducted to validate the setup and procedures. The pilot consists of two short time blocks, during which the focus is on assembling and disassembling the system efficiently, testing the launch mechanism, and verifying camera placement.

The second pilot block focuses more on data collection and sensor handling. Multiple launches are performed, and the sensor data is regularly read and stored. This phase also includes testing adjustments to the setup, such as changing the impact angle, to identify potential practical challenges.

H.6. Data analysis

The analysis consists of both quantitative and qualitative components. The quantitative analysis focuses on the deceleration curves and peak acceleration values obtained from the sensor data. Additionally, the repeatability of the measurements is evaluated using the intra-class correlation coefficient (ICC).

A two-way mixed effects model with absolute agreement is used. Both single-measurement reliability (ICC(3,1)) and average-measurement reliability (ICC(3,k)) are considered. A two-way mixed ANOVA is performed to determine the required mean square values.

In addition to the quantitative analysis, qualitative analysis is performed using video recordings. These recordings provide context for interpreting the sensor data and allow visual assessment of deformation behaviour. Markers placed on the padding enable tracking of deformation patterns.